30th June 2013

SAR Formation Flying

Annex 12. Basis of an Australian Radar Soil Moisture Algorithm Theoretical Baseline Document

Document Version: V01_00

User Advisory Group (UAG)
Prof J.P. Walker, Monash University
Dr R. Panciera, University of Melbourne
Dr A. Monerris, Monash University

Revision History

Version No.	Date	Author	Description of Change
V01_00	30th June 2013	UAG	Initial Release

REPORT BACKGROUND AND SUMMARY

The purpose of the Garada User Advisory Group's (UAG) study into the soil moisture application was to determine a theoretical baseline of requirements for any future Australian sensor. This short summary introduces the report "*Basis of an Australian Radar Soil Moisture Algorithm Theoretical Baseline Document*" where the issues are thoroughly investigated. In what follows, references to a specific, numbered paragraph of the above mentioned report are specified with the number of the paragraph in parentheses.

Timely knowledge of soil moisture content on a national level has important social, economic and environmental consequences, especially in the Murray Darling Basin area of Australia. Such coverage within short periods of time is only possible through a dedicated *spaceborne* mission and Synthetic Aperture Radar (SAR) is the best candidate sensor. This is because it is an active sensor and measurements can be made in all weather conditions and at any time of day. Also, the spatial resolution is better than for passive radiometer sensors (at the expense of worse radiometric accuracy) (1.1.3).

It is shown in the report that the *best* SAR mission for soil moisture is a fully polarimetric P, L or S band SAR sensor while the *minimum* requirement is for a dual polarised (HH and VV) or compact polarimetric L-band system (transmit circular, receive linear). The Garada mission therefore qualifies as among the most able of current or planned SAR missions for soil moisture extraction.

A sensor with carrier frequency between 1 and 5 GHz (into which L band falls) has the maximum sensitivity to soil moisture (1.3.3). Relatively long microwave wavelengths are preferred since lightly vegetated areas can be considered as bare soil for the purposes of extracting soil moisture. Moreover, L-band is a protected band, meaning interference will be minimal (1.3.5). In fact, the Garada SAR instrument is designed to work within a designated International Telecommunication Union frequency band, for minimal interference.

In terms of the orbit requirements, the best mission for soil moisture has a dawn-dusk sun-synchronous orbit. A dawn-dusk sun-synchronous orbit is such that the satellite will image a certain area of the earth at the same local time. Typically the ascending pass (moving from southern to northern latitudes) will be at dawn (6 am) and the descending pass (moving oppositely) will be at dusk (6 pm). The orbit is such that the solar panels on the satellite will have continuous illumination from the sun, meaning more power will be generated so a greater number of acquisitions can be taken. The 6 am overpass minimises the atmospheric effects of the ionosphere on the polarisation of the electromagnetic radiation and thus is optimal for soil moisture extraction (2.3.8).

The orbit selection also affects the revisit time. This is the minimum period of time such that the ground track of the satellite repeats. A relatively short revisit time is preferred for continuous soil moisture monitoring and a requirement on the resolution of 50 metres is derived. This is both to differentiate the capabilities of an Australian spaceborne SAR from the forthcoming SAR missions of other countries, but more importantly, to address the specific needs of Australian users who would depend on a soil moisture product. The forthcoming spaceborne soil moisture missions considered include SAOCOM, ALOS 2 and SMAP and their soil moisture solutions are discussed in detail.

The spatial resolution requirements will vary according to the application. The applications considered include climate modelling, weather forecasting, flood forecasting, broad-acre farming

and irrigation management. The most stringent requirement is for a 50 metre spatial resolution for irrigation management (1.4.1). This becomes the driver for all subsequent requirements. A 50m spatial resolution will also likely be beneficial in environmental protection applications, where for example it can discriminate moisture levels as a function of distance from a river.

The report considers the various soil moisture extraction algorithms in order to determine a *baseline*. There are two broad classes of soil moisture algorithms, the snap-shot based ones and the time-series based ones (3.1.1). Within these categories, there are further divisions, empirical, semi-empirical and theoretical among them. Each may have analytical, ie. closed form or numerical solutions. (3.1.2). The snap-shot based algorithms require only a single image.

A *time series* approach to soil moisture extraction is recommended. This means that multiple images at different times are used to determine the changes in soil moisture levels of the scene (4.1.1). Using images of the same scene from different times allows the phase changes to be measured. The working assumption is that the parts of the image that show changes are related to soil moisture content, while the relatively static parts of the image relate to soil texture and roughness, as well as to topography (4.1.1). Thus, measuring the decorrelation between two images allows the soil moisture content to be determined.

Soil moisture is expected to effect polarisation because it changes the conductivity of the soil. The time series approach can be combined with full polarimetric operation in order to extract information about the dominant scattering mechanisms. Polarimetric operation of the SAR refers to using information about the polarisation of the electromagnetic returns additionally to the phase and amplitude of the received echo. The polarisation information can be exploited to give information about the dominant scattering mechanisms of a scene.

Important to the soil moisture application is the need for good *radiometric calibration*. Calibrating the SAR sensor is needed in order to extract an absolute volumetric soil content from the data (or better yet, the dielectric constant that is related to the soil moisture content). Calibration can be done either using passive corner reflectors (which are ground based and reflect the incoming signal strongly) or active transponders. A study of calibration demands, especially relating to multiple spaceborne sensors (ie. relative calibration) is described (7.2.4).

An analysis of the error budget pertaining to soil moisture retrieval is given. The following are considered: SAR instrument noise, calibration error, physics model error, ancillary data error, conversion error from dielectric constant to volumetric soil moisture, effect of scaling and scene heterogeneity.

Finally the algorithms for extracting soil moisture from SAR data are investigated. Recommendations are given on the best algorithms and the validation procedures. The latter include airborne and field studies to be conducted prior to deployment of the SAR mission. Quality control in the form of post launch validation of the algorithms and their accuracy is recommended. This will involve in-situ soil moisture measurements using probes.

In conclusion, the following report is a comprehensive study of state of the art methods relating to soil moisture extraction from radar data and its recommendations are highly relevant to a future Australian soil moisture SAR mission, such as studied in the Garada program.

PREFACE			**4**
EXECUTIVE SUMMARY			**5**
1.	**INTRODUCTION**		**6**
	1.1.	Overview	6
	1.2.	Importance of Soil Moisture	6
	1.3.	Soil Moisture Measurement Approaches	7
	1.4.	Soil Moisture Applications and their Requirements	8
	1.5.	Basis of Soil Moisture Measurement Using Radar	9
	1.6.	Review of Radar Requirements for Soil Moisture Measurement	13
2.	**REVIEW OF SATELLITE SOIL MOISTURE MISSIONS**		**15**
	2.1.	Overview	15
	2.2.	Sentinel	21
	2.3.	SMAP	22
	2.4.	SAOCOM	23
3.	**APPROACHES TO RADAR SOIL MOISTURE RETRIEVAL USING SNAP-SHOT ALGORITHMS**		**25**
	3.1.	Overview	25
	3.2.	Bare Surfaces using Numerical Surface Backscatter Models	25
	3.3.	Bare Surfaces using Theoretical Surface Backscatter Models	27
	3.4.	Bare Surfaces using Empirical Scattering Models	29
	3.5.	Bare Surfaces using Semi-Empirical Scattering Models	30
	3.6.	Vegetated Surfaces	32
	3.7.	PolSAR and PolInSAR Observations	33
4.	**APPROACHES TO RADAR SOIL MOISTURE RETRIEVAL USING TEMPORAL ALGORITHMS**		**36**
	4.1.	Change Detection Approaches	36
	4.2.	Time-series Approaches	36
	4.3.	Principal Components Analysis	38
	4.4.	Interferometric Techniques	39
5.	**SUMMARY OF APPROACHES TO RADAR SOIL MOISTURE RETRIEVAL**		**40**
	5.1.	Statistical Methods	40
	5.2.	Model Inversion Methods	40
	5.3.	Data Cube Methods	40
	5.4.	Polarimetric Methods	41
	5.5.	Interferometric Methods	41
	5.6.	Change Detection Methods	41
	5.7.	Time Series Methods	41
6.	**CURRENT METHODS PROPOSED FOR RADAR SOIL MOISTURE RETRIEVAL**		**42**

6.1. SMAP Radar Soil Moisture Retrieval Algorithms 42
6.2. Sentinel-1 Soil Wetness Retrieval Algorithms 47
6.3. SAOCOM Soil Moisture Retrieval Algorithms 51
7. RADAR SOIL MOISTURE RETRIEVAL ALGORITHM RECOMMENDATION 52
7.1. Overview 52
7.2. General Observations 53
7.3. Algorithm Recommendations 55
8. SYSTEM SPECIFICATIONS 60
8.1. Overview 60
8.2. SAR System Design Considerations 60
8.3. Summary 71
9. ACCURACY AND FURTHER CONSIDERATIONS 71
9.1. Accuracy Assessment 71
9.2. Risks and Special Cases for Soil Moisture Retrieval 74
9.3. Ancillary Data Requirements 78
9.4. The Way Forward: R&D Requirements 79
10. CALIBRATION AND VALIDATION 82
10.1. Overview 82
10.3. Pre-launch Algorithm Validation 84
10.4. Post-launch Satellite Calibration 86
10.5. Post-launch Algorithm Validation 87
10.6. Validation of Derived Products 88
11. CONCLUDING SUMMARY 89
REFERENCES 91
APPENDIX A. SOME SIGNIFICANT MODEL PARAMETERS 104
APPENDIX B. ACRONYMS 108

PREFACE

This report constitutes the basis for an Algorithm Theoretical Baseline Document (ATBD) of a radar-based soil moisture mission for Australia.

This document draws heavily upon material provided in the report

> M.L. Williams, A. Mitchell and A.K. Milne (2013) Soil moisture retrieval using satellite synthetic aperture radar (SAR): Review of relevant soil moisture retrieval algorithms and recommendations for a SAR soil moisture sensor and algorithm, 105pp.

prepared by Horizon Geoscience Consulting (HGC) for Prof. Walker. The original report is available upon request. HGC staff have been working in close collaboration with Prof Walker and Dr Panciera as part of a User Advisory Group (UAG) for soil moisture estimation from radar during the preparation of their report. While this report does not necessarily reflect the views of HGC, the outcome of this collaboration has culminated in the present document. Some material has also been sourced from the report

> Tanase, M. and Panciera, R. (2011) Towards operational monitoring of key climate parameters from synthetic aperture radar. Research Plan. Cooperative Research Center for Spatial Information (CRC-SI) / The University of Melbourne.

EXECUTIVE SUMMARY

- The preferred radar mission design for soil moisture mapping would be a fully polarimetric S-, L-, P-band system so as to cover the full range of conditions ranging from bare to forested, while the minimum mission would be a dual polarized (HH and VV) or compact polarimetric (providing the current knowledge gaps on compact polarimetry techniques can be filled) L-band system.
- Important factors to consider in the design are RFI mitigation and Faraday rotation/ionospheric correction. A 6AM overpass time would be expected to minimize the Faraday and ionospheric effects.
- An exact orbit repeat with 2-3 day revisit is needed to meet the requirements of most soil moisture applications and retrieval algorithms. A constellation of satellites will be required to achieve this, and thus inter-sensor calibration will be critical for the time-series based retrieval algorithms that are proposed. Use of Gallium Nitride (GaN) technology and SCan On REceive (SCORE) operation with digital beam forming will help limit the number of satellites required to achieve this temporal repeat requirement.
- Presuming the minimum mission with a 2-3day exact orbit repeat is adopted, a 50m spatial resolution of the derived soil moisture product would be required to set an Australian radar soil moisture mission apart from the capabilities of other existing and/or near-term missions, such as Sentinel, SAOCOM and TanDEM-L. Moreover, the 50m resolution would be required to address issues in relation to irrigation scheduling. If this resolution and/or temporal repeat are not achievable, then the possibility of partnering with one of the proposed missions should be explored.
- A time-series soil moisture retrieval algorithm is recommended, making use of frequent radar observations to distinguish backscatter changes due to soil moisture dynamics from those due to changes in surface roughness and vegetation, together with decomposition of fully-polarimetric observations to determine dominant scattering mechanisms within each cell.
- Attention to the retrieval algorithms, related ancillary information and calibration methodologies will be required before committing to a final system design, particularly if compact polarimetric mode is to be adopted. This would require dedicated pre-launch airborne field campaigns that closely mimic the specifications of the proposed mission design. Careful attention to post-launch algorithm validation and final algorithm selection should also be included as a fundamental component of any radar soil moisture mission for Australia.

1. INTRODUCTION

1.1. Overview

1.1.1. Knowledge of the spatial and temporal distribution of soil moisture is critical for economic, social and environmental planning in a water-constrained future. Such information can only be provided on a national basis using remote sensing.

1.1.2. While most applications require absolute soil moisture content on a near-daily repeat, the spatial resolution requirements are highly dependent on the application.

1.1.3. Microwave remote sensing is the only approach to have all-weather observing capabilities, and to have a response that is directly affected by the water content in the near-surface layer of soil. Moreover, radar (active microwave) is required to achieve spatial resolutions that are better than the 10's km spatial resolution provided by radiometer (passive microwave) sensors.

1.1.4. In this report, soil moisture will be understood as the water content in the top 5cm soil surface layer, measured in terms of volumetric units [vol/vol]. While soil water content is often referred to in terms of "relative wetness", it is only an "absolute soil moisture content" that can be directly measured and traced against calibration standards using volumetric field measurements.

1.1.5. The absolute soil moisture value typically has a dynamic range from close to zero, to as much as 0.5 vol/vol in sandy soils; clay soils have a lower dynamic range.

1.2. Importance of Soil Moisture

1.2.1. About 70% of the Earth is covered with water, 97% of which is oceans. Heating of oceans by the Sun keeps the Earth's water in a continuous circulation from the atmosphere to the Earth and back again through condensation, evapotranspiration, and precipitation processes. Some of the precipitation that falls onto the land infiltrates into the ground.

1.2.2. The water in the unsaturated or "vadose zone" of the land surface is usually referred to as soil moisture. The thickness of this zone extends from the soil surface to as much as a few hundred metres below the surface in some regions, depending on soil thickness and groundwater table depth.

1.2.3. Although the water held by soils is a small fraction of the Earth's water budget, soil moisture plays an important role in the water cycle since it controls the proportion of rainfall that percolates, runs off, or evaporates from the land, thus influencing plant growth and flood magnitudes. Moreover, it affects the evapotranspiration that then impacts the precipitation variability within a region (Koster et al., 2004).

1.2.4. Importantly, the near-surface layer of soil moisture that can be observed by satellites i) is what has the greatest impact on flood events, and ii) can be combined with model predictions to estimate root zone soil moisture requirements for agricultural and meteorological applications.

1.3. Soil Moisture Measurement Approaches

1.3.1. In-situ measurements of soil moisture are sparse and their values are only representative of small areas, since soil moisture temporal and spatial variation is large. Such soil moisture networks are also expensive to install and maintain. However, several data bases exist, such as the Global Soil Moisture Data Bank (Robock et al., 2000) and the International Soil Moisture Network (Dorrigo *et al.*, 2011), based on a networks ranging from small research watershed to national coverage. Unlike the United States, Australia has no national soil moisture observing network.

1.3.2. Many model based soil moisture products exist, such as the Australian Water Availability Project (http://www.eoc.csiro.au/awap), but these typically provide information only on wetness in the climatology of the model, meaning that values are not easily used in applications. Moreover, they are typically un-validated.

1.3.3. The alternative to these approaches is remote sensing, with the capability to provide an absolute soil moisture value over large areas on a regular repeat cycle. However, the sensitivity to soil moisture content is highly dependent on the operating frequency of the remote sensing system. The maximum sensitivity to soil moisture is achieved in the lower range of microwave frequencies (Ulaby et al., 1986), which goes from 1 to 5 GHz (wavelength from 30 cm to 5 cm, respectively).

1.3.4. Land surfaces are a mixture of soil, water, and air particles. At microwave frequencies the real part of dry soil and water dielectric constants are approximately 4 and 80, respectively (Jackson & Schmugge, 1989). Thus soil moisture can be estimated from this contrast between the dielectric constant of water and soil particles.

1.3.5. Many works in the scientific literature conclude that microwave radiometry at L-band (1.4-1.427 GHz) is optimal to estimate soil moisture, not only because it is very sensitive to soil moisture, but also because i) it provides all-weather coverage, since the atmosphere at microwave frequencies may be considered nearly transparent, ii) vegetation is semi-transparent, which allows observations of the underlying layers, and iii) it is a protected band (Eagleman & Lin, 1976; Wang & Choudhury, 1981; Jackson & Schmugge, 1991, 1995; Kerr et al., 2000).

1.3.6. Radiometry (passive) and radar (active) microwave remote sensing differ primarily in the source of electromagnetic energy used. Passive sensors record the emission from the ground at microwave frequencies. Active microwave sensors, including Synthetic Aperture Radar (SAR), transmit and receive pulses of microwave energy, and record the time delay (distance) and intensity (backscatter) of the echoed signal.

1.3.7. Radiometers employ very large antennas to measure the typically weak signal from thermal emission. Technical limitations on the antenna size yield a large beam width and thus poor spatial resolution (Lillesand and Kiefer, 1994). Despite their poor spatial resolution, they are less affected by vegetation and surface roughness than radars, making them the preferred option for dedicated soil moisture missions to date.

1.3.8. Active sensors can resolve objects at much finer spatial resolutions than passive systems, but the data are much more difficult to interpret due to their high sensitivity to surface roughness, topography and vegetation effects.

1.3.9. The intended application of the data will determine the most suitable system. The utility of active microwave sensors (Ulaby *et al,* 1976, 1978, 1996; Wang *et al.* 1986; Rombach, 1997) and radiometers (Jackson, 1993; Wigneron, 1998; Du *et al*., 2000) for soil moisture content retrieval has been successfully demonstrated in many studies. Real-aperture radar spatial resolution is determined by the pulse length and antenna beam width, both a function of antenna length. By increasing the length of the antenna, finer spatial resolution is achieved. The technical limitations imposed on antenna length to achieve the desired resolution are circumvented by coherent processing of a large number of return signals along the flight direction, simulating a large antenna, or synthetic aperture, in a method first propose by Carl Wiley in 1951, and first implemented as a Synthetic Aperture Radar (SAR) by the University of Michigan in 1953 (Barbier, 1996).

1.3.10. Although arguments can be made for more accurate passive microwave retrieval (Moran *et al*., 2006), the requirements for spatial resolution and coverage for applications requiring reliable soil moisture data can sometimes only be met using active sensors. It is noted that NASA's Soil Moisture Active Passive (SMAP) mission plans to use a combination of low resolution passive microwave radiometry and higher resolution active SAR to measure soil moisture at moderate (10km) resolution.

1.3.11. While passive microwave soil moisture missions have a 0.04 vol/vol accuracy target, radar products struggle to achieve a 0.06 vol/vol accuracy.

1.4. Soil Moisture Applications and their Requirements

1.4.1. Soil moisture must necessarily be obtained at high accuracy for use in hydrologic and meteorological models (0.04 vol/vol; Wigneron *et al.,* 2000). The soil moisture user community has differing needs in terms of spatial resolution, but almost all require a 2-3day temporal repeat (Kerr *et al.,* 2001). Missions referred to below are described in Section 2. The spatial resolution requirements are as follows:

1. Climate modelling. Most climate models are run with a spatial resolution of 50km or larger with global coverage. Several existing missions are already providing data including SMOS (40km), ASCAT (50km), AMSR (50km) and SMAP (40, 10, 3km).

2. Weather forecasting. Weather forecast models are now being run at relatively high spatial resolution when compared with climate modelling, typically on order of 10km. However, the global coverage requirement is relaxed for this application; such models are typically run for the entire Australian continent and/or over regions encompassing each of the Australian capital cities. Several existing missions are and/or will be able to provide this data globally including SMAP (3 and 10km) and ASAR (1km).

3. Flood forecasting. Flood forecast models are run on catchment scale, typically on order of a few thousand square kilometres. Consequently they have a spatial resolution requirement on order of 1-10km. Several missions will be able to provide this resolution or better globally within the next few years, including SMAP (3km) and ASAR (1km). Others are likely

to be able to provide this data regionally if appropriate negotiations are undertaken, such as SAOCOM (250m) and possibly TanDEM-L (250m).

4. Broad-acre farming. Soil moisture information for farm management, in terms of what to plant and when, is done on the paddock scale, typically on order of 1km for crops like wheat, canola and corn etc. Several missions will be able to meet this requirement including ASAR (1km), SAOCOM (250m??) and possibly Tandem-L (250??m). There are also downscaled products emerging from SMOS and AMSR, by combining the passive microwave products with thermal images. Examples include DisPATCH from SMOS, with a 1km or better resolution (Merlin *et al.*, 2012).

5. Irrigation management. Most irrigation in Australia is done using centre-pivot (on order of 50-100m radius), travel irrigators (on order 50m wide) or using flood irrigation bays (typically not more than about 50m wide and several hundred meters long). To be useful for irrigation scheduling, there is a requirement that the resolution be significantly smaller than the size of these management units, on order of 10m. At the very least a 50m resolution would be required. There are no satellite missions currently able to meet the radar radiometric accuracy required for soil moisture monitoring at 50m resolution. The closest would be thermal derived indices which are limited to clear sky conditions and can be complicated to interpret.

6. Other: There are multiple other incidental uses and users to those identified above. Some of these include vector borne diseases, flood plain management, and bushfire risk, but each of fall into one of the main spatial resolution requirements identified above. There is little justification for spatial resolutions that fall between the 10-50m and 1km scales identified above.

1.5. Basis of Soil Moisture Measurement Using Radar

Overview

1.5.1. Radar backscatter from natural terrain is determined by direct and direct-reflected surface and volume scattering by both soil and vegetation (see Figure 1.1). The magnitude of the various backscatter contributions is highly dependent on soil roughness, vegetation structure and both soil and vegetation dielectric properties (i.e., water content).

1.5.2. The electric field scattered by a rough surface, such as that between moist soil and air, can be described in terms of the surface fields (at the soil/air interface). The surface fields are determined by the surface shape, the incident field strength, the direction and polarization of the incident field, and the dielectric constant of the material. Radar backscatter measurements are measurements of the strengths of scattered electric fields. Thus radar backscatter from rough soil surfaces depends on these same factors.

1.5.3. The potential of microwave remote sensing for the measurement of soil moisture is based on the large contrast between the dielectric properties of liquid water and those of dry soil.

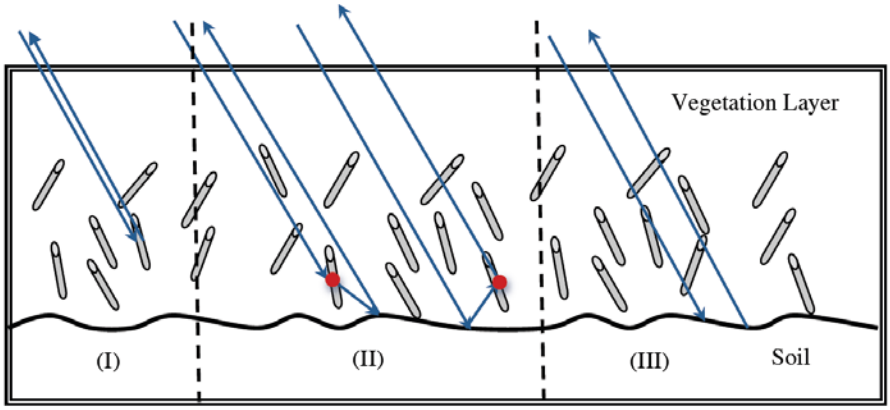

Figure 1.1. Three scattering mechanism (from SMAP ATBD L2/3_SM_A Data Products).

1.5.4. Soil moisture may therefore be estimated using active microwave remote sensing by measuring radar backscatter signals from soil surfaces, inverting these signals to yield estimates of dielectric constant, and converting these into estimates of soil moisture.

1.5.5. Surface properties including roughness and vegetation cover complicate the retrieval of soil moisture and must necessarily be compensated. Roughness can affect backscatter as much as, or more than, soil moisture (Altese *et al.*, 1996, Wutherich, 1997) and there are no simple or straightforward correction methods (Jackson *et al*., 1996).

Dielectric Constant

1.5.6. The relative dielectric constant is the dielectric constant value relative to that of free space, and is a measure of a material's ability to sustain an electric polarisation. When a dielectric material is placed between the plates of a capacitor, the static electric field strength is decreased and the dielectric constant gives the magnitude of the electric field relative to the value it would have in the absence of any medium (Frölich, 1949). The relationship is usually described in terms of the electric displacement, *D*, the electric field *E* and the polarization, *P*:

$$D = \varepsilon E = E + 4\pi P \qquad \text{(Eq. 1)}$$

1.5.7. For a periodic electric field the dielectric constant is a complex quantity which gives both the reduction in magnitude and the phase of the electric field relative to the field in the absence of the dielectric.

1.5.8. Water (e.g. free moisture in a soil) is a polar liquid and therefore a dielectric material. Water molecules carry an electrical polarisation, and may undergo rotations and be further polarised in the presence of electric fields at microwave frequencies. The complex dielectric constant of a dielectric material such as water is given by the Fourier-Laplace transform of the response of the polarization of water to the electric field (Frölich, 1949). The polarization response function can be modelled so as to describe both the contribution to dielectric polarization from electronic polarizability, and the contributions from molecular reorientations in polar fluids such as water (Powles *et al.*, 1987;1988).

1.5.9. The imaginary part of the complex dielectric constant is proportional to the energy loss in dielectrics. The real and imaginary parts vary with frequency and are not entirely independent if the relationship between the displacement and the electric field strength is linear (Frölich, 1949).

1.5.10. Soil, being a mixture of soil particles, air and both bound and free water (Ulaby, Moore and Fung, 1986a) is a dielectric material that displays a strong dependence of dielectric constant on volumetric soil moisture (m_v).

1.5.11. Dry soil, irrespective of frequency, exhibits a real part of the dielectric constant ε' between 2 and 5, and an imaginary part ε'' < 0.05 (Dobson and Ulaby, 1986). For water at 1 GHz ε' is around 80 and ε'' around 4 (Ulaby *et al*., 1986). As the water fraction increases in the soil, so does the amount of free water that is able to move freely around the soil particles, and consequently the soil dielectric constant increases (Topp, 1992). As a result of adding water to dry soil, the value of ε' can increase to 20 or greater (Schmugge, 1983). This difference can be exploited in microwave imaging to estimate m_v.

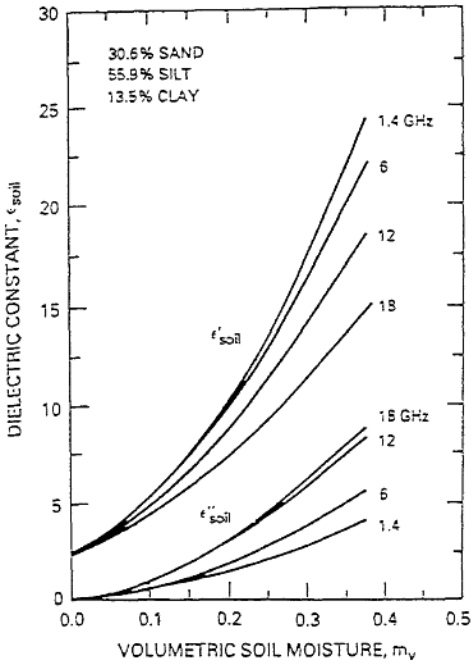

Figure 1.2 Illustration of the response of the real (ε') and imaginary (ε'') parts of the dielectric response to volumetric soil moisture content at four microwave frequencies (Ulaby *et al*., 1986a).

1.5.12. Figure 1.2 illustrates the changing value of the dielectric constant with increasing soil moisture and the response at different microwave frequencies. As the frequency increases, ε' decreases and ε'' increases with increasing soil moisture (Fig. 1, Ulaby *et al.,* 1986). The dielectric constant is affected by the observation frequency and soil properties including soil type, soil water state (whether bound to soil particles or freely occurring), soil temperature, texture and salinity (Schmugge, 1983; Engman and Chauhan, 1995; Ulaby *et al.,* 1986a).

1.5.13. The conversion of an estimate of soil dielectric constant into a soil moisture estimate is a stage common to most soil moisture retrieval algorithms. This requires a model describing the dependence of soil moisture on dielectric permittivity.

1.5.14. The semi-empirical dielectric mixing model of Dobson *et al*. (1985) gives the dielectric constant as a function of soil temperature, moisture, texture, and observation frequency, for both the real and imaginary parts of the dielectric constant, and is valid for frequencies between 1.4 and 18 GHz. At frequencies less than 4GHz, the mixing model does not fully account for the dielectric properties of bound water at low soil moisture contents.

1.5.15. Peplinski *et al*. (1995) extended the semi-empirical dielectric mixing model of Dobson *et al*. (1985) to be valid over the whole range of frequencies between 0.3 and 18 GHz. The model of Peplinski *et al*. (1995) is a popular soil-water-air dielectric mixing model as it represents a practical compromise between the complexity of theoretical modelling and the simplicity of empirical models. It also has validity over a wide range of observation frequencies and accounts for the significant factors of soil texture and temperature. Dielectric mixing models are discussed in more detail in the report.

1.5.16. Mironov (2004) is often being used in place of the models from Peplinski and Dobson due to the fact it works better for sandy soils.

Surface Roughness

1.5.17. Without accurate information on surface roughness, the retrieval of soil moisture with single-wavelength, single-pass SAR is not possible (Moran *et al.,* 2006; Walker *et al.*, 2004). However, the effects of roughness and soil moisture are separable at low frequency (L-band) for bare soil surfaces when fully polarimetric SAR data are available (Hajnsek, 2002). Additionally topographic information is required for incidence angle corrections; such information is available from InSAR, fully polarimetric PolSAR, and other sources. In any event, repeated measurements of surface roughness and fine resolution topographic information are required.

1.5.18. Surface roughness is not an intrinsic property of “random” rough surfaces (commonly used to describe soil surfaces and in the modelling of backscatter). Both frequency and incidence angle determine how “rough” any surface appears to be, so that any description of a surface as rough or smooth must be qualified by reference to the illuminating (microwave) radiation. A surface that appears rough at X-band may appear smooth at L-band or P-band, and at grazing incidence and scattering angles all surfaces begin to appear smooth. The distinction between rough and smooth, although somewhat poorly defined, is important, since only for smooth surfaces may the effects of surface roughness and dielectric permittivity upon backscatter be de-coupled (Hajnsek *et al*., 2002, 2003a/b; Williams, 2008).

1.5.19. As wavelength increases, soil surfaces appear increasingly smooth, and ground-volume scattering can increase in significance as the specular field increases. Ground-volume scattering is influenced by ground moisture content, and the contribution to backscatter from ground-volume interactions can be estimated using polarimetry (Hajnsek *et al*., 2009) and polarimetric SAR interferometry (Cloude and Williams, 2005; Neumann *et al*. 2010).

1.5.20. Surface roughness may vary more over time and space in managed ecosystems such as cropland, as compared to natural ecosystems and dense forest. The consistent row structure of crops creates a periodic pattern that complicates the interpretation of data (Beaudoin *et al*., 1990, Giacomelli *et al*., 1995). Surface roughness of paddocks will likely change in imagery acquired on sequential satellite passes with a revisit time of 30 days or more

(Wutherich, 1997). Data acquired from different satellite orbit tracks may incur large differences in view angle, and so surface roughness may change with respect to field direction (Wutherich, 1997).

1.5.21. Past backscatter modelling was limited in that models were invalid outside their roughness domains, with approximations applicable either to smooth or rough surfaces (Tsang, Kong and Shin, 1985; Ogilvy, 1991; Thorsos and Jackson, 1991). These limitations were in large part relaxed with the development of the Integral Equation Method (IEM) for calculating surface backscatter coefficients, although even this model was generally applied to surfaces characterized by a single-scale roughness, described by the two classical parameters of root mean square (RMS) height and "correlation length". It has been observed that natural rough surfaces are not single-scale, but multi-scale (Davidson *et al*., 1998, 2000) and the IEM has been adapted to use multi-scale correlation functions (Manninen 1997). The multi-scale nature of naturally rough soil surfaces has serious implications for the estimation of correlation lengths: correlation length estimates vary according to the size of the area sampled. If forward modelling is used in a soil moisture retrieval algorithm, consistency of sampling area should be maintained.

Vegetation Scattering

1.5.22. Vegetation cover absorbs and scatters some of the incident radiation, and in so doing, reduces the sensitivity of the microwave signal to soil moisture content. Absorption is influenced both by the vegetation water content (Schmugge, 1985) *and* the structure of vegetation since the *effective* dielectric constant of a random medium contains a contribution from the spatial correlation of the local dielectric constant in mean field theory (Frisch, 1968).

1.5.23. The amount of scattering is determined by canopy structure and geometry (van de Griend and Engman, 1985), as well as the water content and biomass of the vegetation. The effect of vegetation is also dependent on radar imaging parameters including wavelength, view angle and polarisation (Ulaby *et al*., 1986). The effect of vegetation may be reduced by increasing the wavelength of observation (Brown *et al*., 1992; van Zyl, 1993). Schmulluis and Furrer (1992) obtained good results over crops using L-band. Shorter wavelength C- and X-band data are more sensitive to vegetation cover, although there is a greater chance of penetration when vegetation is dry (Brown *et al*., 1992).

1.5.24. Grassland areas can be problematic, with large volumes of moist leaf litter that masks the relationship between backscatter and soil moisture (Sano *et al*., 1998). According to Ulaby *et al*. (1996), active microwave remote sensing has demonstrated potential to measure the volumetric moisture content of the near-surface soil layer with an RMS error of 0.035 vol/vol at low frequencies (e.g., <2 GHz) providing the vegetation cover is less than 15cm.

1.6. Review of Radar Requirements for Soil Moisture Measurement

1.6.1. A number of studies have addressed radar optimal sensor configuration for soil moisture retrieval.

1.6.2. Due to the sensitivity of the backscattering coefficient to surface roughness and vegetation

cover, and the differing effect of various combinations of frequency and incidence angle, there has been a great deal of discussion in the literature about an "optimum" configuration for active microwave remote sensing with satellites. The recommendations that have been made in literature differ from one researcher to the next, so a brief review of the recommendations that have been made is presented below.

1.6.3. Soil moisture measurement using active microwave remote sensing observations is difficult due to the competing effects of soil moisture content and surface roughness. It has been noted by Chen *et al.* (1995) that the larger the incidence angle the larger the sensitivity to soil moisture content, but because of the increasing influence of surface roughness, there must be a compromise. As frequency is increased the active microwave remote sensor becomes more sensitive to surface roughness for all soil moisture conditions and sensitivity to soil moisture content decreases.

1.6.4. To minimise the roughness effects that may often dominate the active microwave remote sensing data in agricultural fields (e.g., Koolen *et al.*, 1979; Beaudoin *et al.,* 1990), an early scatterometer study by Ulaby *et al.* (1978) suggested that the optimum parameters are frequencies from 4 to 5GHz with HH polarisation having an incidence angle between 7° and 17° from nadir. This agrees closely with the recommendation made earlier by Ulaby and Batliva (1976) who suggested that optimum parameters are a frequency of 4GHz with HH or VV polarisation having an incidence angle between 7°and 15° from nadir, for bare fields. Operation of a SAR at such low incidence would of course require enhanced bandwidth in order to maintain range resolution.

1.6.5. Altese *et al.* (1996) have shown that the effect of surface roughness on backscattering is minimised by a sensor configuration having an incidence angle of around 20° and observation frequency between 4.5 and 7.5GHz. Altese *et al.* (1996) also found that the effect of roughness correlation length *l* on backscattering was less than for surface roughness, with its effect minimised at an incidence angle around 30° and observation frequency less than 6GHz. However, Beaudoin *et al.* (1990) have shown that a significant effect on backscattering can be expected from the periodic rows of row crops at all incidence angles except around 5°, with a maximum effect in the range of 25° to 40°. In addition, Dobson and Ulaby (1986) have suggested that the orbital sensor intended for soil moisture sensing should have an orbital inclination greater than 15° from polar orbit in order to minimise the effects of row direction at most latitudes.

1.6.6. Soil moisture estimates with C-band SAR data have been found to be better at both high and low incidence angles rather than using a single incidence angle (Srivastava *et al*., 2003, Baghdadi *et al*. 2006).

1.6.7. Although roughness effects can be minimised by using a sensor with a low incidence angle, this configuration of look angle is very unlikely on a spacecraft system, as the resolution decreases with decreasing incidence angle according to $1/\sin\theta$ (Autret *et al.,* 1989). Therefore, if a low incidence angle is not acceptable, Autret *et al.* (1989) suggest that the best configuration for soil moisture measurement requires the simultaneous use of two polarisations (HH and VV) with an incidence angle greater than 35°.

1.6.8. To minimise the effect of *vegetation* on soil moisture sensing, Dobson and Ulaby (1986) concluded that the optimum parameters should be frequencies of less than 6GHz and

incidence angles of less than 20°. Using these observation parameters, both direct scattering by the vegetation and the effective attenuation loss related to the two-way transmission through the canopy are minimised. At higher incidence angles, the backscattering contribution of the canopy increases and is dominated by the return from vertically aligned stalks and cobs, whereas leaves dominate the canopy loss component. Of course this early study was conducted long before the potential of SAR polarimetry to separate the various scattering mechanisms was fully appreciated.

1.6.9. It has also been noted that the co-polarised measurements of σ^o_{hh} and σ^o_{vv}, and their linear combinations, are the best choice for estimation of soil moisture content, as they are most sensitive to soil moisture changes and least sensitive to calibration accuracy and vegetation cover (Shi *et al.,* 1997). The influence of surface roughness can be minimized using, for example, the co-polarized HH/VV ratio (Chen, 1995). Furthermore, co-polarised channels can be calibrated directly with passive targets like corner reflectors, while cross-polarised channel calibration relies upon measurements made on the co-polarised channels (van Zyl, 1990), and is hence less accurate. Dubois *et al.* (1995a) have noted that to achieve 0.04 vol/vol accuracy in soil moisture content requires a 0.5dB accuracy of the relative calibration and 2dB accuracy in the absolute calibration.

1.6.10. For ERS, which operated at a characteristic incidence angle of 23° (VV polarisation and frequency of 5.3 GHz/C-band), the roughness and vegetation effects would be minimised. Soil moisture inversion from ERS data for regions with short vegetation cover (plant biomass less than 1 kg m^{-2}) appeared possible to Dobson (Dobson *et al.*, 1992), although it should be stressed that this study was theoretical and considered only one characteristic soil surface.

1.6.11. An understandable rule of thumb is that soil moisture retrieval is improved by using more than one measurement. For example multi-frequency measurements of σ° provided better estimates of soil moisture over those derived from single frequencies (Rao *et al*., 1993).

1.6.12. A consensus derived from the literature would indicate that low incidence angles, long wavelengths (L-band) and single HH or multiple polarizations, including quad-polarimetry or compact-polarimetry are the pre-eminent sensor configurations required for soil moisture estimation.

2. REVIEW OF SATELLITE SOIL MOISTURE MISSIONS

2.1. Overview

2.1.1. For the purpose of this review, the emphasis of the discussion is on space-borne active microwave remote sensing for soil moisture content estimation, although some mention is made to the role of passive microwave remote sensing.

2.1.2. Despite the recent losses of PALSAR and ENVISAT SAR sensors, SAR systems are on the increase, and new SAR missions will mean that SAR data is more widely available. Some characteristics of past, contemporary and planned satellite Synthetic Aperture Radars are summarized in Table 2.1.

Table 2.1 Characteristics of major space-borne SAR systems (Barrett *et al.,* 2009).

Platform	Sensor	Band	Polarisation	Highest Spatial Resolution(m)	Swath Width (km)	Mission
SEASAT	SAR	L	HH	25	100	June-Oct 1978
SIR-A	SAR	L	HH	40	50	Nov 12-15th 1981
SIR-B	SAR	L	HH	25	30	Oct 5-13th 1984
Almaz-1	SAR	S	HH	13	172	Mar 31st 1991-Oct 17th 1992
ERS-1	AMI	C	VV	30	100	July 17th 1991-Mar 10th 2000
JERS-1	SAR	L	HH	18	75	Feb 11th 1992-Oct 12th 1998
SIR-C/X-SAR	SIR-C X-SAR	L,C,X	VV,HH,HV, VH, HH	30	10-200	April 1994 Oct 1994
ERS-2	AMI	C	VV	30	100	April 21st 1995-
RADARSAT-1	SAR	C	HH	10	100-170	Nov 28th 1995-
SRTM	C-SAR X-SAR	C,X	VV,HH HH	30	50	Feb 11th – 22nd 2000
ENVISAT	ASAR	C	VV,HH,HH/VV HV/HH,VH/VV	30	100-400	Mar 1st 2002-
ALOS	PALSAR	L	Quad-pol	10	70	Jan 24th 2006-
TerraSAR-X	X-SAR	X	Quad-pol	1	10-100	June 15th 2007-
RADARSAT-2	SAR	C	Quad-pol	3	10-500	Dec 14th 2007-
COSMO/ SkyMed Series	SAR-2000	X	Quad-pol	1	10-200	June 8th & Dec 8th 2007-
TecSAR	SAR	X	HH, HV, VH, VV	1	40-100	21st Jan 2008
SAR-Lupe	SAR	X	-	<1	-	Dec 2006 & Jul 2008-
Kondor-5	SAR	S	HH,VV	1	-	2009
TanDEM-X	SAR	X	Quad-pol	1	10-150	2009
RISAT	SAR	C	Quad-pol	3	30-240	2009
HJ-1C	SAR	S	HH, VV	20	-	2009
ARKON-2	SAR	X, L, P	-	2	-	2011
Sentinel-1	C-SAR	C	Quad-pol	5	80-400	2011
MapSAR	SAR	L	Quad-pol	3	20-55	2011
KompSAT-5	SAR	X	HH, HV, VH, VV	20	100	2011
SAOCOM-1	SAR	L	Quad-pol	7	50-400	2011
RADARSAT Constellation Mission	SAR	C	Quad-pol	3	20-500	2012 – 2014
SMAP	SAR	L	HH, HV, VV	3km	30-1000	2012
DESDynI	SAR	L	Quad-pol	25	>340	2015

2.1.3. Prior to 2002, civilian satellite SARs were capable only of single channel (i.e., frequency) and mode (i.e., polarisation) observations, wherein the influences of both surface roughness and vegetation on backscatter cannot easily be resolved from that of soil moisture. The launch of ENVISAT marked the beginning of a move towards multi-configuration sensors, with the Advanced Synthetic Aperture Radar (ASAR) featuring greater capability in terms of coverage, range of incidence angles, polarization and modes of operation than any of its predecessors.

2.1.4. The increasing number of SAR satellites now available and the higher spatial resolution along with shorter revisit intervals offers greater potential than ever to improve the quality with which surface soil moisture can be retrieved from radar data (Baghdadi *et al.*, 2008).

2.1.5. Of the contemporary and planned radar missions, the ones most suitable for soil moisture monitoring are ESA's Sentinel-1, NASA's SMAP and CONAE's SAOCOM. A discussion regarding algorithm development for soil moisture retrieval from these missions may be found in Section 6.

2.1.6. The passive microwave missions dedicated to soil moisture measurement include SMOS and SMAP. However, soil moisture products have also been derived from sensors with non-optimal wavelengths such as AMSR-E and AMSR2.

2.1.7. ESA launched the Soil Moisture and Ocean Salinity (SMOS) satellite in November 2009, with the aim of measuring soil moisture and ocean salinity for use in climate and hydrological

forecasting (Kerr *et al.*, 2001;2010). SMOS provides a global revisit time of 3 days, and its only payload is an L-band 2D imaging radiometer. The spatial resolution is of 35 – 50km and the incidence angle range of 0 – 50°. The "Disaggregation based on Physical And Theoretical scale Change" (DisPATCh) model (Merlin *et al.*, 2012) is being used to disaggregate the low resolution SMOS soil moisture product to high resolution (1km), thus allowing the use of SMOS data across small scale applications. DisPATCh uses as input the evaporative fraction of each 1km pixel derived from spectral data obtained from MODIS (Moderate Resolution Imaging Spectroradiometer), which implicitly takes into account the moisture distribution at the 1km scale. This model has been developed using data from the OzNet soil moisture network (www.oznet.org.au; Smith *et al.*, 2012).

2.1.8. The Soil Moisture Active Passive (SMAP) mission is a joint effort of NASA's Jet Propulsion Laboratory (JPL) and Goddard Space Flight Center (GSFC). The target launch date is October 2014 (Entekhabi *et al*. 2010). SMAP development is drawing on the heritage of the Hydrosphere State (Hydros) mission (Entekhabi *et al*. 2004). SMAP will provide 3km radar-only soil moisture product, considered a research product, as well as 40km radiometer only and 10km active-passive downscaled products.

2.1.9. The Advanced Microwave Scanning Radiometer - Earth Observing System (AMSR-E), operated by JAXA and onboard NASA's Aqua satellite operated at 6 dual polarized frequencies, centred at 6.9, 10.6, 18.7, 23.8, 36.5 and 89.0 GHz (Draper *et al.,* 2009). AMSRE-E has been in orbit since 2002, but routine observations ceased in October 2011. The spatial resolution of each individual band ranged between 5.4 and 56 km. Global soil moisture measurements were available every 2 days (Njoku *et al.,* 2003). The Global Change Observation Mission 1st – Water (GCOM-W1), a continuation of AMSR-E, was launched in May 2012. The GCOM comprises two satellites, GCOM-W, a microwave radiometer, for observing water circulation changes and GCOM-C, a multi-channel optical imager, for monitoring climate changes. The Advanced Microwave Scanning Radiometer 2 (AMSR2) is onboard GCOM-W1. Like its predecessor, AMSR2 uses six frequencies ranging from 7 to 89 GHz. Each scan observes an area of approximately 1,450 km, so providing coverage of 99% of earth's surface in 2 days. GCOM-W1 is the first of three planned missions, which would extend AMSR measurements out for the next 15 years.

2.1.10. The Advanced SCATterometer (ASCAT) on board Metop-A was launched in October 2006 and it's the successor to the ERS1 and ERS2 scatterometers. ASCAT is a real aperture radar operating at 5.255 GHz (C-band) and using vertically polarised antennas. Two sets of three antennas measure the electromagnetic backscatter in two 500 km wide swaths, one each side of the satellite ground track. Soil wetness is retrieved from ASCAT scatterometer data using the TU Wien change detection method (Wagner et al. 1999a,b,c; Wagner and Scipal, 2000; Wagner et *al.*, 2003). Since December 2008 the European Organization for the Exploitation of Meteorological Satellites (EUMETSAT) has been disseminating global 25km ASCAT surface soil wetness data in near real-time (within 135min after sensing) over its broadcast system EUMETCast.

2.1.11. Hornacek *et al*. (2012) suggested that ESA's proposed Sentinel-1 system, the successor to ENVISAT ASAR, could be used to provide an operational service to derive 1km soil wetness data using change detection algorithms developed and demonstrated with ENVISAT ASAR Global Monitoring mode, and in the ASCAT. The Sentinel-1 mission consists of two polar-orbiting C-Band SAR satellites designed to map the European land mass once every four days

in interferometric wide swath mode (IWS), and the global land surface once every 12 days (MacDonald, Dettwiler and Associates Ltd, 2011). It is expected that Sentinel-1A will be launched mid-2013 and Sentinel-1B about 18 to 24 months later.

2.1.12. SAOCOM (Spanish for Argentine Microwave Observation Satellite) is a planned Earth observation satellite constellation of the Argentine Space Agency (www.conae.gov.ar/eng/satelites/saocom.html). Originally launch was announced for 2010 (1A) and 2011 (1B), but delays have pushed the launch dates back (tentatively) towards 2014 and 2015 respectively for 1A and 1B satellites. SAOCOM 2A and 2B satellites are due for launch in 2019 and 2020 respectively. Those two satellites along with four X-band SAR equipped COSMO-SkyMed satellites from the Italian Space Agency ASI would form the Italian-Argentine System of Satellites for Emergency Management (SIASGE) constellation. While SAOCOM is not planned to provide data over Australia, it may be possible to partner with them to get downloads for Australia.

2.1.13. There is also the proposed TanDEM-L of DLR (the German Aerospace Center), an interferometric L-band sensor for measuring dynamic earth processes (Moreira *et al.,* 2011), but this is still at the conceptual phase. The mission concept comprises two satellites flying in close formation, with PolInSAR and single- and repeat-pass interferometric imaging modes. The design of TanDEM-L will facilitate systematic observation of above ground biomass, earth surface deformation, snow and ice movements, changes in surface soil moisture and land use, and ocean surface currents. As this mission is still in the conceptual phase, it may be possible for Australia to become a partner on this mission.

2.1.14. Due to funding cuts, the DESDynl (Deformation, Ecosystem Structure, and Dynamics of Ice) mission of NASA is on indefinite hold. The mission was scheduled for launch in 2017, and featured a ~10m resolution L-band SAR system with multiple polarizations. Repeat-pass InSAR would have been used for surface deformation and ice sheet dynamics measurements, and PolSAR for biomass estimation and spatial variability of ecosystem structure. The DESDynI radar employs a novel imaging technique called “SweepSAR” that allows wide swath (~240km) imaging at full resolution and full polarization (Rosen et *al.*, 2011). As in the case of TanDEM-L, it may be possible for Australia to become a partner on this mission should the funds become available in the future.

2.1.15. Technical specifications of these and other satellite missions relevant for soil moisture applications are provided in Table 2.2. Further information is provided in the following Sections.

2.1.16. Any soil moisture mission for Australia would need to differentiate itself from the capabilities of these existing and anticipated missions.

Table 2.2. Technical specifications of satellite missions relevant to soil moisture applications (SP: HH or HV or VH or VV, DP: HH+HV or VV+VH, QP: HH+HV+VH+VV, CL: RH+RV or LH+LV).

Sensor	Freq. Band	Orbit	Incidence Angle (°)	NESZ	Rad. Stability	Swath (km)	Spatial resolution	Imaging modes	Soil moisture dedicated (Y/N)	Single/Constellation	Launch / Notes
BIOMASS	432 - 438 MHz (6MHz)	672 km, sun-synch, 17day RC	26-33	-27dB	0.35dB	40 – 60	-	-	N	Single	Space Object Tracking System Interference limits operation
PALSAR II	1257.5MHz (24,42MHz FP)	628 km, sun-synch, 14 day RC	8-70	-28dB	0.2dB	50 – 70	-	Spotlight Stripmap ScanSAR	N	Single	Aug. 2013 GaN, up/down chirp
TerraSAR-L	1.2575GHz (80MHz max)	630km, sun-synch, 14 day RC	20-45	-30dB	-	40 – 70	-	-	N	Single	Concept, DLR, designed for repeat-pass IFSAR
NovaSAR	3.2GHz (25MHz)	580 km, sun-synch,	16-34	-	-	15 – 20	-	-	N	Single	Concept, SSTL/ESA, not yet approved
Sentinel-1	5.410GHz (30MHz)	Near polar sun-synch, 693km 12-day, 175 orbit repeat cycle 3-6 days Europe 6-12 days Global	31-46 23-37 20-47 20-47	-22dB	< 1dB (3sigma)	>250 20(x20) >80 >410	5mx20m 5mx5m 5mx5m 20x40m	C-band (5410MHz) Dual(HH+HV,VV+VH) Single (HH, VV) Dual(HH+HV,VV+VH) Dual(HH+HV,VV+VH)	N	2 sat	Mid. 2013 (1A) 2015 (1B) 12 day RC for a single satellite
SMAP	1.26GHz	670km,	40	-30dB	0.5dB	1000	1-3km	L-band VV, HH, HV	Y	Single	Oct. 2014

	(15kHz)	sun-synch 2-3 days					40km	L-band radiometer			
SAOCOM	1.275GHz (21 MHz)	Sun-synch 620 km 97.89° 16 days (1 Sat) 8 days (Const)	17-50 17.6-47 17.6-49	-35dB	0.25dB	20-40 100-150 220-350	10m 30-50m 50-100m	Stripmap SP/DP TopSAR narrow SP/DP/QP TopSAR wide SP/DP/QP/CL	Y	4 sat	1A 2014-2019 1B 2015-2020 2A 2015-2020 2B 2016-2021
TanDEM-L	-	-	-	-	-	-	-	PolInSAR	Y	2 sat	2019
GCOM-W1 (AMSR-2)		700 km 2 days RC	55	-	-	1450	3- 35km	14 channels, 6 freq, dual pol (7.3, 10.65, 18.7, 23.8, 36.5, 89 GHz)	Y	Single	2012
SMOS	1.413 GHz	Sun-Synch 756 km 32.5° 3 days	0 - 50	-	-	1000	35-50km	2D Imaging Radiometer (H and V pol)	Y	Single	2009
AMSR-E	6.9-89 GHz	705 km 47.4° 2 days	55	-	-	1445	5.4 – 56km	12 channels, 6 freq, dual pol (6,9, 10.6, 18.7, 23.8, 36.5, 89.0 GHz)	Y	Single	2002-2011

2.2. Sentinel

2.2.1. The Sentinel series is being developed by the European Space Agency (ESA) for continuation of operational applications using C-band SAR (MacDonald, Dettwiler and Associates Ltd, 2011). The Sentinels constitute the first series of operational satellites responding to the Earth Observation needs of the European Union (EU) — ESA Global Monitoring for Environment and Security initiative. ESA is currently undertaking the development of 3 Sentinel mission families. Each Sentinel is based on a constellation of 2 satellites in the same orbital plane, which allows to fulfil the revisit and coverage requirements, and to provide a robust and affordable operational service.

2.2.2. Sentinel-1 has been designed to address primarily medium to high resolution applications through a main mode of operation that features both a wide swath (250 km) and high geometric (5 m × 20 m) and radiometric resolution. Over sea–ice and polar zones or certain maritime areas, an extra-wide swath mode may be used to satisfy the observation requirements of certain service providers (e.g. sea–ice monitoring), in order to ensure in particular wider coverage and better revisit time by sacrificing geometric and radiometric resolution.

2.2.3. The Sentinel-1 mission consists of two polar-orbiting C-Band SAR satellites designed to map the European land mass once every four days in interferometric wide swath mode (IWS) and the global land surface once every 12 days using the 2 satellite constellation.

2.2.4. Based on Sentinel-1 acquisition modes, Table 2.3 outlines the anticipated science products:

Table 2.3. Anticipated science products from Sentinel-1 (MacDonald, Dettwiler and Associates Ltd, 2011).

Acquisition mode	L1 product	Resolution class	L2 product	L2 product component
StripMap (SM)	SLC		OCN	OSW, OWI, RVL
	GRD	FR. HR, MR		
Interferometric Wide Swath (IW)	SLC		OCN	OWI, RVL
	GRD	HR, MR		
Extra Wide Swath (EW)	SLC		OCN	OWI, RVL
	GRD	HR, MR		
Wave Mode (WV)	SLC		OCN	OSW, RVL
	GRD	MR		

(L1 Product types include SLC: Single-Look Complex, and GRD: Ground Range Multi-look Detected. Product resolutions include FR: Full Resolution, HR: High Resolution, MR: Medium Resolution. L2 Product types include OCN: Ocean. L2 Product Components include OSW: Ocean Swell spectra, OWI: Ocean wind field, and RVL: Radial Surface Velocity).

2.2.5. Sentinel-1 level 1 products will contribute to a range of operational applications including oil spill and ship detection, arctic sea ice mapping, land-surface motion detection, forest monitoring, and soil wetness estimation.

2.2.6. Sentinel-1 level 2 products will contribute to numerical weather predication and wave forecasting and modelling.

2.2.7. It is expected that Sentinel-1A will be launched mid-2013 and Sentinel-1B about 18 to 24 months later.

2.3. SMAP

2.3.1. SMAP sensor and algorithms are being designed to meet the Level 1 requirements for soil moisture which state "… The baseline science mission shall provide estimates of soil moisture in the top 5cm of soil with an error of no greater than 0.04 vol/vol (one sigma) at 10km spatial resolution and 3-day average intervals over the global land area excluding regions of snow and ice, frozen ground, mountainous topography, open water, urban areas, and vegetation with water content greater than 5kg/m^2 (averaged over the spatial resolution scale)…"

2.3.2. The SMAP instrument incorporates an L-band radar and an L-band radiometer that share a single feed horn and parabolic mesh reflector. The reflector is offset from nadir and rotates about the nadir axis, providing a conically scanning antenna beam with a surface incidence angle of approximately 40°. The provision of constant incidence angle across the swath simplifies the data processing and enables accurate repeat-pass estimation of soil moisture (and freeze/thaw) change. The 6m diameter reflector yields a 3dB antenna footprint of 40km for the radiometer and 1km for the radar.

2.3.3. The goal is to combine the attributes of the radar and radiometer observations (in terms of their spatial resolution and sensitivity to soil moisture, surface roughness, and vegetation) to estimate soil moisture at a resolution of 10km, and freeze-thaw state at a resolution of 1-3km. A radar-only soil moisture product will have a 3km spatial resolution.

2.3.4. SMAP planned data products are listed in Table 2.4. Level 1B and 1C data products are calibrated and geo-located instrument measurements of surface radar backscatter cross-section and brightness temperatures derived from antenna temperatures. Level 2 products are geophysical retrievals of soil moisture on a fixed Earth grid based on Level 1 products and ancillary information; the Level 2 products are output on half-orbit basis. Level 3 products are daily composites of Level 2 surface soil moisture and freeze/thaw state data. Level 4 products are model-derived value-added data products that support key SMAP applications and more directly address the driving science questions.

2.3.5. The 10-km soil moisture requirement will be met for SMAP by combining the radar and radiometer measurements in an algorithm that optimizes the high-resolution attribute of the radar with the higher accuracy attribute of the radiometer, as described in the L2_SM_AP ATBD (Seung-bum Kim *et al*., 2012).

2.3.6. The 3-km radar-only soil moisture product (L2_SM_A) is considered a research product for SMAP and is not expected to be as accurate as either the 40km radiometer only (L2_SM_P) or active-passive downscaled (L2_SM_AP) SMAP data products, especially under more densely vegetated conditions (~3-5kg/m^2). The SMAP mission has targeted 0.06 vol/vol as the L2_SM_A accuracy goal, for vegetation water contents up to 5 kg/m^2. It is acknowledged that this may not be feasible at the higher vegetation amounts.

2.3.7. The 3-km radar only product is currently considering a range of retrieval algorithm approaches, as described in the L2_SM_A ATBD.

2.3.8. The SMAP radiometer measures the four Stokes parameters that characterize the polarization state of the microwave radiation at 1.41GHz. The third Stokes parameter measurement can be used to correct for possible Faraday rotation caused by the ionosphere, although such Faraday rotation is minimized by the selection of the 6am/6pm sun-synchronous SMAP orbit (Yueh, 2000; Freeman and Saatchi, 2004).

2.3.9. At L-band anthropogenic Radio Frequency Interference (RFI), principally from ground-based surveillance radars, can contaminate both radar and radiometer measurements. The measurements of the SMOS mission indicate that in some regions RFI is present and detectable. The SMAP radar and radiometer electronics and algorithms have been designed to include features to mitigate the effects of RFI.

2.3.10. To combat RFI the SMAP radar utilizes selective filters and an adjustable carrier frequency in order to tune the pre-determined RFI-free portions of the spectrum while in orbit. The SMAP radiometer will implement a combination of time and frequency diversity, kurtosis detection, and use of fourth Stokes parameter thresholds to detect and where possible mitigate RFI effects.

Table 2.4. Anticipated SMAP Data Products

Product	Description	Gridding (Resolution)	Latency	
L1A_TB	Radiometer Data in Time-Order	-	12 hrs	Instrument Data
L1A_S0	Radar Data in Time-Order	-	12 hrs	
L1B_TB	Radiometer T_B in Time-Order	(36x47 km)	12 hrs	
L1B_S0_LoRes	Low Resolution Radar σ_o in Time-Order	(5x30 km)	12 hrs	
L1C_S0_HiRes	High Resolution Radar σ_o in Half-Orbits	1 km (1-3 km)	12 hrs	
L1C_TB	Radiometer T_B in Half-Orbits	36 km	12 hrs	
L2_SM_A	Soil Moisture (Radar)	3 km	24 hrs	Science Data (Half-Orbit)
L2_SM_P	Soil Moisture (Radiometer)	36 km	24 hrs	
L2_SM_AP	Soil Moisture (Radar + Radiometer)	9 km	24 hrs	
L3_FT_A	Freeze/Thaw State (Radar)	3 km	50 hrs	Science Data (Daily Composite)
L3_SM_A	Soil Moisture (Radar)	3 km	50 hrs	
L3_SM_P	Soil Moisture (Radiometer)	36 km	50 hrs	
L3_SM_AP	Soil Moisture (Radar + Radiometer)	9 km	50 hrs	
L4_SM	Soil Moisture (Surface and Root Zone)	9 km	7 days	Science Value-Added
L4_C	Carbon Net Ecosystem Exchange (NEE)	9 km	14 days	

2.4. SAOCOM

2.4.1. SAOCOM (SAtélite Argentino de Observación COn Microondas, Spanish for Argentine Microwaves Observation Satellite) is a planned Earth observation satellite constellation of the Argentine Space Agency (Comisión Nacional de Actividades Espaciales) CONAE. SAOCOM is a joint proposal by CONAE, Argentina and ISA, Italy, for a 4 satellite constellation with

application in soil moisture mapping. It is anticipated that observations acquired by SAOCOM will contribute to agricultural, hydrological and health applications, natural resource management and disaster monitoring and management.

2.4.2. The SAOCOM series are Argentina's first Remote Sensing mission carrying instruments on board which operate at microwave wavelengths, including an L-band full polarimetric SAR and a thermal infrared camera. Four satellites are planned, SAOCOM 1A, 1B, 2A and 2B. Each will be equipped with an L-band full polarimetric SAR. Each weighs 1600 kg and their main purpose will be monitoring for the prevention of disasters. The first two satellites are currently under simultaneous development.

2.4.3. Originally launch was announced for 2010 (1A) and 2011 (1B) but delays and further delays have pushed the launch dates back tentatively towards 2014 and 2015 respectively for 1A and 1B satellites. SAOCOM 2A and 2B satellites are due for launch in 2019 and 2020 respectively.

2.4.4. Along with four X-band SAR equipped COSMO-SkyMed satellites from the Italian Space Agency ASI, SAOCOM will form the Italian-Argentine System of Satellites for Emergency Management (SIASGE) constellation.

2.4.5. The L Band SAR will operate at 1.275 GHz and will be right-observing (with possible left-observing capability) from a frozen, quasi-circular, sun-synchronous orbit at 620 km altitude. The satellite will have a 16 day revisit time, with an 8 day revisit for the twin-constellation (1A and 1B). SAR imagery will have 10–100 m resolution, in 30–350 km swath widths at 20-50° incidence with anticipated radiometric accuracy of 0.25 dB (full mission) and 0.05 dB (within a scene).

2.4.6. Available polarization modes include single (HH or VV), double (HH/HV or VV/VH), quadrupolar (HH, HV, VH and VV) and Compact mode Circular-Linear (CL-POL) whereby the system transmits one circular polarization (right or left) and receives two linear polarizations simultaneously (RH and RV or LH and LV).

2.4.7. SAOCOM 1A operation modes include stripmap, TOPSAR (narrow and wide) in all linear polarization modes, TOPSAR Narrow linear polarization modes, and a technological mode TOPSAR Wide CL-POL (designed exclusively for soil moisture assessment in the Pampa Húmeda region).

2.4.8. Despite advances in sensors and methodologies, the development of robust methods for estimating surface soil moisture has been problematic. Consequently, many different techniques and algorithms have been developed for soil moisture content retrieval, using various modes of SAR measurements.

2.4.9. The coverage by SAOCOM will be limited, as it is not intended to be a global mission. The baseline acquisitions will include a large part of Europe for exclusive use by ASI (Italian Space Agency), and Argentina/South America for exclusive use by CONAE. Acquisitions by other users and for other parts of the world will need to be negotiated.

3. APPROACHES TO RADAR SOIL MOISTURE RETRIEVAL USING SNAP-SHOT ALGORITHMS

3.1. Overview

3.1.1. A standard approach to biophysical parameter retrieval, such as soil moisture inversion, is to interpret the measured signals at the time of measurement using models: fitting the model signal by varying the model parameter values (of which soil moisture is one). This process is referred to here as snap-shot algorithms, and is distinct from others that use two or more acquisitions that are distributed through time.

3.1.2. Snap-shot models for surface backscatter may be divided into several categories: theoretical, empirical or semi-empirical, with analytical or numerical solution approaches. They may also include single polarisation or polarimetric solutions. In each case the nature of the random rough surface must be specified, along with the imaging parameters. The parameters include (soil) dielectric constant, wavelength, polarisation and incidence angle. The surface description is often limited to two parameters, RMS surface height and correlation length, which are not always sufficient to describe natural surfaces due to the multi-scale nature of roughness (Davidson *et al.,* 1998/2000, Manninen, 1997).

3.1.3. The use of such single-scale models to recover soil moisture from multi-scale natural surfaces often leads to retrieval ambiguities. Thus, while theoretical models may have justification from the point of rigour, in practice their use may be limited by the availability of proper surface descriptions, or their ease of application.

3.1.4. Surface roughness and correlation may be inverted at the same time as soil moisture, but only if supported by multi-frequency or polarisation measurements, and providing the roughness conditions meet the validity constraints of the model. In general *a priori* information on the surface properties is required, making soil moisture retrieval over large areas problematic. Additionally, even when surface information is available, its limitations do not permit the full description of the surface properties, and the restrictive assumptions made when deriving analytic backscatter expressions imply that they can seldom be used to invert data to a high degree of accuracy when measured over natural surfaces.

3.2. Bare Surfaces using Numerical Surface Backscatter Models

3.2.1. Numerical methods include Method of Moments (MoM) (Tsang *et al*. 2001), the Extended Boundary Condition Method (EBCM) (Kuo and Moghaddam 2007), the finite element method (Lawrence *et al*., 2010; Lou *et al*., 1991) and the finite difference time domain method (Chan *et al*. 1991).

3.2.2. “Fast” methods to further improve computational efficiency have also been developed, including the Sparse Matrix Canonical Grid (SMCG) method (Johnson *et al*. 1996), the Physical Based Two Grid (PBTG) method (Li and Tsang 2001), and the multilevel UV method (Tsang *et al*. 2004). Fully 3D simulations of Maxwell equations (where the height function z=f(x,y) of the rough surface varies in both horizontal directions) are required to predict realistic surface behaviours.

3.2.3. The 3D full wave method of moments simulations based on the “Numerical Maxwell Model in 3 Dimensions” simulations (NMM3D) began in the mid-1990’s (Tsang *et al*. 1994; Tsang *et*

al. 2001). The NMM3D of the Univ. Washington (UW) was selected as the benchmark forward model for the bare surface class for SMAP and was used to compute L-band 40° 3-D surface backscattering for 200 cases including varying surface RMS heights, correlation lengths, and soil permittivities for co-polarization (Huang *et al*. 2010) and cross-polarization (Huang and Tsang 2012).

3.2.4. Numerical methods, which avoid approximations beyond those used to model the surface topographies but require Monte Carlo simulations and much greater computational costs, have also been employed by SMAP researchers to obtain bare surface scattering predictions.

3.2.5. The numerical calculations were used to create interpolation tables (or "data cubes") wherein interpolated values are within 0.2 dB of the original data values. The maximum RMS height considered for SMAP was 0.21 wavelength (ks=1.32 which is about 5cm at L band, where k and s are the wave number and RMS height) so that the cases simulated and the interpolations used can be applied to cover a wide range of interests.

3.2.6. These results were compared with the Dubois empirical model (Dubois *et al*. 1995), SPM, KA, and AIEM. In parallel, a group in the Univ. Michigan Group used a stabilized EBCM method (Duan and Moghaddam 2011) and computed results up to ks=1. Results of the UW NMM3D look-up tables were compared with field measurements of co- and cross-polarized backscattering (Oh *et al*. 1992). The field data included measurements of soil permittivities, RMS heights, and correlation lengths (which latter should be used subject to the previous caveats regarding natural surfaces). The soil surface correlation functions were also measured and found best matched by exponential correlation functions. These ground truth parameters were simulated with NMM3D using the exponential correlation function description. Comparison of NMM3D predictions and measured data shows that good agreement is achieved. The cross polarization results of NMM3D are also in good agreement with experimental data.

3.2.7. For both non-woody and woody vegetation on vegetated surfaces the primary approach utilized was a "discrete scatterer" approximation (Lang and Sidhu 1983; Tsang *et al*. 2000), in which each vegetation object, such as a cylinder or disk, is assumed to scatter independently. Scattered fields calculated in the mean field model from each vegetation component are summed and averaged over size and orientation distributions in a coherent model that accounts for vegetation structure.

3.2.8. A first order iterative solution of the radiative transfer equation (Karam *et al*. 1992; Tsang *et al*. 1985) yields similar predictions but neglects a coherent double bounce effect. Several variations of the discrete scatterer model exist (Arii *et al*. 2010; Chauhan *et al*. 1994), depending on the fidelity with which the vegetation-ground interaction term is treated, the number of vegetation layers included, the method utilized to compute scattering from vegetation and surface components, and the approach used for estimating attenuation.

3.2.9. A notable example of a coherent SAR simulation model for forests, suitable for frequencies between L-band and P-band, is PolSARproSIM (Williams, 2006, earth.eo.esa.int/polsarpro). Although restricted to simulation of forests, the software has been used widely to demonstrate the utility of various biophysical parameter retrieval algorithms because of its high fidelity and proper inclusion of important scattering mechanisms and their inter-dependence.

3.3. Bare Surfaces using Theoretical Surface Backscatter Models

3.3.1. In principle, if the surface topography and surface fields (e.g., roughness and dielectric constant) are known, backscatter from a surface can be calculated through application of the Stratton-Chu integral (see e.g. Ulaby *et al*., 1982), which is an analytical solution of Maxwell's equations, and embodies Huygen's principle for a rough surface. In practice exact analytical solutions are intractable, and full numerical solutions are computationally expensive, although increasingly accessible.

3.3.2. Despite complexity hurdles theoretical models may be preferred over empirical and semi-empirical models as the models are valid for a range of different sensor configurations, and incorporate directly the effect of surface parameters on backscatter response (Altese et al., 1996). Theoretical models, for the most part, describe the general trend in backscattering coefficient with changes in surface roughness (including RMS surface height, correlation function and correlation length) and soil moisture. However, the complexity of some of the models and the restrictive assumptions of their simplifications may limit their use for inversion as a result of failure to meet validity ranges or lack of agreement with experimental observations (Oh et al., 1992; Dubois and van Zyl, 1994; Dubois et al., 1995b). This is often bacause knowledge of surface roughness is required for soil moisture inversion, and incomplete knowledge of surface statistical description can have profound implications for backscatter predictions.

3.3.3. As a result of the complexity of the surface scattering problem a number of approximations were developed that yielded simplified expressions for surface backscattering coefficients. These simplifying approximations were restricted for use to those surfaces for which the simplifying assumptions were valid.

3.3.4. For example the Small Perturbation Method (SPM) describes the scattering of waves from slightly rough surfaces (Rice, 1963). The SPM assumes that surface variations are much smaller than the incident wavelength (recall that surface "roughness" is wavelength and incidence angle dependent). The SPM solves for the surface fields in the Stratton-Chu equation using a series expansion which is truncated on the assumption of small surface slope. The zeroth-order solution is just that which would be observed for a perfectly smooth surface. The first-order solution, the most commonly discussed, provides a simple expression for backscatter, but predicts no depolarization in the backscatter direction; this deficiency is corrected in the second-order solution. The SPM has been used to study rough surface scattering for surfaces with small height variation compared to the wavelength and with slope smaller than unity. The SPM (or Bragg model) has also been adapted for use in what is effectively a "two-scale" approach for use with polarimetric SAR data: discussion of this methodology is left to a later section.

3.3.5. The Kirchhoff Approach (KA) and the Physical Optics Method (POM) use the "tangent plane approximation" to represent the surface fields on a rough surface as those that would exist on the tangent plane at that point. The local Fresnel reflection coefficients (which depend upon the dielectric permittivity through the soil composition and water content) are used to calculate the tangent fields. Given a surface correlation function it is possible to derive tractable analytic expressions for backscatter in the KA. These are of limited validity however, and the KA can only be used to study backscatter from surfaces with large radius of curvature (relative to the wavelength of the incident radiation). For a full discussion of the ranges of validity of the SPM and KA the reader is referred to Thorsos and Jackson (1991).

The Geometrical Optics (GO) solution is a high-frequency asymptotic solution to the KA diffraction integrals derived using the method of stationary phase (Tsang, Kong and Shin, 1985).

3.3.6. The use of integral equations in the study of surface scattering is by no means new (e.g. Morse and Feshbach, 1953). The Integral Equation Method (IEM) of Fung and Chen (1992) united both KA and SPM models in an attempt to extend their applicability over a wider range of roughness conditions and frequencies. Although it contains a number of approximations (Fung, 1994), the IEM demonstrates the capacity to describe backscattering behaviour of a randomly rough bare surface over wide ranges of roughness and correlation length for Gaussian and exponentially correlated surfaces, and takes both single and multiple surface scattering into account through the use of tangential surface field estimates that extend beyond the use of Fresnel reflection coefficients in the KA. The IEM has been employed to model backscatter from multi-scale surfaces more representative of real rough surfaces (Manninen, 1997), but the range of validity of the IEM in the multiscale formulation is not yet clear.

3.3.7. Perhaps because of its wide range of validity the IEM has become arguably the most widely used radar backscatter model and has been found to be particularly suitable for retrieving soil moisture from single-wavelength, single-pass SAR measurements. However, in all such cases, an *a priori* measure of surface roughness was required (e.g., Tansey and Millington, 2001).

3.3.8. Altese *et al.* (1996) used an approximate version of the IEM, valid for surfaces with small to moderate roughness (Appendix A Table A.1). Only the single scattering component of the IEM was considered and only the real part of the relative dielectric constant was used, with the assumption that the surface correlation function is isotropic and could be represented by either Gaussian or exponential models.

3.3.9. As a result of successful applications of the IEM to soil moisture retrieval, there have been numerous refinements, improvements, and additions to the IEM that will certainly encourage its continued use. To reduce the complexity of the IEM application, algorithms have been developed based on fitting of IEM numerical simulations for a wide range of surface roughness and soil moisture conditions (Chen *et al*., 1995; Shi *et al*., 1997). The results are a look-up table of IEM simulations that serve to directly relate SAR surface backscattering coefficient to theoretical model predictions over bare and sparsely vegetated surfaces with known radar parameters. These simplified IEM-based algorithms require fewer parameters and are much easier to use with remotely sensed data.

3.3.10. Another critical refinement of IEM was the incorporation of vegetation backscatter effects into the soil moisture inversion algorithm. The original IEM was developed for bare soil conditions only, although the retrieval algorithm performed well for sparsely vegetated areas. Bindlish and Barros (2001) formulated an IEM vegetation scattering parameterization. They reported that the application of the modified IEM led to an improvement in the correlation coefficients between ground-measured and SAR-derived soil moisture estimates from 0.84 to 0.95. The incorporation of vegetation scattering may expand IEM applications to moderately vegetated sites and improve applications in arid and semiarid regions where soil moisture is so low that the soil contribution may be equal to the magnitude of the vegetation contribution.

3.3.11. The IEM model has also been refined to include a penetration depth model (Boisvert *et al.,* 1997). Studies have reported problems in IEM-based soil moisture retrieval due to an increase in the penetration depth of the incident wave when the soil moisture was low (e.g., Wiemann, 1998). As a result, modelled soil moisture could not be compared with ground measurements because the IEM did not account for the fact that microwave penetration exceeded the layer where the soil moisture was measured (Wiemann, 1998). Boisvert *et al.* (1997) offered three approaches to refine the IEM to account for variations in beam penetration depth. They reported that the correction allowed reliable comparisons among different SAR configurations and took into account the daily variations in the beam penetration with soil moisture.

3.3.12. Semi-empirical calibration of the IEM model has been proposed and applied to compensate for the uncertainty in the effect of the correlation length on the backscatter. As correlation length is not only the least accurate but also the most difficult to measure of the parameters required in the model, it is proposed that it be replaced by a calibration parameter that would be estimated empirically from experimental databases of radar images and field measurements (Baghdadi et al., 2004)

3.3.13. The general consensus of studies using SAR measured backscattering coefficient with radar backscatter models is that the retrieval of soil moisture with single-wavelength, single-incidence, single-pass SAR data is not possible without information about the surface roughness. The results also demonstrate the need for continuous measurement of surface roughness and fine-resolution information about surface topography, if soil moisture is to be monitored accurately with single-wavelength SAR data. When SAR data with consistent ground truth information are available, it is possible to test the many existing retrieval algorithms and select those that perform best with the available sensor data. This is an approach to be recommended.

3.4. Bare Surfaces using Empirical Scattering Models

3.4.1. The most widely published empirical models apply simple linear regression techniques to SAR backscatter and observed soil moisture (Bernard *et al*., 1986; Bruckler *et al*., 1988; Ragab, 1995). Bruckler *et al*. (1988) applied a simple second order regression equation:

$$\sigma°dB = a.m_v + b \qquad \text{(Eq. 2)}$$

where m_v is the volumetric soil moisture and a and b are empirical regression coefficients and σ°dB is the backscattering coefficient in decibels. Dobson and Ulaby (1986) determined, unsurprisingly perhaps, that the “a” and “b” coefficients were dependent on surface roughness and soil “texture” respectively.

3.4.2. Some of the limitations inherent to empirical models include the requirement of a large number of experimental observations for statistical robustness (Oh et al., 1992), validity over a narrow range of imaging (frequency, incidence angle, polarization) and soil (roughness and moisture) parameters (Walker, 1999), and poor extrapolation to areas outside of those used in model development (Chen et al., 1995; Dubois et al., 1995b). However Oh et al. (1992) suggest that empirical backscatter models have advantages over theoretical models since many natural surfaces do not meet the validity requirements of the

models, and those that do yield poor results against experimental observations.

3.4.3. In the 1990's, more advanced empirical non-linear regression models were developed (Appendix A Table A.2), including Oh's model (Oh *et al.,* 1992) and the Dubois-van Zyl model (Dubois and van Zyl, 1994; Dubois *et al.,* 1995a,b).

3.4.4. The empirical model developed by Oh *et al.* (1992) employed polarimetric backscatter measurements acquired using a truck-mounted scatterometer (LCX POLARSCAT). Full polarimetric data were collected at X-, C- and L-band frequencies over a 10 – 70° incidence angle range, and for a variety of soil roughness and moisture conditions. The reference ground data comprised measurements of RMS height, correlation length and dielectric constant over a finite area.

3.4.5. The model was developed using the magnitudes of the measured data. Good agreement between measured and modelled data was achieved within the ranges $0.1 \leq ks \leq 6$, $2.5 \leq kl \leq 20$ and $0.09 \leq mv \leq 0.31$, where k is the wave number, s is soil RMS height, l is soil correlation length, and mv is the moisture content The model was inverted to predict RMS height and moisture content from multi-polarized radar data

3.4.6. Dubois *et al.* (1995b) developed an empirical model for estimation of soil moisture and RMS height using radar data also acquired by truck-mounted scatterometers (LCX POLARSCAT and RASAM). The Dubois algorithm was optimised for bare soil surfaces and requires 2 co-polarized measurements at a frequency between 1.5 and 11 GHz. Best results are obtained under the conditions $kh \leq 2.5$, $mv \leq 0.35$ vol/vol and $\theta \geq 30°$ (incidence angle).

3.4.7. Excluding use of the HV backscatter in retrieval models has been shown to reduce the sensitivity of the algorithm to cross-talk and system noise, simplify calibration, and increase robustness when vegetation is present (Dubois *et al.,* 1995b), although cross-talk is generally lower than -20dB so this is not a significant issue. Since it is designed for bare soil surfaces, the algorithm underestimates soil moisture and overestimates RMS height in the presence of dense vegetation (NDVI > 0.4). A simple criterion based on the $\sigma°_{HV}/\sigma°_{VV}$ ratio is used to identify areas where inversion of the model is not affected by vegetation. It is noted here that the HV backscatter is now reintroduced into the algorithm as an aid to classifying land cover, a theme that will be apparent in other work. Inversion accuracy was assessed using in situ measurements and the scatterometer data, as well as SIR-C and AIRSAR data, and found to be < 0.042 vol/vol soil moisture.

3.5. Bare Surfaces using Semi-Empirical Scattering Models

3.5.1. Semi-empirical backscatter models might be considered an improvement over empirical backscatter models as they either i) originate from a theoretical model and use simulated or experimental data to simplify the model, or ii) use simulated data from a theoretical model to develop an empirical one that models backscatter response over a wider range of conditions (Walker, 1999). Semi-empirical models tend not to incur the site-specific limitations often found with empirical models. Model parameter details are provided in Appendix A Table A.3.

3.5.2. Oh *et al.* (1994) developed a semi-empirical backscatter model based on available theoretical models (SPM and KA) and extensive experimental observations collected from a

truck-mounted multi-frequency (X-, C- and L-band), polarimetric scatterometer. Backscatter measurements were obtained over a 20 – 70° incidence angle range, with 10° steps and under a variety of soil moisture and roughness conditions. The model is an extension of their previous empirical model (Oh et al., 1992) and includes the magnitude and phase of the backscatter. The co-polarization ratio ($\sigma°_{HH}/\sigma°_{VV}$), cross-polarization ratio ($\sigma°_{HV}/\sigma°_{VV}$) and degree of correlation for co-polarization phase difference were found to be most sensitive to surface parameters.

3.5.3. Chen *et al.* (1995) developed a semi-empirical backscatter model based on the single scattering terms of the IEM. The model is based on multiple linear regression of IEM simulated data. The model proved a simple and successful tool for retrieving of bare soil moisture with known radar parameters.

3.5.4. Another semi-empirical backscatter model based on the single-scattering IEM was developed by Shi et al. (1997). The algorithm was applied to quad-polarized backscatter measurements acquired at L-band by the AIRSAR and SIR-C instruments. Good agreement was found between the single-scattering IEM simulations and L-band backscatter over a wide range of soil moisture and roughness conditions (Shi et al., 1997). Co-polarized backscatter and ratios showed the greatest sensitivity to soil moisture variation, as one might expect, confirming the significance of the approach adopted by Dubois. Model inversion of co-polarized AIRSAR and SIR-C backscatter measurements over bare and sparsely vegetated fields resulted in soil moisture and surface roughness RMSE of 0.034vol/vol and 1.9dB respectively.

3.5.5. The algorithm is expected to not incur the same site-specific limitations typical of an empirical model derived from a limited observation set, as the regression was based on a large dataset simulated for a wide range of surface parameters and at fine intervals (Shi et al., 1997). However, further testing of the algorithm at other sites with ground and SAR data is required to assess its wider application. Further improvement of the algorithm would require consideration of vegetation effects.

3.5.6. Moran *et al.* (2000) used the difference in wet and dry season ERS backscatter measurements to normalize the effects of roughness and topography. Moran indicates that the effects of non-dense vegetation (on the change signal) were found to be negligible for identical sensor configurations and could be ignored (Dobson *et al.,* 1992; Lin and Wood, 1993; Demircan *et al*., 1993; Dubois *et al.,* 1995b; Chanzy *et al.* 1997). Moran also noted that in many areas vegetation is too dense to be able to monitor soil moisture with only C-band wavelength (Wever and Henkel, 1995; Wang *et al.,* 1996).

3.5.7. Quesney *et al.* (2000) applied standard radar equations to estimate soil moisture content at accuracies of ±0.04-0.05 vol/vol using ERS measurements. Site selection was guided by an existing vegetation classification and in situ measurements which helped identify low biomass vegetation. First order radiative transfer modelling was used to correct the backscatter response for the effect of vegetation. Sites were classified according to roughness based on furrow direction as observed by the radar. Empirical relationships were then derived between radar backscatter and in situ soil moisture for each class and applied to all target sites in the ERS image. It was concluded that the same algorithm was applicable to wheat fields throughout November to August, excluding May and June (Quesney et al., 2000).

3.5.8. It is noted that although radiative transfer modelling may be appropriate at C-band for low biomass vegetation, radiative transfer models often contain inappropriate approximations for extinction coefficients, and cannot be readily used to model backscatter when vegetation structure is important. For such instances coherent backscatter modelling is more appropriate.

3.6. Vegetated Surfaces

3.6.1. In areas with denser vegetation, the vegetation component has to be taken into account by the retrieval algorithm in order to obtain accurate estimates of soil moisture. Consequently, the effect of vegetation volume scattering has to be quantified and removed from the total backscatter in order to estimate the surface component, which used in subsequent steps for the retrieval of the parameters of interest. Estimating the vegetation volume scattering component also allows for a more accurate retrieval of the vegetation characteristics (e.g., biomass, height, etc.).

3.6.2. Simple empirical models have been developed based on the increase of the radar backscattering coefficient with biomass according to observational data (Ulaby *et al.,* 1986). The model parameters are highly specific to a single plant structural type (i.e., monospecies plant population) and sensor characteristics (frequency, polarization and incidence angle), strongly limiting their application to large areas.

3.6.3. In theoretical models of radar scattering, the vegetation canopy is normally treated as a uniform layer of some specified height containing a random distribution of scatterers (Attema and Ulaby, 1978; Eom and Fung, 1984; Fung and Ulaby, 1978; Karam and Fung, 1988; Lang and Sidhu, 1983; Tsang and Kong, 1981; Tsang *et al*. 2000). The advantage of the discrete approach is that the results are expressed in terms of quantities such as plant geometry and orientation statistics that are easily related to the biophysical properties of individual plants and can be measured objectively. This generally involves a large number of structural parameters. Two major challenges are encountered when modelling the backscatter behaviour of a vegetation canopy. The first relates to the difficulties in specifying model parameters that adequately describe the canopy. The second relates to the mathematical complexity in resolving the inverse problem due to the large number of variables and parameters, which makes their inversion difficult (Lang and Sahel, 1985). This is the motivation for the semi-empirical models.

3.6.4. The basic approach for semi-empirical modelling of the vegetation scattering is the Water Cloud Model (WCM). Basic conceptual assumptions in the WCM approach include: i) the vegetation is represented as a homogeneous horizontal cloud of identical water spheres, uniformly distributed throughout the space defined by the soil surface and the vegetation height; ii) multiple scattering between the canopy and the soil can be neglected; iii) the only significant variables are the height of the canopy layer and the cloud density, with the latter assumed to be proportional to the volumetric water content of the canopy. In this context, the WCM represents the power backscattered by the whole canopy as the incoherent sum of the contribution of the vegetation and the contribution of the underlying soil which is attenuated by the vegetation layer.

3.6.5. In WCM models, the canopy is represented by "bulk" variables such as leaf area index (LAI) or total water content, and because of the parsimonious use of parameters, these models can be easily inverted.

3.6.6. Once the model is parameterized it is possible to estimate the relative contributions of vegetation and surface to the total backscatter and, subsequently, to retrieve soil moisture from the surface component using bare surface models (Dubois *et al*. 1995; Fung *et al.* 1992; Oh, 2004).

3.6.7. Most semi-empirical models used for soil moisture and/or vegetation parameters retrieval (Bindlish and Barros 2001; Gherboudj *et al.,* 2011; Santoro *et al.,* 2002) are based on the WCM. The models differ in the way the vegetation is parameterized, ranging from crop-specific parameterization (Attema 1978; Gherboudj *et al.*, 2011) to more general relationships for a variety of vegetation types (Bindlish and Barros 2001).

3.6.8. The strong sensitivity of the WCM parameters to changes in canopy structure (i.e., land-cover type) restricts a generalized approach. However, in principle, it should be possible to develop a unique set of parameters for each class of vegetation (defined by its geometric structure).

3.6.9. The WCM in its original form ignores multiple scattering within the vegetation layer and scattering between the vegetation and soil is ignored. The reduced attenuation at low frequencies (L-band) could increase soil-vegetation interaction for crops with significant returns from stems (e.g., corn), in which case the soil-vegetation backscatter should be accounted for.

3.7. PolSAR and PolInSAR Observations

3.7.1. The application of fully polarimetric SAR (PolSAR) and compact polarimetry for soil moisture retrieval has also been investigated. Measurement of polarimetric parameters such as coherence (γ), entropy (H), and alpha angle (α) have been used to study the dependence of the polarimetric signature on land cover changes and on surface parameters such as soil moisture and surface roughness (Barrett *et al*. 2009). The key advantage of PolSAR is the capacity to measure the full suite of polarimetric attributes pertaining to a target. While previous spaceborne SARs have operated in a single fixed polarisation for both transmission and reception (e.g., Radarsat-1, ERS-1 & 2), more recent SARs operate with dual (ENVISAT ASAR) or fully (Radarsat-2, TerraSAR-X) polarimetric capabilities. This facilitates measurement of a target's scattering *amplitudes* in all combinations of the two linear polarisations: S_{HH}, S_{HV}, S_{VH} and S_{VV}. Full measurement of the scattering matrix in any single (e.g. linear) basis permits the construction of the scattering matrix in any polarization basis and permits a full description of the target backscattering characteristics at the observation frequency.

3.7.2. For monostatic observation $S_{HV} = S_{VH}$ for reciprocal scatters, and is a valid assumption for most natural targets. Under reciprocity, the Sinclair/Jones scattering matrix (the set of four scattering amplitudes) can then be expressed as a three-vector, the Pauli vector, and the average of the outer product of this vector forms the 3 x 3 polarimetric coherency matrix. For fully developed speckle the coherency matrix represents all the information required for

a full description of the polarimetric clutter distribution for distributed targets, such as bare soil surfaces or crop fields etc.

3.7.3. Polarimetric signatures can provide detailed information on different scattering mechanisms. Compared to single-channel SAR, the benefits of improved data quality and accuracy of results afforded by polarimetry are significant (Barrett *et al*. 2009). As with single-channel SAR, the presence of vegetation is a significant inhibitor to accurate retrieval of soil moisture, but multichannel polarimetric SAR data offer increased ability to both detect and compensate for the effects of overlying vegetation on the observed signal (e.g. Dubois use of HV for vegetation discrimination).

3.7.4. Compensation for vegetation effects has been tackled in two main approaches, including target decomposition algorithms and polarimetric SAR interferometry (PolinSAR). Target decomposition aims to deconstruct the backscattered signal into the various combinations of scattering contributions within each resolution cell. A detailed review of available decomposition algorithms is found in Cloude and Pottier (1996) and Lee et al. (2004). The two most widely used decomposition theorems are the Freeman decomposition (Freeman and Durden, 1998) and its variations, and the Cloude-Pottier or eigenvector decomposition (Cloude and Pottier, 1996, 1997).

3.7.5. The Cloude-Pottier decomposition uses the diagonalisation of the coherency matrix (T) to represent the backscattered signal as the sum of three scattering mechanisms. The first component is attributed to surface scattering and the second and third components represent contributions from secondary or multiple scattering terms (such as direct vegetation and ground-vegetation scattering). Following decomposition, a number of models can be applied to quantitatively estimate soil moisture and surface roughness using the surface scattering term. The extended Bragg or X-Bragg model (Hajnsek, 2001) is an extension of the Small Perturbation Model (SPM), which assumes reflection symmetry and takes into account cross-polarisation and depolarisation effects. Good agreement between inverted and ground measurements was demonstrated in Hajnsek *et al.* (2003b, 2009) using the X-Bragg model. Several studies have also demonstrated the retrieval of surface parameters from the derived entropy (H), anisotropy (A) and alpha angle (α) of the Cloude-Pottier decomposition.

3.7.6. Anisotropy was found to be sensitive to surface roughness (Hajnsek *et al*., 2002; Cloude *et al.*, 2000), while the entropy and alpha angle parameters were effective in estimating surface soil moisture (Allain *et al*. 2003). The utility of the entropy/alpha decomposition model was extended by Cloude (2007) in a dual polarized version which expanded its use beyond that of fully polarimetric data. In a simulation study it was demonstrated (Williams, 2008) that compact polarimetry can be combined with the X-Bragg model to retrieve soil moisture and roughness values for bare soil surfaces that are in accordance with values recovered through the use of full polarimetry.

3.7.7. The inclusion of polarimetric phase information in the form of complex correlation coefficients has also demonstrated sensitivity to surface parameters. Mattia *et al.* (1997) found a significant relationship between the circular polarisation coherence (γ_{RRLL}) and surface roughness while minimising the impact of the dielectric constant. Similar results were achieved by Hajnsek *et al.* (2003), Schuler *et al.* (2002) and Malhotra *et al*. (2003).

3.7.8. Similarly, Hajnsek *et al.* (2002) found high correlation between the linear polarisation coherence $\gamma_{(HH+VV)(HH-VV)}$ (Hajnsek, 2001) and surface roughness and its independence from soil moisture content. Cloude and Corr (2002) applied polarimetric backscattering coefficients and developed a new ratio for soil moisture estimation that is insensitive to variations in surface roughness.

3.7.9. More recently, attempts have been made to exploit the characteristic polarimetric signatures of different scattering mechanisms to aid retrieval of soil moisture from soils under vegetation (Hajnsek *et al*., 2009). L-band PolSAR images permitted the decomposition of the scattering signature into canonical scattering components and their quantification: primarily into direct, volume and soil-vegetation terms. Simple canonical scattering models were used to decompose the polarimetric signature into these components in a manner similar to that used for forest discrimination. Five different decomposition approaches using different models for the individual scattering contributions were investigated and validated, with each yielding a similar level of performance. The study indicated that the X-Bragg model (Hajnsek *et al*., 2003) showed a clear performance advantage at L-band since it was able to better model increased cross-polar return from agricultural fields, due to surface scatter rather than volume scatter. The work also indicated that signatures were more reliable for mature crops, and that soil moisture estimation was possible from both direct-surface and surface-volume scattering components as theory suggests.

3.7.10. The combination of polarimetric SAR with SAR interferometry (PolInSAR) has potential to aid soil moisture inversion below forests. In their study Cloude and Williams (2005a/b) decomposed the polarimetric coherency into volume and surface (direct-ground and ground-volume) terms, and indicate that for L-band observation of forests, the separation of these terms using PolSAR alone can be unreliable. Using PolInSAR the surface-to-volume scattering ratio may be estimated and related to soil moisture, since increasing the soil moisture increases the surface reflectivity and enhances both direct-surface and surface-volume scattering. The study showed, using robust forward modelling, that whilst the polarimetric entropy and HH backscatter were insensitive to soil moisture changes below forests, a new polarimetric parameter, the Negative Alpha Value, showed strong dependence upon soil moisture. The technique was applied to L-band airborne SAR data, with retrieved soil moisture values for forested areas found to be consistent with soil moisture measurements from nearby open ground. The theory was expanded (Neumann *et al*., 2010) and used with airborne L-band SAR data to recover forest parameters, but not soil moisture. The technique has not been tested with satellite SAR data.

3.7.11. Quite recently, a simplified distorted-Born Approximation model for scattering of P-band microwaves by forests was used to recover both forest biophysical parameters (RMS height and biomass) and soil moisture (My-Linh Truong-Loi *et al*., 2012). The algorithm took into account three significant low-frequency scattering components: volume, double-bounce and surface, and the inversion process used the Levenberg-Marquardt non-linear least-squares method to estimate the structural parameters. The results showed that the inversion process had a root-mean-square error lower than 0.05 vol/vol for soil moisture, 24Mg/ha for biomass and 0.49cm for roughness, considering a soil moisture of 0.4 vol/vol, roughness equal to 3cm and biomass varying from 0 to 500Mg/ha with a mean of 161Mg/ha. This work suggests that P-band observation may be suitable for retrieval of soil moisture.

4. APPROACHES TO RADAR SOIL MOISTURE RETRIEVAL USING TEMPORAL ALGORITHMS

4.1. Change Detection Approaches

4.1.1. Change detection approaches rely on the assumption that extraneous surface properties, including for example, soil texture, roughness and vegetation, exhibit gradual or limited change over time, and so any change observed is assumed to originate from a change in soil moisture (Engman, 1990; Engman and Chauhan 1995).

4.1.2. This approach affords high potential for operational monitoring of soil moisture using single-wavelength/single-polarisation, repeat SAR observations (Engman, 1994). Multi-temporal observations can be used to minimise the effect of vegetation and roughness and so maximise the sensitivity of backscatter to changes in soil moisture (Moran *et al.,* 2006). Naturally many studies have attempted to exploit data from available SAR systems which in the past has generally meant C-band, and in some cases L-band.

4.1.3. The main drawback of change detection approaches is that they provide relative soil moisture change, in the form of an index of "wetness" between two extremes (wet and dry), rather than an absolute soil moisture estimation in terms of volume of water per volume of soil.

4.1.4. Wagner and Scipal (2000) used a multi-year time-series of ERS scatterometer images with a spatial resolution of 50km to develop a library of backscatter behaviour for each pixel. The behaviour of σ° with incidence angle over time was used to determine roughness and vegetation, and normalize σ° to a reference incidence angle of 40°. Relative soil wetness is then estimated by comparing σ° to reference backscatter values for wet and dry soil conditions.

4.1.5. Wickel *et al.* (2001) used 10 RADARSAT images acquired over 1 month to monitor changes in soil moisture in fields of wheat stubble. All images were first corrected for variations in incidence angle. Fields with significant temporal variation in roughness were then identified and excluded. A multi-temporal regression of day-to-day differences in backscattering coefficient and soil moisture was calculated, and achieved a strong correlation ($r^2 = 0.89$).

4.1.6. Lu and Meyer (2002) trialled a similar approach but incorporated both SAR intensity and phase information to initially discriminate changes in soil moisture from changes in surface roughness. Changes in soil moisture were detected ranging from 0.05 - 0.2 vol/vol.

4.2. Time-series Approaches

4.2.1. Time series approaches differ from change detection techniques in that they make use of the temporal information to constrain the retrieval of a time series of absolute volumetric soil moisture rather than a "wetness index". This is done by selecting an opportune observation window so that the other factors affecting the backscatter (roughness and vegetation) can be considered constant, and either ignored all together or retrieved as a constant value over the observation window, depending on the method.

4.2.2. Balenzano *et al.* (2011) investigated the use of dense time-series C- and L-band SAR, acquired by DLR's E-SAR airborne system to map temporal changes in soil moisture content in cropland area. A soil moisture retrieval algorithm was proposed to transform temporal series of backscatter ratios between subsequent days into soil moisture content values. Under the simplifying assumption that the backscatter response is just due to ground response attenuated by vegetation canopy (i.e., volume scattering was not dominant) and that roughness surface is unchanged, it was found that the ratios between backscatter on subsequent days was a simple and effective technique of decoupling vegetation and roughness effects from changes in soil moisture.

4.2.3. The results demonstrate the capacity to retrieve soil moisture over the entire growing season for crops that are relatively insensitive to volume scattering (winter wheat at C-band or winter rape (canola) at L-band for example), with accuracies of 0.05–0.06 vol/vol. Under these circumstances, systematic retrieval of soil moisture would first require a classification step to identify crop classes whose backscatter is not dominated by volume scattering. Extension of the method to multi-polarized data such as for the SMAP mission is currently underway.

4.2.4. Kim *et al.* (2011) used time-series co-polarised (HH and VV) backscatter measurements to retrieve soil moisture and roughness. The approach was based on inversion of a numerical model (Maxwell Model in 3 Dimensions, NMM3D) for bare soil using a pre-computed lookup table (LUT) of σ° derived from numerical Maxwell model simulations. Surface roughness is assumed constant over the time-series and so only one surface roughness RMS height estimate is retrieved, highly reducing the number of retrieved variables and therefore making use of temporal information to constrain the soil moisture retrieval. This approach is the basis of the baseline radar algorithm implemented for the SMAP mission (see Section 6.4).

4.2.5. An RMS error of 0.044 vol/vol for soil moisture was achieved, with a correlation coefficient of 0.89 between estimated and in situ data (Kim *et al.,* 2011). The relative accuracy of surface roughness estimates was found to be 10 – 30 % of in situ measurements.

4.2.6. Kim *et al.* (2011) indicated that application of the time-series method could be extended to vegetated surfaces by including more dimensions in the look-up-table, such as vegetation water content. Initial results show high accuracy estimates of soil moisture content, largely attributed to inclusion of the time-series information which helps mitigate attenuation and surface scattering from the vegetation layer.

4.2.7. Pierdicca *et al.* (2010) demonstrated the retrieval of soil moisture content over cropland using multitemporal radar (AirSAR C-band) and optical (Landsat) images. The approach corrects for incremental vegetation effects and incorporates multi-temporal data within an inversion model based on the Bayesian maximum posterior probability estimator.

4.2.8. The vegetation correction models the variation of that part of the backscattering coefficient due to soil properties as a linear function of the variations with respect to the first time step of the measured backscatter and biomass (Pierdicca *et al.* 2010).

4.2.9. There was good correlation between measured and modelled soil moisture content (correlation coefficient of 0.72, RMSE = 0.036 vol/vol). This presents a reasonable estimation

given the presence of dense canopy cover. Model performance was improved using multi-temporal data as opposed to a single radar acquisition (Pierdicca *et al.* 2010).

4.3. Principal Components Analysis

4.3.1. Principal Components Analysis (PCA) is an established image transformation technique whereby a highly correlated, multi-dimensional dataset is reduced and transformed to a limited set of uncorrelated bands/variables. PCA linearly transforms the data into a new coordinate system, with the axes placed orthogonal to each other (Verhoest *et al.*, 1998). In so doing, the useful components of the data are separated from the noise, and significant spatial patterns in the data are enhanced (Barret *et al.,* 2009). The first principal component (PC) contains the largest percentage of the total variance, and hence highest information content.

4.3.2. The PC method is entirely different from any other method described in that it does not provide an absolute soil moisture or a soil wetness value, but rather a "saturation potential index" based on an assumption of terrain-dominated soil moisture distribuion along a slope (at steady-state). This might be a useful method for providing approximate, large scale soil moisture wetness information long after rainfall events (where soil moisture patterns "tends" to follow the terrain elevation). However it is currently of little value when high-resolution soil moisture dynamics need to be monitored.

4.3.3. Verhoest *et al.* (1998) applied PCA to a winter time-series of 8 ERS-1/2 images acquired in Belgium and found that soil moisture could be separated from other influential factors such as topography and land cover. Effects due to local incidence angle (LIA), land cover and soil moisture were isolated in the first 3 PCs.

4.3.4. The first PC (PC1) accounted for 76.6 % of the total variance, the second PC (PC2) 6.6 %, the third PC (PC3) 5.9 %, and the remaining PCs < 4 %.

4.3.5. PC2 revealed a strong spatial structure, with the highest values clustered along the drainage network (Figure 4.1). Comparison with a drainage map derived from a digital soil map of the catchment revealed that poorly drained soils in the valley correspond well with areas of high PC2 values (Verhoest *et al.*, 1998). This suggested the radar was responding to soil moisture as determined by the drainage characteristics of the basin.

4.3.6. PC1 correlated well with LIA derived from a catchment DEM, indicative of the influence of topography on total variance. PC3 correlated well with Landsat derived land cover, indicative of the influence of land cover and land use on the radar response.

4.3.7. Further research will require testing the robustness of the approach using non-winter images and other test sites.

4.3.8. Kong and Dorling (2008) applied PCA to 12 multi-temporal ASAR wide swath images acquired over a 2-year period (150m resolution) and demonstrated potential for routine monitoring of soil moisture throughout the agricultural growing season and at different levels of roughness and vegetation cover. ASAR VV polarization was selected due to greater capacity for penetration of vegetation compared to HH. Of ASAR's imaging modes, the wide swath mode presents the best compromise due to high temporal revisit capability (3-5 days)

and extensive coverage (400 x 400 km).

4.3.9. PC1 contained the largest percentage of total variance (41.7 %). PC2 contained 14.7 % of the total variance, and was found to be positively correlated with dry days and negatively correlated with wet days. High PC2 values were located near watercourses with sandy soils, and low PC2 values were found on up slopes with clay soils. The spatial patterns in the PCA were consistent with soil moisture and rainfall-runoff dynamics in the catchment (Kong and Dorling, 2008).

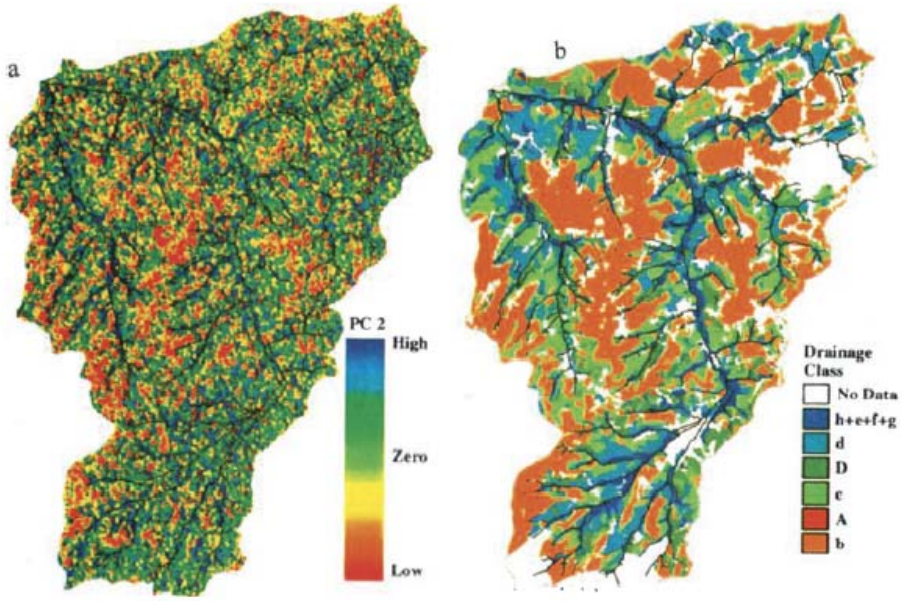

Figure 4.1 Relationship between PCA and soil moisture: a) Second PC image derived from ERS-1/2 data, and b) Catchment drainage map (Verhoest *et al.*, 1998).

4.4. Interferometric Techniques

4.4.1. Repeat pass interferometry (InSAR) was initially developed for topographic mapping purposes. InSAR exploits the phase information of the signal to calculate the interferometric coherence between 2 or more SAR images, providing complementary information to that obtained in the amplitude (Barrett *et al*., 2009). The phase difference calculated from 2 SAR images with slightly different imaging geometries can be used to generate a DEM of the surface.

4.4.2. The application of InSAR to estimating the change in soil moisture has yielded some promising results. Previous studies have demonstrated a correlation between interferometric coherence and relative soil moisture (Borgeaud *et al*., 1996; Wegmüller, 1997; Lu and Meyer, 2002; Zhang *et al*., 2008). The combination of coherence and amplitude may improve the estimation of surface parameters (Ichoku *et al.,* 1998).

4.4.3. Phase decorrelation of the signal occurs due to changes in viewing geometry (baseline) and change in surface scattering between two image acquisitions (i.e., temporal change, Zebker and Villasenor, 1992). Furthermore, both lab and field experiments have demonstrated that

changes in soil moisture lead to decorrelation (Nesti *et al*., 1998; Luo *et al*., 2001; Srivastava and Jayaraman, 2001). Temporal decorrelation is sensitive to the sensor wavelength, and so temporal effects are greater at C-band than L-band (Zebker and Villasenor, 1992).

4.4.4. Hajnsek *et al.* (2002, 2003) used the decorrelation caused by the additive signal-to-noise ratio (γSNR) in two single-pass interferometric images (thereby avoiding temporal decorrelation) to extract surface parameters (soil moisture and surface roughness), and found high sensitivity of interferometric coherence to soil moisture variations, particularly for low roughness values.

4.4.5. Topographic variations and surface displacement also contribute to InSAR phase shifts. By subtracting two interferograms, these two components can be separated out in the process of Differential Interferometry (DInSAR). There are only few studies on the use of DInSAR for estimation of soil moisture (Gabriel *et al*., 1989; Nolan *et al*., 2003a,b; Hajnsek and Prats, 2008).

4.4.6. The interferometric approach has the potential to detect line-of-sight surface height variation on the order of millimetres. However, since a surface generally shrinks as it dries, and the microwave penetration depth also increases, topographic phase changes can potentially be confused with those due to soil moisture.

5. SUMMARY OF APPROACHES TO RADAR SOIL MOISTURE RETRIEVAL

5.1. Statistical Methods

5.1.1. These methods include approaches such as linear regression.

PROS: Simple; do not require *a priori* knowledge of surface conditions.

CONS: Require observation data to train the method; cannot be adapted to conditions different than the training data.

5.2. Model Inversion Methods

5.2.1. These methods include approaches such as empirical, semi-empirical and theoretical models.

PROS: Depends on parameters which can be related (more or less directly) to surface physical properties.

CONS: Validity is restricted to the conditions used for model development. Models must be validated against a wide range of field data. Choice of model requires terrain scattering characterization.

5.3. Data Cube Methods

5.3.1. These methods include the computation of data cubes using highly complex numerical models that cannot be easily inverted.

PROS: Detailed simulation of scattering across a wide range of conditions can be included.

CONS: Numerical models are complex with many parameters and with high computational burden, but the use of pre-computed data cubes reduces the burden. Models must be validated against a wide range of field data.

5.4. Polarimetric Methods

5.4.1. These methods include the use of data with multiple polarisations.

PROS: Requires no or limited *a priori* knowledge of surface conditions; can provide ancillary estimates of surface parameters other than soil moisture (e.g., roughness). Provides additional information for land cover scattering classification for inversion model choice, permits separation of scattering mechanisms and isolation of surface backscattering components, particularly when combined with interferometry, provides better separation of the effects of surface roughness from soil moisture, even with dual (HH,VV) polarimetry, provides observables sensitive to soil moisture and invariant to LOS rotation.

CONS: Requires proper radar cross-channel amplitude and phase calibration accuracy.

5.5. Interferometric Methods

5.5.1. These methods include the use of interferometric analysis using two images observed from slightly different vantage points, either from the same pass or from a repeat pass in a different orbit.

PROS: Requires no or limited *a priori* knowledge of surface conditions; can provide ancillary estimates of surface parameters other than soil moisture (e.g., roughness); is sensitive to even weak ground scattering under vegetation cover.

CONS: Requires fine radar cross-channel amplitude and phase calibration accuracy when used polarimetrically. Repeat coherence affected by temporal decorrelation e.g. changing Faraday rotation between observations.

5.6. Change Detection Methods

5.6.1. These methods typically include use of a long time sequence of observations for a single polarisation combination to determine maximum and minimum values that represent the wet and dry extremes. These are then used to interpolate intermediate values.

PROS: Require limited *a priori* knowledge of surface conditions.

CONS: Provides relative soil wetness rather than absolute soil moisture; requires stability of surface conditions (i.e., scattering mechanism) during the observation period.

5.7. Time Series Methods

5.7.1. These methods include the use of fully polarimetric data across a sequence of dates, ideally representing a variation in moisture conditions over a relatively short period of time.

PROS: Any method capable of yielding a soil moisture estimate from a single observation can be incorporated into a time-sequence method. Requires limited *a priori* knowledge of surface conditions; can provide ancillary estimates of surface parameters other than soil moisture (e.g., roughness).

CONS: Requires stability of surface conditions during the observation period if constant roughness is to be assumed during the observation window, although this assumption is not essential (see Section 7).

6. CURRENT METHODS PROPOSED FOR RADAR SOIL MOISTURE RETRIEVAL

6.1. SMAP Radar Soil Moisture Retrieval Algorithms

6.1.1. The SMAP mission is expected to provide a 3km spatial resolution soil moisture product globally with a 3 day repeat. The SMAP satellite is currently carrying several optional soil moisture algorithms for its radar products, according to its radar-only ATBD (L2_SM_A, Kim et al., 2012). It is not expected to make a final choice until some point after launch, when it is had the opportunity to conduct some initial validation studies

Snap Shot Retrieval

6.1.2. The SMAP radar has three L-band measurement channels (HH, VV, HV) from which soil moisture can be estimated using a single acquisition. The estimation of soil moisture is an inversion of forward models facilitated by the data cubes. The estimation is challenging, because there are many parameters in the forward models that are unknown (or uncertain) *a priori* (e.g., s, ε_r, l and VWC), and must therefore be estimated as part of the retrieval, or be provided through ancillary data.

6.1.3. SMAP researchers believe that soil moisture retrievals are insensitive to errors in knowledge of the correlation length over a wide range of soil moisture, roughness, and correlation lengths (Kim *et al*. 2012b). An exponential correlation function that describes empirical measurements (Mattia *et al*. 1997; Shi *et al*. 1997) has been chosen, and is not considered as an unknown during the retrieval.

6.1.4. With three measurement channels, the largest number of free parameters that can be estimated is three. For SMAP, the three parameters chosen are dielectric constant (equivalently, soil moisture), soil surface roughness height, and vegetation water content.

6.1.5. The impact of vegetation structure is accounted for by development of separate models for different land cover classes: evergreen, deciduous broadleaf, and needle forests; mixed forests; closed and open shrub lands; woody savannahs; savannahs; grasslands; wheat/rice; corn/soybean croplands; cropland/natural vegetation mosaics; and barren or sparsely vegetated areas.

6.1.6. The complexity of the non-linear forward models precludes a closed-form analytical solution. Direct numerical inversion of a complicated forward model is also not feasible for global soil moisture retrieval at 3 km resolution. However, a lookup table representation of a complicated forward model was demonstrated to be an accurate and fast approach for retrieval (Kim *et al*. 2012b). Because the SMAP radar has three measurement channels, and

three primary retrievables (dielectric constant, surface roughness, and vegetation water content), the forward models can be pre-computed for a given land surface class, for discrete values covering the full range of the three parameters, and represented as a "data cube" (Kim *et al*. 2012a; van Zyl 2011). Merits of the data cube search are summarized below:

- avoid numerical or analytical inversion that is often not feasible for a sophisticated forward model (Moghaddam *et al*. 2000);
- achieve the same inversion accuracy as the numerical or analytical inversion by adopting a fine interval for the data cube axis, as demonstrated in van Zyl (2011);
- conveniently replace and update a forward model while retaining the same retrieval formulae.

6.1.7. One vegetation axis represents the vegetation structure and dielectric properties by an allometric equation relating volume to weight of the vegetation. The representation of vegetation effects is clearly a simplification, considering that numerous vegetation parameters produce different backscatter coefficients. However, the axis dimension cannot be too large, and for "snapshot" retrieval options the dimension cannot exceed the number of independent observations. This simplification will result in errors in the soil moisture retrieval.

6.1.8. Only the real part of the complex relative permittivity is used, to keep the number of unknowns to 3. It is assumed that the imaginary part of the dielectric constant can be directly related to the real part for specific soil texture information. The results remain dependent on both real and imaginary parts of the permittivity, particularly for cases when the real part of the soil dielectric constant is less than 5.

6.1.9. The data cube for the grass surface, developed by the Univ. Washington, is shown as an example in Figure 6.1. The data cube has the NMM3D simulation for the surface backscatter and the Body of Revolution model for vegetated contributions.

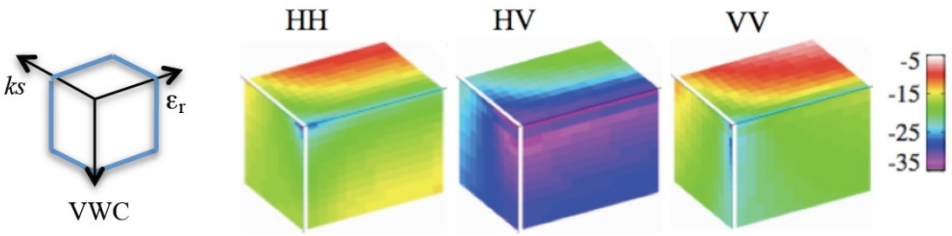

Figure 6.1 Data cubes of σ_0 (backscattering coefficient) for a grassy surface (units dB m^2/m^2). The ks axis ranges from 0.03 to 1.1, the real part of permittivity axis from 3 to 30, and the vegetation water content (VWC) from 0 to 3kg/m^2.

6.1.10. The snapshot retrieval over the pasture surface was found to be poor, showing a retrieval error of 0.105 vol/vol, which indicates that effects of the overlying vegetation have not been

properly compensated. The evaluation results suggest the limited applicability of the snapshot retrieval.

6.1.11. The SMAP algorithm research team report that a new algorithm to estimate bare surface soil moisture using dual-polarization L-band backscattering measurements, proposed in Sun *et al*. (2009), is being adapted for snapshot retrieval over vegetated surfaces. This algorithm uses a semi-empirical model to describe the backscattering coefficients as a product of two functions: a dielectric function that reflects the soil moisture information approximated by the polarization magnitudes as described by the Small Perturbation Model at L-band, and a roughness function that describes the overall effects of the surface roughness at the different polarizations. The relationship between the HH and VV surface roughness parameters is required for the algorithm to be of use. Estimates of the HH VV surface roughness parameter have been obtained using AIEM forward modelling for a wide range of soil moisture and surface roughness conditions.

6.1.12. Initial versions of all of the 16 data cubes are currently available, but with limited validation using existing *in situ* observations. Because "forward model" error is a key concern for SMAP radar soil moisture retrievals, validation of the data cubes will continue throughout the calibration validation period.

6.1.13. The backscatter coefficients of data cubes do not include the "Kp" noise; multiplicative Gaussian random noise with a magnitude of 0.9 dB (1-sigma) is anticipated that includes speckle (0.7dB), relative calibration error (0.35dB), and contamination from radio frequency interference (0.4dB). Application of the noise-free data cubes to the noisy SMAP data will result in retrieval errors and the errors are included in the retrieval error budget.

Time-series Retrieval

6.1.14. The SMAP baseline approach (Kim *et al*. 2012a,b) is a multichannel time-series retrieval algorithm that searches for a soil moisture solution such that the difference between computed and observed backscatter is minimized in the least squares sense.

6.1.15. The algorithm retrieves s, and then the real part of dielectric constant (ε_r), using a time series of N co-polar backscatter measurements. There are thus 2N independent input observations and N+1 unknowns, consisting of N ε_r values and one s value (since s is presumed not to change over the period of the 2N observations). The VWC is permitted to vary throughout the time series.

6.1.16. The least-square minimization of the cost function is implemented using forward model lookup tables or "data cubes", which are interpolated values of forward model outputs for a wide range of soil moisture, RMS height and VWC values.

6.1.17. Vegetation effects are included by selecting the forward model's σ° at the VWC level given by an ancillary source, or using the SMAP radar HV measurements.

6.1.18. Another change detection approach is also under development (Kim and van Zyl, 2009). After the SMAP radar data are accumulated for a moderate time period, nominally six months, an expression will be derived to relate the backscattering cross section to soil moisture. This expression will depend on the biomass level, and the cross-polarization will be used to compensate the biomass variation over time: how this will be implemented is

being studied.

6.1.19. Hajnsek (2009) and Neumann (2010) have already indicated how to isolate volume scattering from fully polarimetric L-band data. Woodhouse (2010) has used the PolInSAR ground-to-volume scattering ratio to estimate biomass, and My-Linh Truong-Loï (2012) has demonstrated recovery of soil moisture and forest parameters using a model-based approach with L-band quad-pol data. It is likely that these approaches will also be tested.

6.1.20. In addition to the use of time-series observations coupled with large-scale forward modelling exercises and field testing, the SMAP algorithm developers are also considering use of the change detection method employed for ASCAT data (Wagner *et al*. 1999a/b/c; Wagner and Scipal, 2000; Wagner *et al*., 2003).

6.1.21. The proposed time series SMAP soil moisture retrieval algorithm flow (L2_SM_A, Kim et al., 2012) is presented in Figure 6.2.

6.1.22. The portion of the flowchart through the land surface classification is the initial processing done as a precursor to the actual retrievals. The L2_SM_A processor reads in 1km resolution σ° from the SMAP L1C_S0. The 1km data in natural units are aggregated onto the km EASE grid, during which various quality flags are applied. Three quality flags are derived using the 3 km σ°: freeze-thaw state (see L3_FT_A ATBD), radar vegetation index, and transient water body. Static and dynamic ancillary data are sampled for each pixel of the L2_SM_A product. The σ° values from the past time are sampled and used by the time-series algorithm. For each 3 km pixel, land cover class information is obtained from the mostly annual ancillary data. The land cover information allows the choice of an appropriate data cube for each pixel. The retrieval over the different land cover classes is spatially assembled to create a half-orbit output, followed by the conversion from the dielectric constant to soil moisture.

Algorithm Evaluation

6.1.23. Preliminary field tests have used two data sets. The first test data were measured by a truck-mounted scatterometer at 1.25GHz and 40° incidence angle over four bare surface sites during a two-month period, with up to 11 temporal samples per site (Oh *et al*. 2002). The second test data were collected by the airborne Passive/Active L-band Sensor (PALS) instrument at 1.26GHz at the incidence angle centred at 38° during the 1999 Southern Great Plains (SGP99) experiment over the Little Washita Watershed near Chickasha, Oklahoma (Jackson and Hsu 2001; Njoku *et al*. 2002).

6.1.24. The snapshot retrieval algorithm was tested with the two sets of field campaign data and showed that the bare surface retrieval had an RMSE of 0.055 vol/vol. It was also found that the retrieval error increased for larger soil moisture.

6.1.25. The time series interpolation tables or “data cubes” generated for SMAP have also been tested against field observations in order to provide estimates of accuracy for subsequent soil moisture retrievals.

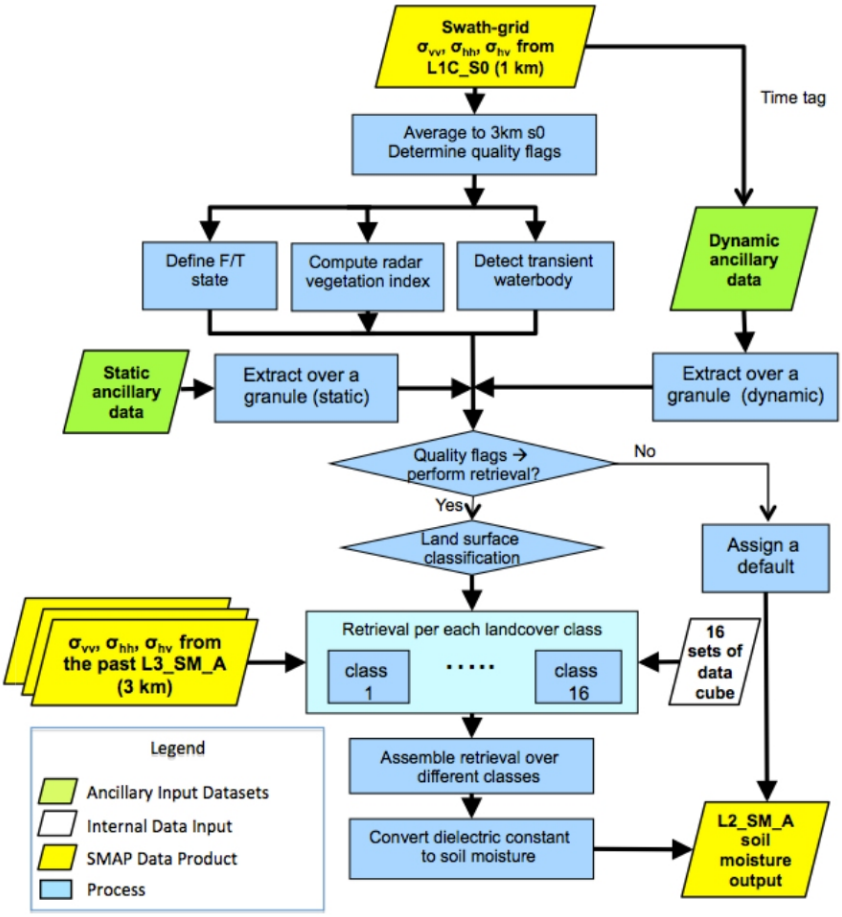

Figure 6.2 Proposed SMAP soil moisture retrieval algorithm L2_SM_A (Kim *et al.*, Algorithm Theoretical Basis Document SMAP L2 & L3 Radar Soil Moisture (Active) Data Products).

6.1.26. The VWC varied from site to site between 0.16 and 2.5kg/m^2. Temporally the roughness, correlation length and VWC remained constant throughout the test periods. The bare surface retrieval has an RMSE of 0.044 vol/vol after compiling the retrievals over the 4 *in situ* locations. The time-series retrieval over the pasture surface has an RMSE of 0.054 vol/vol. The slightly larger error for the pasture surface may reflect the effect of vegetation.

6.1.27. For each field of the 1999 Southern Great Plains (SGP99) experiment, a constant offset in terms of dB was estimated to minimize the difference between observed backscatter and predicted backscatter using the time series of co-pol backscatter observations. The SMAP research team considered this to be associated with a bias in the data cube predictions associated with the vegetation scatterer density. The existence of this bias is of some concern as it might suggest a systematic error in the forward modelling process.

6.1.28. That new soil moisture algorithms for general or global retrievals are still under development at this stage speaks loudly to the difficulty of designing a single algorithm to work for a wide range of natural soil conditions.

6.2. Sentinel-1 Soil Wetness Retrieval Algorithms

6.2.1. The Sentinel-1 mission is expected to provide a 1km spatial resolution soil wetness product globally with a 6 day repeat. A number of institutes worldwide are engaged in algorithm development, which has focussed on adaption of the TU Wien change detection method that has been applied to ASAR (Hornacek *et al*., 2012a).

Change Detection Retrieval

6.2.2. The improved temporal and radiometric resolution (0.05 - 0.07dB when aggregated to 1km) and Interferometric Wide Swath (IWS) imaging mode afforded by Sentinel-1 are key to the potential for global monitoring of surface soil wetness.

6.2.3. The TU Wien method to be used was originally developed for ERS scatterometer data, and later adapted to MetOp ASCAT and ENVISAT ASAR data (Hornacek *et al.* 2012b). The basic idea behind the change detection algorithm is to attribute natural surface backscatter changes over short timescales mainly to variations in soil moisture, while assuming that vegetation or surface roughness are assumed to be constant or only slowly varying (Kim and Van Zyl, 2009).

6.2.4. The algorithm is as follows:

$$\sigma°(m_v,t) = \sigma°_{dry}(\theta_{char}) + Sm_s(t) \qquad \text{(Eq. 3)}$$

where $\sigma°(m_v,t)$ are backscatter measurements in dB, $\sigma°_{dry}(m_{v\ char})$ is the dry reference backscatter at characteristic local incidence angles, and $m_s(t)$ is the surface soil moisture at time t.

6.2.5. Surface soil water saturation is thus retrieved by:

$$m_s(t) = [\sigma°(\ m_v,t) - \sigma°_{dry}(m_{v\ char})\ ]/\ S \qquad \text{(Eq. 4)}$$

6.2.6. The sensitivity S to changes in surface soil moisture is estimated by the observed dynamic range $\sigma°_{wet}(m_{v\ char})$ - $\sigma°_{dry}(m_{v\ char})$ of backscatter measurements at the location under consideration, where $\sigma°_{wet}(m_{v\ char})$ is the wet reference at θ_{char}.

6.2.7. The respective references with respect to characteristic incidence angle could be obtained and stored per gridpoint of a global grid at 1km resolution (Hornacek *et al*., 2012). HH polarisation is preferred due to greater penetration of vertically oriented vegetation (e.g., grasses and crops).

6.2.8. Retrieval error is determined by the noise of the IWS mode and uncertainties in model parameters.

6.2.9. The proposed near real time soil wetness processor (S2M-NRT) is illustrated in Figure 6.3. Requisite pre-computed model parameters corresponding to the input 1 minute DEM-geocoded IWS mode ground-range multi-look detected (GRD) slice at 1km resolution are

identified. Requisite model parameter tiles are mosaicked and resampled to the grid of the input geocoded slice. Using the input backscatter and reference measurements, surface soil water saturation is computed for every pixel of the input slice.

6.2.10. A binary mask (flag image) is also generated as an indication of the reliability of the soil wetness product. Certain land cover classes are flagged as they are not suited to retrieval. These include urban, evergreen broadleaf forest, water bodies, barren or sparsely vegetated, snow or ice. Pixels are also masked if temporal correlation between DEM-geocoded backscatter at 1km and aggregated coarser scale measurements (25km) lies below a defined threshold.

6.2.11. The Institute of Photogrammetry and Remote Sensing (IPF), TU Vienna, has, through the ESA DUE TIGER SHARE project, developed operational processing chains for deriving 1km resolution soil wetness products using ENVISAT ASAR ScanSAR data. The method is similar to that described above for use in Sentinel-1 using HH polarisation data (Pathe *et al.,* 2009).

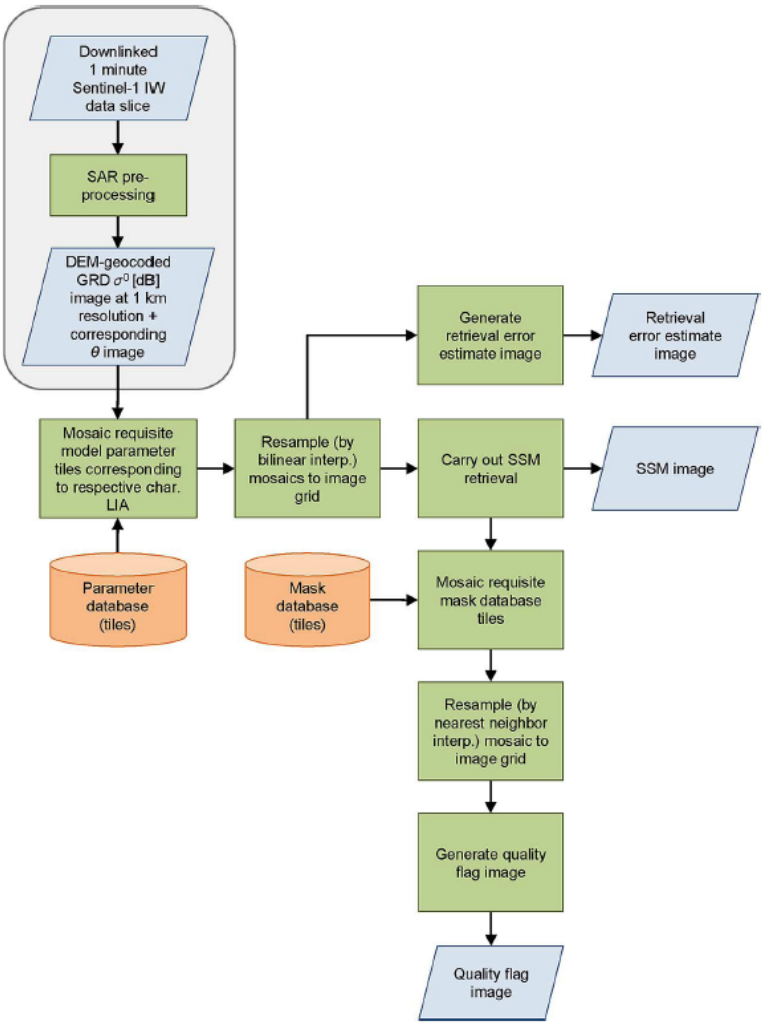

Figure 6.3 Processing chain of the proposed NRT soil wetness processor (S2M-NRT; Hornacek *et al*., 2012).

6.2.12. The model is quite simple in that all model parameters are derived directly from the ASAR time-series for each pixel (Wagner *et al.,* 2009).

6.2.13. Demonstration of the method over a 181,182km^2 area (697 ASAR GM images) in Oklahoma revealed that the retrieval error was dominated by the high noise level of the ASAR GM backscatter measurements (1.2dB). Comparison against 1km aircraft data showed almost no skill at less than 10km spatial resolution (Mladenova et al., 2011).

6.2.14. The improved spatial, temporal and radiometric resolution of Sentinel-1 IW mode and addition of cross-polarised channels (HV or VH) should make for a straightforward transfer of the ASAR GM change detection method to Sentinel-1, with some improvements (Wagner *et al.,* 2009).

6.2.15. Doubkova *et al.* (2012) evaluated the ASAR GM soil wetness error product using independent soil wetness estimates derived by the grid-based landscape hydrological model (AWRA-L), part of the Australian Water Resources Assessment system (AWRA). Predicted and computed RMSE showed a high level of spatial and quantitative agreement. The RMSE was predicted within accuracy of 0.04 vol/vol of saturated soil moisture over 89% of the Australian continent (Doubkova *et al.*, 2012). The error estimates promote confidence in the retrieval error model and derived error estimates.

6.2.16. Given the similar configuration of ASAR GM and Sentinel-1, it would appear that a similar retrieval error estimation method can be applied (Doubkova *et al.*, 2012). With the improved radiometric resolution of Sentinel-1, soil moisture estimation errors are likely to be an order of magnitude less than ASAR GM however.

Time-Series Retrievals

6.2.17. Balenzano *et al.* (2012) applied the "Soil MOisture retrieval from multi-temporal SAR data" (SMOSAR) algorithm to dense time-series ASAR data acquired over study sites in Germany and Italy. SMOSAR was developed within the framework of the ESA GMES Sentinel-1 soil moisture algorithm development project.

6.2.18. The SMOSAR algorithm demonstrates the capacity to monitor soil moisture in agricultural landscapes throughout the growing season for crops not dominated by volume scattering. This is achieved through inversion of temporal changes of radar backscatter, rather than absolute backscatter values (Balenzano *et al.*, 2012).

6.2.19. Given a dense time-series of SAR data (revisit time of 6-12 days), the SMOSAR algorithm is applied under the assumption that the backscatter change between two acquisitions is largely related to the change in soil moisture, rather than a temporal change in vegetation biomass or surface roughness (typically incurred over a few weeks).

6.2.20. The prototype processing chain for SMOSAR is shown in Figure 6.4. Dense time-series single or dual polarised C-band SAR images are transformed into time-series soil moisture maps over agricultural sites. Ancillary land cover and soil textural information are required. Overall accuracy, and accuracy as a function of spatial resolution, polarisation and site location, are computed.

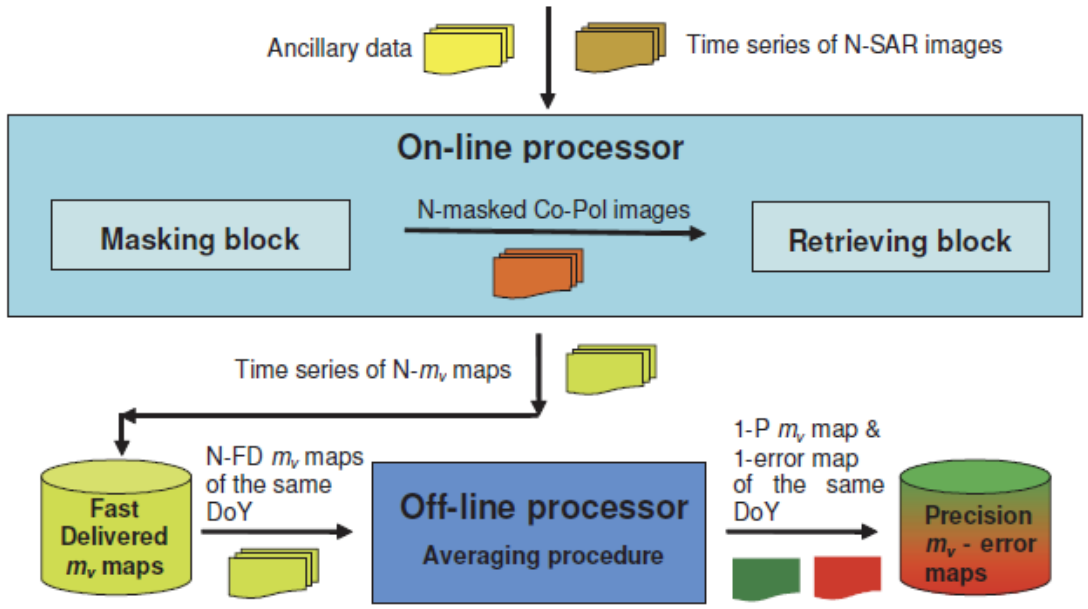

Figure 6.4 Prototype SMOSAR processing chain (Balenzano *et al.*, 2012).

6.2.21. Soil moisture can be retrieved with an accuracy of 0.05 vol/vol at HH polarisation. The results support the future use of time-series Sentinel-1 data for soil moisture estimation at high spatial resolution.

Artificial Neural Network and Bayesian Retrievals

6.2.22. Paloscia *et al.* (2012) proposed two approaches to soil moisture retrieval in light of future Sentinel-1 acquisitions and near real time processing. The first approach was based on Artificial Neural Network (ANN) retrieval from sing acquisitions, and represented the best compromise between retrieval accuracy and processing time. The second approach was based on Bayesian Maximum Probability (MAP) using multi-temporal processing, which allowed for increased retrieval accuracy at the cost of processing time.

6.2.23. The ANN comprised a feed-forward multilayer perceptron with two hidden layers. Archive bare soil backscatter and ground measurements available from previous experiments, and data simulated using the IEM and Oh models were used to train the ANN. Input parameters included randomly variable incidence angle (20-50°), standard deviation of soil height (1-3cm), correlation length (4-8cm) and dielectric constant (5-45). Around 10,000 iterations were run to produce a set of backscattering coefficients for each soil parameter set.

6.2.24. Vegetation effects were taken into account by simulating the backscatter as a function of soil backscatter and the VWC using the Water Cloud Model. VWC was related to NDVI using a semi-empirical relationship. The model was iterated 10,000 times to obtain a set of backscattering coefficients for each soil and vegetation parameter set. This dataset was used to train a new ANN. An RMSE of 0.0093 vol/vol was obtained for HH polarisation. Worse results were obtained using VV polarisation, with an RMSE of up to 0.029 vol/vol.

6.2.25. In the case of dual polarisation images, and in the absence of NDVI, the ratio between cross- and co-polarised backscattering coefficients (polarisation ratio, PR) showed good sensitivity to vegetation. Re-training the ANN resulted in an RMSE of 0.013 vol/vol for retrieved soil moisture.

6.2.26. Using the Bayesian approach, time-series radar data was integrated with the retrieval algorithm based on Bayesian Maximum Posterior Probability (MAP) statistical criterion (Paloscia *et al.*, 2012). A quality index was computed for each soil moisture estimate in the process. A simulation was run comprising input time-series backscatter measurements of bare soil derived from Oh's model, randomly variable soil moisture and speckle noise derived from multi-looking. Both RMSE and R^2 were significantly improved using a time-series of around 4 - 6 images.

6.2.27. Pierdicca and Pulvirenti (2012) outline an operational system for implementation of the multi-temporal MAP algorithm, as illustrated in Figure 6.5.

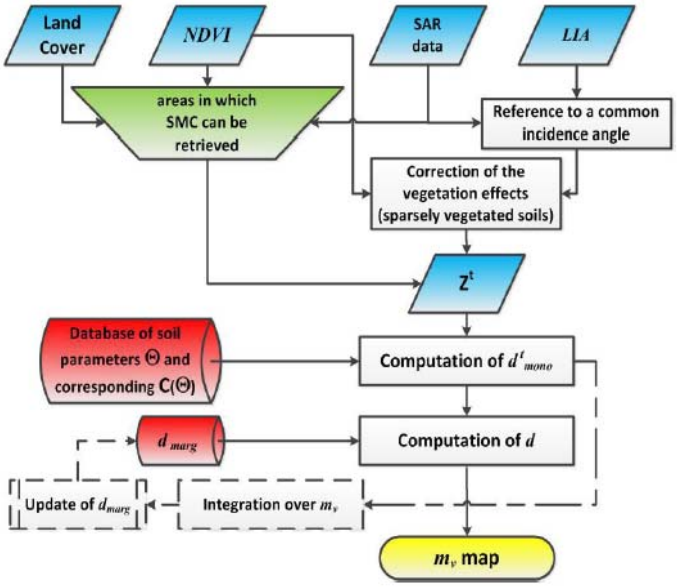

Figure 6.5 Processing chain for multi-temporal MAP algorithm (Pierdicca and Pulvirenti, 2012).

6.3. SAOCOM Soil Moisture Retrieval Algorithms

6.3.1. The SAOCOM mission is expected to provide a 700m spatial resolution soil moisture product for select regions on an operational basis with a 6 day repeat. However, little detail is available on the SAOCOM retrieval algorithm, and there are no ATBD's in the public domain.

6.3.2. The contributions to backscattering coefficient from soil permittivity, surface roughness and vegetation cover at specific incidence angles and wavelength (L-band) will be developed from field experiments over the Pampa's region. Simulations will be performed using the Peplinsky-Dobson and Topp's dielectric models (Frulla *et al*., 2011).

6.3.3. Similarly to SMAP, numerical forward models will be used in the simulations to generate

data cubes for each vegetation type. The more robust algorithms are expected to be those that use co- (HH and VV) and cross-polarized (HV) backscattering coefficients. For bare soil or low vegetated surfaces the data cubes flatten to planes (Frulla *et al.*, 2011). In such cases SAOCOM analysis will apparently use only the backscattering coefficient from the two co-polar inputs, although there are good arguments for using cross-polar returns, since co-polar ratios are terrain-orientation dependent, whereas coherency matrix element ratios are line-of-sight rotation independent (Hajnsek *et al.*, 2003; Williams, 2008; Lee *et al.*, 2000). The proposed architectural design of the SAOCOM soil moisture processor is presented in Figure 6.6 (Frulla *et al.*, 2011).

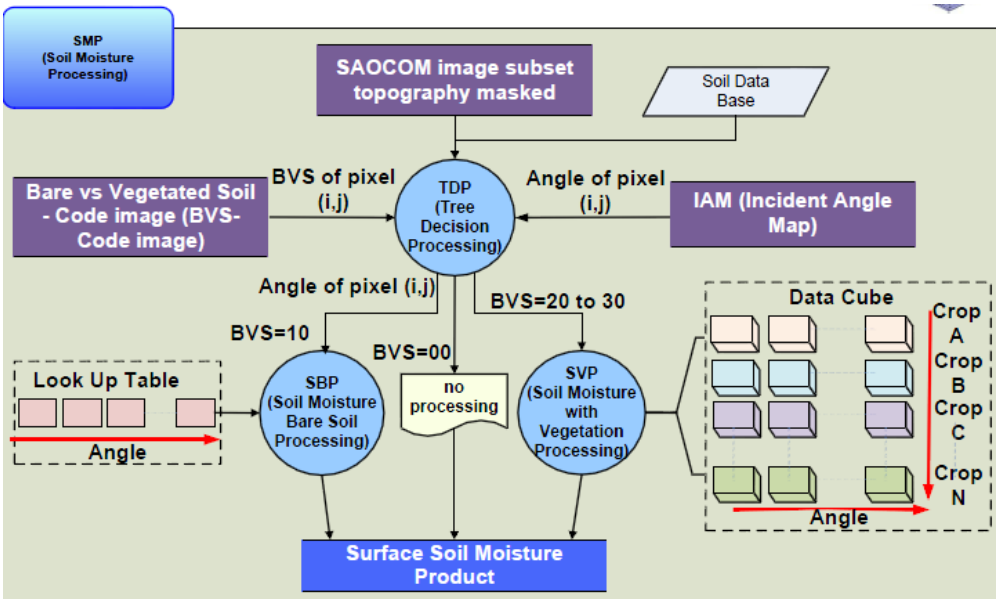

Figure 6.6 Architectural design of SAOCOM soil moisture product retrieval (Frulla et al., 2011).

7. RADAR SOIL MOISTURE RETRIEVAL ALGORITHM RECOMMENDATION

7.1. Overview

7.1.1. For soil moisture retrieval, microwave remote sensors are clearly preferred over optical and thermal sensors, as they are largely unaffected by cloud cover, haze, rainfall, and aerosols, and respond to the soil properties even in the presence of vegetation, rather than simply vegetation colour or temperature.

7.1.2. In order to achieve spatial resolutions better than 10's km, radar rather than radiometer approaches are required. However, radar is more affected by soil roughness and vegetation than radiometers, typically resulting in a lower accuracy for derived soil moisture content.

7.1.3. The higher spatial resolution of radar as compared to radiometers yields challenges to achieve high temporal repeats from a single satellite. The use of multiple satellites results to achieve temporal repeat requirements can result in calibration challenges, especially for time-series and change detection approaches, where high relative calibration accuracies between the multiple sensors is required.

7.1.4. A major limiting factor in the quantitative estimation of soil moisture is separation of the individual scattering effects from surface roughness and vegetation. Moreover, the return signal is not only a function of the physical and electrical properties of the target, but also of the wavelength, polarisation and incidence angle of the radar sensor.

7.1.5. Several general conclusions can be drawn from the preceding review.

7.2. General Observations

7.2.1. Forward modelling has a role to play in soil moisture retrieval algorithm development, but only when supported by field campaigns. Of the tractable approximate theoretical models available, the IEM offers the widest range of validity and can be used to help generate a database of backscattering coefficients characterised by surface roughness and soil moisture values. Numerical surface scattering calculations have an additional role to play in this regard. Models must properly account for the true multi-scale nature of i) natural surfaces and ii) artificial surfaces such as ploughed fields. The models must also account for both the attenuation due to vegetation and the scattering by vegetation over a wide range of frequencies.

7.2.2. If radar is to be used on an operational scale for soil moisture mapping, then soil roughness parameterization through in situ measurement is not an option. This can be circumvented using techniques that either i) do not require information on surface roughness (e.g., change detection techniques), or ii) characterize the surface roughness (e.g., time-series techniques, polarimetry, multi-angle viewing, laser scanning).

7.2.3. Frequency choice is important, and high frequencies (C-band, X-band or higher) are not appropriate for direct retrieval of soil moisture (although they may have a partial role in land cover discrimination in a retrieval algorithm) since the backscatter at these frequencies shows significant dependence upon surface roughness and is strongly influenced by vegetation. At lower frequencies (L-band and perhaps S-band, although little experimental evidence is available for S-band), the surface roughness effects on backscattering decouple from soil moisture effects, and the impact of vegetation on the signal decreases, making soil moisture retrieval more reliable. At even lower frequencies (P-band and lower), surface backscattering coefficients decrease and RFI become more prevalent. This reduces signal to noise, and impedes biophysical parameter recovery. Furthermore, for space-based observation, the effects of Faraday rotation are increasingly important at lower frequencies, and this introduces another source of error into soil moisture retrieval algorithms. However, for heavily vegetated areas, for example below dense forests, P-band may offer the only option for soil moisture retrieval. For moderately vegetated areas L-band is most appropriate.

7.2.4. Multichannel data yield better results than single channel observations. If only single channel polarization data are available then HH may be preferred as it appears more sensitive to soil moisture. However, with only a single polarization channel it is not possible to separate the effects of soil moisture and roughness without multi-temporal observations, and only then with the assumption of constant soil roughness. At minimum one would anticipate measurement of both HH and VV linear polarization scattering amplitudes. A system designed for dual co-polar operation, that can transmit and receive in both H and V

polarizations, is inherently capable of fully polarimetric (FP) operation (although there may be associated design costs for FP). Full polarimetric operation is required for polarimetric calibration even if only the co-polar channels are to be used in soil moisture retrieval. However quad polarization (FP) operation is recommended over dual co-polar operation as it permits better soil/vegetation discrimination and correction for terrain slope effects. Measurement of the full complex scattering matrix in any polarization basis permits synthesis of the scattering matrix in all polarization bases and makes accessible algorithms that use (for example) linear polarization scattering amplitudes from measurements of (say) circular scattering amplitudes. If fully polarimetric operation represents too high a cost, then hybrid "compact" polarimetric modes (in particular transmit circular, receive linear H and V) offer an advantage over traditional dual polarimetric systems which record a co-polar and cross-polar return, which latter is low for rough surfaces.

7.2.5. Terrain effects have received little attention in the literature, yet it is clearly understood that terrain slope alters, and mixes, the scattering amplitudes (Lee *et al*., 2000). If fully polarimetric data are used to recover Line of Sight (LOS) rotation independent quantities, such as polarimetric coherency matrix eigenvalues, and soil moisture content retrieval is based on these, then terrain slope effects can be safely ignored. However, if only co-polar channels are to be employed then terrain slope must be accounted, in addition to local incidence angle, which is itself LOS rotation independent. How this may best be achieved without measuring the response in the full polarimetric basis would be the subject of additional research.

7.2.6. Multi-temporal data lead to improvements in the performance of soil moisture retrieval algorithms over that observed with single acquisition data. Repeat observation intervals on the order of 2-3 days or less are desirable. Whilst multi-temporal, single polarization channel data may permit change detection of soil moisture content, this is only possible with some underlying assumption regarding soil roughness stability. In general, multi-temporal data incur variation in local incidence angle at the pixel level. Corrections for incidence angle effects are indicated for multi-temporal data, and such corrections are best achieved with multi-channel polarimetry.

7.2.7. The inversion of soil moisture content from multichannel and multi-temporal signals can be achieved through the use of trained neural networks or look-up tables constructed with a combination of forward modelling and observation. In order to use these approaches the land cover must first be categorised into classes wherein the scattering effects of overlying vegetation can be quantified and corrected, at wavelengths for which the effects of vegetation are not severe. Data cube construction and/or neural network training must be done for each of the classes, and the forward and/or numerical models used must be of high fidelity, capable of accurately predicting the effects of combined soil surfaces and a wide variety of vegetation, under different conditions, imaged at different frequencies, polarizations, resolutions and incidence angles.

7.2.8. Scale is still an issue using radar, which at low resolution can compound the effects of multi-scale processes, e.g., topography, surface roughness and soil moisture variations and vegetation effects at different spatial resolutions. It is difficult to characterise surface roughness at "field" scales because of spatial variations/spatial heterogeneity of soil parameters, in addition to the fact that soil surface characteristics may be non-stationary or self-similar, thus presenting a limitation to bio-physical parameter retrieval using satellite

imagery. At large scales or low resolutions, pixel values are averages and local surface roughness and soil moisture variability are obscured, which is limiting for hydrological applications. Further studies are needed on the application of filtering and averaging techniques to address the scale issue.

7.2.9. Active microwave remote sensing with SAR is capable of providing much finer resolution than passive microwave remote sensing. However passive microwave measurements are not redundant, and can be used to i) constrain soil moisture content retrievals based on active measurements, and ii) provide estimates of the Faraday rotation angle to correct fully polarimetric SAR measurements at lower (L-band and below) frequencies. Although total electron content (TEC) estimates, and hence Faraday rotation estimates, are available from different sources, correction of the effects of Faraday rotation is only possible (without the need for additional targets) if the complete scattering matrix is measured. Compact polarimetric modes, in particular transmit single circular and receive dual linear modes, are attractive since they imply enhanced swath coverage and reduced power requirements. Estimation and correction of Faraday rotation for compact polarimetric SAR appears possible, but requires three different target types and orientations, and places strict requirements on the transmit channel imbalance which cannot be corrected after transmission.

7.2.10. Based on the preceding literature review and case studies, and the general observations listed above, the following recommendations for a soil moisture retrieval algorithm are made.

7.3. Algorithm Recommendations

7.3.1. A combination of fully-polarimetic, passive and active microwave remote sensing is recommended: with synthetic aperture radar operating at S-band to L-band for bare soil surfaces, at L-band for moderately vegetated areas, and between L-band and P-band for forests. Bandwidth and other SAR system design considerations are the subject of Section 8. If constraints prohibit the use of fully polarimetric data then compact polarimetric operation should be considered with circular transmit and linear receive combinations.

7.3.2. The algorithms should closely follow those proposed for SMAP and SAOCOM missions, and combine multi-temporal observations at intervals of 2-3 days in order to properly sample the dynamics of soil moisture variation.

7.3.3. The channel backscatter complex amplitudes should be measured and if required adjusted for terrain slope either estimated through polarimetry, or using the best available DEM and knowledge of the imaging geometry.

7.3.4. The SAR instrument requires careful calibration. The data calibrations, radiometric and polarimetric, should be validated using external targets and monitored regularly. Faraday rotation should be estimated for each observation and correction made for this in the scattering (and emission) amplitudes.

7.3.5. The measured scattering amplitudes should be converted to backscattering coefficients using the best available DEM. These in turn should be subject to terrain illumination

correction, which should in addition generate a local incidence angle layer. Polarimetric coherency matrices should be estimated from single look complex data along with the backscattering coefficients, as soil moisture retrieval will use these where available. The information derived from decomposition of the coherency matrix could be used in several ways: i) un-supervised classification of land surface scattering mechanism for each pixel, for pre-classification of land cover and categorization of retrieval cases (e.g., agricultural land, urban areas, water bodies); ii) aid the selection of the appropriate forward modelling hyper-cubes based on vegetation structure information; iii) direct estimation of vegetation parameter inputs of the hyper-cubes, such as vegetation water content, mean angle of scatterer orientation or scatterer density, iv) detect sudden surface changes (e.g., tillage, harvest) that could be disruptive to the accurate retrieval of surface parameters, and v) direct inversion of soil moisture and surface roughness for bare surfaces, and from corrected coherency matrix information for vegetated surfaces.

7.3.6. Observations and all available auxiliary data should be used to recover land cover classifications for selected scattering classes in order that the effects of vegetation on the returned signal may be estimated and corrected. This stage could involve decomposition techniques that affect an estimation of vegetation cover simultaneously with the estimation of the surface contribution to polarimetric coherency. These techniques are model-based and will require considerable development, particularly in the case of forested areas.

7.3.7. Forward modelling and field observation should be used to create data (hyper) cubes, which now include the variation in both (terrain normalized) backscattering coefficients and quantities derived from the polarimetric coherency matrices. The hyper-cubes will characterize the variation of these observables in terms of, as a minimum, soil permittivity, roughness (ks), vegetation (vector of attenuation and scattering parameters) and incidence angle. Interpolation can be achieved by fitting suitable parametric hyper-surfaces to the hyper-cube information. For surface scattering, Advanced Integral Equation Model (AIEM) or numerical models are preferable since they do not require approximate parameterization or tuning parameters inherent to empirical or semi-empirical models. For vegetation, coherent scattering models are preferred over radiative transfer models.

7.3.8. Volumetric soil moisture could be used rather than soil dielectric permittivity. However, the permittivity, being a more fundamental physical property, is preferable as it is independent of soil compositional properties, therefore reducing the number of axes of the data hyper-cube.

7.3.9. It is envisioned that data hyper-cubes will be generated independently from the actual soil moisture processor, although there is likely to be some feedback between the essentially independent development processes, particularly regarding the interface to the reference set. As long as the interface format is maintained, data hyper-cubes may be updated, perhaps using improved forward modelling. Updated hyper-cubes can then be used with the existing soil moisture processor.

7.3.10. Hyper-cubes are required for each of the selected vegetation scattering class (i.e. land surface class with distinctive scattering behaviour) and each sensor configuration (frequency, polarization, incidence angle). Data hyper-cubes for a variety of land covers and crop types have already been produced for the SMAP and SAOCOM missions. Such cubes require testing for vegetation conditions typical of Australia, or any other area outside the

areas of interest to SAOCOM and SMAP against which those models have been tested. Additional data hyper-cubes will be required for the land covers of interest not matching those already studied, and for polarimetric observables beyond the channel backscattering coefficients not yet considered in the SMAP and SAOCOM methodologies.

7.3.11. Soil permittivity retrieval shall be performed by minimizing a cost function (e.g. weighted sum of squares of differences between measured and interpolated observables) using the time series of multi-channel observations in a least squares process. Where the data permit direct retrieval of soil permittivity and roughness estimates (e.g. Dubois HH, VV and XBragg full-pol) these may be combined with those recovered from the hyper-cubes in the cost function. Soil permittivity estimates from SAR at fine resolutions may be constrained to agree (closely if not precisely) with coarse resolution estimates from passive remote sensing.

7.3.12. If fully-polarimetric SAR data are available, surface parameters such a surface roughness and vegetation water content can be retrieved at each time-step together with permittivity (ie., unconstrained retrieval). Since in general the time-scale of the changes in surface roughness and vegetation is longer than that of soil moisture, a possible alternative approach is that of assuming constant vegetation and surface roughness conditions during the observation window, so that any changes in backscatter can be attributed to soil moisture changes (plus a random component due to the radar measurement error). Only one value of surface roughness and vegetation parameter(s) are then retrieved over a defined observation window, together with a time-series of soil permittivity (ie., constrained retrieval). This approach has two main advantages: i) it does not require fully polarized scattering matrix at each and every time-step, since soil permittivity can be derived from compact or dual-polarimetric observations under the assumption of constant surface roughness and vegetation, and ii) the time-series information helps reduce the impact of the backscatter measurement error which would affect the retrieval at individual time steps, because the value of roughness and vegetation parameters are chosen to minimize, in the least-square sense, the difference between simulated and observed SAR parameters at all time-steps within the observation window. Therefore it is applicable to a mission design which involves frequent (e.g., 2-3 days) dual-polarized acquisitions with less frequent (e.g., 1-2 weeks) fully-polarized acquisitions.

7.3.13. The drawback of the constrained retrieval option is that changes in surface conditions within this window (e.g., tillage, harvest, vegetation growth) will deteriorate the performance of the approach. In such a case by constraining surface roughness and vegetation parameters to fixed, but possibly erroneous, values, further error is introduced into soil moisture estimates. Unconstrained retrieval of roughness and vegetation status conducted in parallel with constrained retrieval might, however, indicate where the approximation of constant soil roughness/vegetation is valid so that advantage might be taken of any accuracy improvements in soil moisture estimates that use this assumption.

7.3.14. Abrupt changes, such as tillage and harvest, should be detected to correctly position observation windows, whether using the constant or variable roughness assumptions, and this implies sampling on time intervals short enough to permit wide sample windows over anticipated time intervals between abrupt changes. Sampling at full-channel capacity, coupled to retrieval without the assumption of constant surface roughness, should be robust to abrupt changes that do not alter soil moisture, but of course abrupt changes are likely to be followed by soil moisture changes, for example harvesting will tend to dry the soil in the

absence of precipitation, and this is an argument for ensuring the capability to detect abrupt changes through frequent sampling.

7.3.15. Slower changes such as vegetation growth will be more difficult to detect. Again polarimetric analysis might be helpful in this sense. However, it is suggested that an optimized observation window should be selected to minimize these changes. The optimization of the observation window is a developmental task.

7.3.16. Note that whilst full-polarimetry is optimal, it does come at a cost, both in power and swath width, and therefore coverage. Thus, whilst the optimal SAR sensor would be capable of fully polarimetric operation, it may be desirable to operate the sensor in compact or dual-pol modes for some portions of the observation cycle. Operation below full-polarimetry will however incur a risk (discussed in following sections) in the estimation and correction for the effects of Faraday rotation, and this will have an impact upon both the accuracies of the soil moisture retrievals, and the land cover scattering class classifications.

7.3.17. The computational cost of minimizing the cost function will depend on both the number of dimensions of the data cube and the resolution at which the hyper-surfaces are interpolated. Hyper-cubes with higher dimensionality can be generated to include other surface or vegetation factors known to impact the backscatter (e.g., surface correlation length, soil texture/composition, vegetation height or structural parameters, with the caveats (see earlier) regarding the non-stationary nature of surfaces and the correct choice of multi-scale correlation lengths with regard to observation resolution). This could result in improved soil moisture retrievals, provided there are sufficient independent observables from multi-channel (e.g. polarimetic, incidence angle diverse, ancillary) data, but a higher computational cost of the search algorithm. Soil permittivities may be converted to soil moisture estimates using a dielectric model appropriate to the soil types in the area of interest and which best fits the field data for the area of interest (e.g. Peplinski, 1995 with later corrections).

7.3.18. Land cover classification for each observation yields a land cover time series which can be used to determine the correct hyper-cube set and retrieval model for polarimetric coherency work. The land cover will be used to determine which method will be used to separate the bare-soil contribution to observed signals. For bare surfaces the extended Bragg model can be used with full- or compact-polarimetric data, or the Dubois model with dual, HH and VV data, to recover soil permittivity and roughness estimates directly. These estimates could be used to optimise the hyper-cube inversion, and/or as a component of the cost function. For moderately vegetated areas, L-band polarimetric data can be analysed in terms of a Freeman-Durden type decomposition to yield the bare-surface contribution to the polarimetric coherency, which can then be used with the extended Bragg model, and the hyper-cubes as described above. For forested areas the use of P-band data is recommended in a manner similar to that suggested for the L-band data in moderately vegetated areas.

7.3.19. It should be highlighted that, particularly in the case of agricultural crop with strong phenological dynamics, the relative strengths of the scattering mechanisms change during the vegetation-growing cycle, and depending on it, the relationship between the various scattering components and soil moisture will vary. This behaviour is the underlying reason that the land cover classification is divided into separate vegetation scattering classes, rather than simply by crop species, since a crop may be classified in a variety of scattering classes

throughout the growing season. The choice of retrieval algorithm, or set of hyper-cubes, will depend upon the scattering vegetation class, and not the crop species or class.

7.3.20. Having SAR observations available at fixed incidence angle would reduce the number of variables and simplify the inversion problem. The local incidence angle is highly important in determining backscatter properties. Whilst a repeat orbit could limit the variation of local incidence angle for any particular point, it could not ensure the same incidence angle everywhere due to terrain variations. Thus the soil moisture inversion algorithm must be able to accommodate different incidence angles. Waiting for an orbit to be repeated could place a limit on the frequency of observation, and on the versatility of the system. Incidence angle diversity at a single site could be seen as advantageous in the same way that other multi-channel approaches have been shown to be advantageous. Thus, both algorithm and system design should consider incidence angle variation and not be constrained to a single incidence angle.

7.3.21. A fixed azimuth view angle between subsequent SAR observations is important for time series and change detection algorithms, and for agricultural fields where returns are influenced by azimuthal surface asymmetries (e.g., periodic crop rows, plant rows) that cause changes in backscatter and polarimetric coherency matrix with azimuthal angle. This implies an exact repeat orbit for each overpass.

7.3.22. It is crucial to highlight that the application of fully-polarimetric coherency matrix, whilst providing additional information on terrain orientation and vegetation cover, implies stringent, additional requirements for the polarimetric calibration of the SAR system. In particular, accurate calibration of the cross-talk, channel imbalance and relative phase are essential. Polarimetric decomposition techniques are sensitive to system noise, and therefore good Signal-to-Noise Ratio (SNR) is required, together with noise filtering and suppression techniques which preserve the polarimetric information content of the data. . Accurate external polarimetric calibration permitting the use of polarimetric techniques is possible, even in the presence of Faraday rotation, and the suppression of noise in polarimetric data can be undertaken using standard tools.

7.3.23. Performance of the algorithm should be optimised during the development phase and repeatedly monitored thereafter to ensure stability using additional field data. The algorithm performance will vary with vegetation cover but should achieve (in the presence of 0.5dB noise) a retrieval error better than 0.06 vol/vol for vegetation water content up to 2kg/m^2 and soil moisture content up to 0.4 vol/vol. Performance will depend upon scale and resolution of the desired product. It is important that a spatially and temporally varying error estimate be provided together with the reported soil moisture.

7.3.24. As satellites can only directly measure the near-surface layer of soil at discrete instances in time, and there is a need for continuous soil moisture data over the root zone, land model data assimilation approaches to providing such a product should also be developed.

8. SYSTEM SPECIFICATIONS

8.1. Overview

8.1.1. The various candidate algorithms for applying radar data to soil moisture estimation have uncertainties and limitations. Some of the algorithms involve temporal change approaches rather than snap-shot algorithms. Final algorithm selection will impose differing requirements on the orbit and calibration requirements. Consequently, any new mission should plan around the most conservative requirements (full polarimetric capability, exact orbit repeat, minimum spacecraft dependent calibration differences, etc.) to provide greatest flexibility in the algorithm selection right up to and even after launch.

8.1.2. The ultimate design of any orbital SAR mission is the result of a number of compromises. For example higher resolution demands greater bandwidth and transmitted power, or improvements in azimuth resolution require higher pulse repetition frequencies that result in smaller possible swath widths (the theoretically achievable SAR azimuth resolution is one half of the antenna length independent of altitude).

8.1.3. A complete system design for even a single SAR system is beyond the scope of the current task, and recommendations have been made for essentially three or at least two SAR systems: S-band/L-band for bare surfaces, L-band for vegetated surfaces and P-band for forested surfaces.

8.1.4. Rather than attempt a SAR design exercise, the following discusses relevant parameters of SAR systems and their relationships, and comments on the probable values of these parameters based on existing or conceived SAR systems, particularly those that may be suited to soil moisture retrieval.

8.1.5. The process of task-dependent SAR-system design is one that should be conducted at the start of any SAR-project.

8.2. SAR System Design Considerations

8.2.1. The design of SAR a system is dependent on the application for which it is intended; in this case soil moisture retrieval. Typically, the specifications provided to the design engineer would include:

Ground range and azimuth resolution
Incidence angle range
Desired swath width
Wavelength
Polarizations
Sensitivity, expressed as Noise Equivalent Sigma Zero (NESZ)
Radiometric accuracy, expressed as Signal-to-Noise Ratio (SNR)

8.2.2. The recommendations of the previous Section indicate a preference for multiple frequency band operations, polarimetric operation, 2-3 day repeat observation, with wide area coverage at good resolution, national coverage, a requirement for topographic information, and ultimately soil moisture information retrieval at scales of 1km or better, according to the application.

Resolution Requirements

8.2.3. Based on the preceding recommendations it is anticipated that the SAR soil moisture system be capable of ground resolutions of the order of 10m or better.

8.2.4. This figure may seem excessively fine given the suggestion that soil moisture product resolution of only order of 1km is required for most applications. However, for irrigation scheduling pixel sizes of less than 100m resolution will be required. At a resolution of 17m in range and 9m azimuth (azimuth resolution is generally finer than range resolution), 100m resolution only represents around 65 independent backscatter samples.

8.2.5. For fully developed speckle single look complex SAR pixel backscatter cross sections are exponentially distributed. *N* independent samples yield an estimate of the mean backscatter cross section with error $1/\sqrt{N}$ of the mean (radiometric accuracy). Quoted accuracy requirements from the literature generally indicate less than 0.5dB uncertainty in the absence of noise. A 0.5dB error corresponds to an uncertainty of ~12% of the mean, or an independent sample size of ~67. A 0.3dB error requirement on estimates of backscattering coefficient corresponds to an independent sample size of ~195, or a resolution of around 10m in ground range and 5m in azimuth if the soil moisture product resolution is around 100m. Note that the above calculation is valid when the system SNR ratio is high, i.e., when it is determined primarily by the number of looks and is not limited by the SNR (this may not be true for smooth and/or dry bare surfaces, particularly for HV measurements). Low SNR will increase the number of independent samples required to achieve the same accuracy according to $1/\sqrt{N}$ *(1+1/SNR)

8.2.6. Slant range resolution is given by $\delta_{Rs} = c/2B$, where *c* is the speed of light and *B* is the frequency bandwidth. Ground range resolution depends upon incidence angle θ and is given by $\delta_{Rg} = c/2B\sin\theta$. Azimuth resolution can be approximated by half the real aperture length (i.e. half the length of the antenna) $\delta_{Az} = D/2$ if the sampling rate is sufficient. Thus requirements on resolution translate into bandwidth and antenna length requirements. Given our two examples of ~18m (range) by 9m (azimuth) or 10m (range) by 5m (azimuth) this suggests that the bandwidth (which must be contained in legal limits) at a nominal 45° incidence should be between respectively 12MHz and 21MHz and the antenna length should be between respectively 18m and 10m, for a S-, L- or P-band system.

8.2.7. PALSAR II, SMAP and SAOCOM all suggest antenna areas of the order of 30m^2, with antenna lengths of around 10m. NovaSAR appears to have a rather small antenna, even taking into account the higher frequency. Aside from BIOMASS, which suffers severe Tx restrictions at P-band, and SMAP which reports a rather low bandwidth and resolution, reported SAR system bandwidths are of the order of 21MHz or higher. It is noted that Tx restrictions are possible at S-band that could restrict the reported NovaSAR bandwidth and limit its range resolution.

8.2.8. It should be noted that a bandwidth of 21MHz will ensure the resolution requirement at satisfied at angle equal or higher than 45°, while for lower incidence angle the range resolution will increase according to $\delta_{Rg} = c/2B\sin\theta$

Orbit Properties

8.2.9. The orbital velocity can be approximated by

$$V \cong \sqrt{\frac{GM}{(R+h)}} \qquad \text{(Eq. 5)}$$

where G is the universal gravitational constant ($G \approx 6.67384 \times 10^{-11}$ m^3 kg^{-1} s^{-2}), M is the Earth mass ($M \approx 5.9736 \times 10^{24}$ kg, $GM \approx 3.986 \times 10^{14}$ m^3 s^{-2}), R is the Earth radius ($R \approx 6.371 \times 10^6$ m), and h is the satellite altitude.

8.2.10. As satellite altitude increases, orbital speed decreases and the satellite has further to go to complete the orbit. The period is the distance travelled in an orbit divided by the speed, i.e.

$$T \cong 2\pi\sqrt{\frac{(R+h)^3}{GM}} = 2\pi\sqrt{\frac{(R+h)^3}{\mu}} \qquad \text{(Eq. 6)}$$

8.2.11. Since the Nyquist azimuthal sampling rate must be such that pulses are separated by less than half the antenna length along-track, so the PRF is related to the satellite altitude. The SNR is also related to the satellite altitude, and is better for lower orbits, which in turn implies increased PRFs and hence thinner swaths. The achievable pulse power depends also upon SAR technology and pulse duration. Gallium Nitride technology permits greater peak pulse powers. Longer pulses affect the PRF and range ambiguity design space.

8.2.12. Over the observed range of satellite altitudes from Table 2.2 it can be calculated that the orbital velocity varies from roughly 7.6km/s (period 1.57h) at 500km altitude down to 7.5km/s (period 1.64h) at 700km altitude. Lower altitudes yield improved SNR or a reduction in power for fixed SNR, but also mean increased atmospheric friction and a need to carry and use more fuel to maintain orbit over the intended lifetime of the sensor.

8.2.13. A near-polar (orbital inclination between 96.5° and 102.5°), sun-synchronous orbit will permit near-global coverage and can be selected to have repeat ground-track characteristics that appear to be desirable for the soil moisture retrieval task.

8.2.14. Sun-synchronous orbits exploit the orbit perturbation caused by the Earth's non-spherical gravitational field. By choosing the correct inclination and altitude of the satellite orbit, the right ascension of the ascending node can be made to process at the same rate as the Earth revolves around the Sun, in a sun-synchronous orbit. It is an orbit for which the plane of the satellite orbit is always the same in relation to the Sun. It can also be defined an as orbit for which the satellite crosses the equator at the same local time each day.

8.2.15. A sun-synchronous orbit is not fixed in space. It must move 1° per day to compensate for the Earth's revolution around the Sun. Since the Earth makes one revolution (360°) around the Sun per year, it is possible to calculate the rate of change of the Sun's right ascension:

0.9856473°/solar day. The sun-synchronous design equation is

$$\cos i + \frac{2\dot{\lambda} a^{3/2}(1-e^2)^2}{3J_2 R_{eq}^2 \sqrt{\mu}} = 0 \qquad \text{(Eq. 7)}$$

where i is the inclination angle, $\dot{\lambda}$ is the orbital rate of the Earth (0.9856473°/solar day), a is the semi-major axis, e is the orbital eccentricity, J_2 is the coefficient for the second zonal term, R_{eq} is the Equatorial radius of Earth, and μ is the gravitational constant of the Earth.

8.2.16. Whilst the repeating ground track governing equation is

$$\frac{(K/N)}{(\omega_e - \dot{\lambda})} - \frac{1}{(\dot{\omega} + \dot{M})} = 0 \qquad \text{(Eq. 8)}$$

where K is the number of orbits in repeat cycle, N is the number of days in repeat cycle, ω_e is the inertial rotation rate of the Earth, $\dot{\omega}$ is the argument of perigree perturbation, and $\dot{M}$ is the mean anomaly perturbation.

8.2.17. These two equations form a non-linear pair that requires solution using numerical techniques to estimate the Kozai mean semi-major axis and orbital inclination of the sun-synchronous orbit with the chosen repeating ground-track criteria.

8.2.18. Such modelling is beyond the scope of the present task. However it is noted that repeat-cycle periods quoted in Table 2.2 range between 12 and 17 days. The stated optimum repeat time is 2-3 days. Based on this evidence alone one might conclude that multiple satellites are required to achieve the desired repeat observation rate. However, detailed modelling of the possibilities is required before one would be able to draw such a conclusion.

Incidence Angles

8.2.19. Low incidence angles were seen to be desirable from the point of view of soil moisture retrieval, but low incidence angle implies poor resolution in the range direction, and therefore reduced sample size and increased uncertainty in soil moisture estimation. There is also a connection between antenna size and wavelength that limits the range of possible incidence angles (measured at the ellipsoid) and affects achievable swath width.

8.2.20. The range of incidence angles reported in Table 2.2 is anywhere between 8 and 70°. The SMAP mission is being designed to operate above 40°, even though the algorithm review suggested that lower incidence angles are to be preferred.

8.2.21. For a spherical Earth approximation swath width for incidence angles in the range 20-45° and altitudes between 500-700km are in the range of 280-375km.

Sensitivity

8.2.22. The radar equation, also known as the radar range equation, is the fundamental equation of radar. For a SAR system a useful version of the radar equation is the single-look signal (or clutter) to noise ratio (SNR or CNR) (e.g. Ulaby *et al*., 1982):

$$CNR = \frac{P_{Tx-avg} G^2 \lambda^3 \delta_{Rg} \sigma_o}{2(4\pi)^3 R_s^3 k_B T_{sys} V_s L} = \frac{P_{Tx-avg} A^2 \eta^2 \delta_{Rg} \sigma_o}{8\pi R_s^3 \lambda\, k_B T_{sys} V_s L} \qquad \text{(Eq. 9)}$$

where P_{Tx-avg} is the average transmitted power, η is the radiation efficiency, A is the antenna area, $G = \frac{4\pi A \eta}{\lambda^2}$ is the antenna gain, λ is the carrier frequency, δ_{Rg} is the ground range resolution, σ_o is the backscattering coefficient, R_s is the range (slant range), k_B is the Boltzmann's constant, T_{sys} is the system equivalent noise temperature, V_s is the satellite speed, and L are the losses (e.g. electronic, signal processing, atmospheric etc.)

8.2.23. The sensitivity is usually defined in terms of NESZ. This is defined as the clutter level (backscattering coefficient) that produces a received power equal to the thermal noise power, and is found by setting the CNR equal to unity in the previous equation, i.e.

$$NE\sigma_o = \frac{2(4\pi)^3 R_s^3 k_B T_{sys} V_s L}{P_{Tx-avg} G^2 \lambda^3 \delta_{Rg}} = \frac{8\pi R_s^3 \lambda\, k_B T_{sys} V_s L}{P_{Tx-avg} A^2 \eta^2 \delta_{Rg}} \qquad \text{(Eq. 10)}$$

8.2.24. Reported NESZ values for the systems listed in Table 2.2 are in the range -22dB to -35dB.

8.2.25. For an average power of 700W, antenna gain of 34dB (typically over 30dB for space-borne SAR), L-band wavelength of 24cm, ground-range resolution of 10m, slant range of 840km, system temperature of 580K, losses of 7dB and orbital speed of 7.6km/s the NESZ value is -29.3dB, which is squarely in the reported range.

8.2.26. Operating at lower altitude, increasing average Tx power and antenna size and efficiency will all serve to improve the NESZ and improve the sensitivity of the system. For example, an increase of average transmission power to 2000W in the previous calculation yields a decrease in NESZ to -33.9dB, again within the reported range.

The "Mythical" Minimum Antenna Area

8.2.27. The titular description acknowledges the study by Freeman *et al*. (2000) which showed that the following arguments really only apply if the SAR system design is constrained for maximum swath width as well as finest resolution.

8.2.28. Start by noting that the maximum illuminated swath on the ground has width

$$W_{g(\max)} \cong \frac{\lambda R}{D_{el}\cos\eta} \qquad \text{(Eq. 11)}$$

where R is the mid-swath slant range, D_{el} is the width of the antenna in elevation, and η is the incidence angle.

8.2.29. To avoid velocity ambiguity a SAR must have a PRF of at least twice the velocity divided by the antenna length: $PRF \geq 2V_s / D_{az} = V_s / \delta_{az(\min)}$. With a 10m long antenna and a speed of 7.6km/s the minimum PRF is around 1.5KHz.

8.2.30. For short pulses, the requirement for range unambiguous operation (inside the desired swath) implies that $2R_{far}/c < 2R_{near}/C + IPP$ where $IPP = 1/PRF$ is the inter-pulse period and the slant ranges mark the near and far limits of the desired swath. Thus the desired swath in slant range is bounded by $W_s \leq (R_{far} - R_{near}) < c\,IPP/2 = c/2PRF$.

8.2.31. Or to put it another way the PRF has an upper bound of $PRF < c/2(R_{far} - R_{near})$.

8.2.32. So $W_s \leq c/2PRF$ and $PRF \geq V_s/\delta_{az(\min)}$ so that $W_s \leq (c/2V_s)\delta_{az(\min)}$ or $W_s/\delta_{az(\min)} \leq c/2V_s$. Note that for Low Earth Orbit (LEO) satellites the value of $c/2V$ is nearly constant at 2×10^4.

8.2.33. Given that the slant range swath is related to the ground range swath by $W_s = W_g \sin\eta$, a constraint on the antenna area can be obtained as:

$$\frac{W_{s(\max)}}{\delta_{az(\min)}} = \frac{2\lambda R\tan\eta}{D_{az}D_{el}} < \frac{c}{2V_s} \qquad \text{(Eq. 12)}$$

$$\text{and thus } A_{eff} > \frac{4V_s\lambda R}{c}\tan\eta.$$

8.2.34. This bound on the effective antenna area A_{eff} applies only when the SAR design requires maximum swath width and minimum (finest) azimuth resolution. However may SAR systems have been operated with effective antenna areas less than this by operating with a PRF less than the nominal Doppler bandwidth, and recording returns over a *desired* swath width that is less than the *maximum* swath width (Freeman, 2000).

8.2.35. Although SAR antennas may be smaller in area than this constraint implies this does not mean that SAR antennas can be arbitrarily small. The size of the antenna has significant impact on the gain and therefore on the SNR which must be taken into account. The brief discussion presented here is no substitute for a rigorous treatment of the calculation of

range and azimuth ambiguity levels, which must be considered in a robust design process.

8.2.36. There is recent interest in the use of multi-channel SAR systems that, for example, have a single Tx module and multiple Rx modules that are designed to overcome the minimum antenna area constraint (Ma, 2011; Wang, 2012). In such systems a small Tx-aperture is implemented to illuminate a wide area and the Rx antenna is split into multiple sub-apertures with independent receiver channels. Since each individual antenna does not meet the minimum antenna area constraint, range and/or Doppler ambiguities inevitably pollute the recorded echoes. However coherent processing in either the temporal or the Doppler domains that combine the aliased signals received by all sub-apertures enables a single output signal free of ambiguities.

8.2.37. Nevertheless we can be guided by the constraint which can be used to yield an indication of the anticipated antenna size. For an L-band system with a mid-swath range of 800km and a mid-swath incidence of 45° the minimum effective antenna area is around $20m^2$. Note that the effective area is usually related to the actual area by an efficiency constant so that the actual area is greater. Taking into account the efficiency factor, this estimate is consistent with the antenna areas reported in Table 2.2. For S-band the antenna minimum area is reduced to approximately $8m^2$. The NovaSAR antenna area is reported at $3m^2$, so that one might anticipate NovaSAR will employ multi-channel techniques and/or have a desired swath less than maximum. At P-band the antenna area constraint yields an estimated effective area of $60m^2$, in keeping with the BIOMASS sensor actual reported antenna area.

Ambiguities

8.2.38. The previous criterion on antenna size provides only around 6dB suppression for ambiguous targets at the edge of the swath. This level of suppression applies also in azimuth (Doppler) where the Nyquist sampling rate does not entirely prevent spectrum components from being aliased into the main part of the spectrum. For the given range and azimuth antenna patterns the PRF should be selected to yield low range and azimuth ambiguity noise contributions.

8.2.39. The Doppler processing bandwidth is bounded by the PRF. Using less than the full bandwidth can help filter out significant Doppler spectrum aliased into the main Nyquist window, permitting improved ambiguities noise levels at the cost of azimuth resolution.

8.2.40. The integrated ambiguity to signal ratio (ASR) is written as a function of fast time, or equivalently the cross-track position in the image. Evaluation of the expression for the ASR requires knowledge of the two-dimensional antenna pattern, and of the target reflectivity to be formulated in terms of the Doppler frequency and the time delay.

8.2.41. This information is unavailable and estimation of the ASR for the proposed soil moisture retrieval SAR system lies beyond the task description. However the ambiguities are important and it is possible to comment on what the likely ambiguity levels will be. The following is a very brief discussion of the origin of azimuth and range ambiguities in a conventional SAR. The advent of SMART SAR systems with SCan On Receive (SCORE) algorithms will affect the expressions for ambiguities given here. Once again it is completely beyond the bounds of this task to give a full SAR system design.

8.2.42. It is noted that the total integrated ambiguity ratio for the proposed BIOMASS P-band system is of the order of -20dB. Younis *et al*. (2010) have proposed a SMART X-Band SAR that uses SCORE and report RASR below -40dB and AASR values below -40dB rising to -20dB at near range. DLR have also proposed that the Tandem-L system will have RASR values typically between -50dB and -40dB across a 350km swath in fully-polarimetric strip-map operation (with a bandwidth of 85MHz, orbit altitude of 760km, repeat cycle of 8 days, incidence angles between 26.3 and 46.6°, average Tx power of 96W and a PRF of 2.365kHz).

8.2.43. It is anticipated that a soil-moisture SAR system designed to detect low backscattering coefficients from dry, smooth surfaces will require a design that permits a low total ambiguity.

Azimuth Ambiguity

8.2.44. The ratio of the ambiguous signal to the desired signal, within the SAR correlator azimuth processing bandwidth, is commonly referred to as the azimuth ambiguity to signal ratio (AASR). The integrated AASR can be estimated using the following equation (Curlander, 1991):

$$AASR = \frac{\sum_{m\neq 0} \int_{-B_p/2}^{B_p/2} G^2(f + m \times PRF)\, df}{\int_{-B_p/2}^{B_p/2} G^2(f)\, df} \qquad \text{(Eq. 13)}$$

where G^2 is the two-way far field antenna power pattern in which it is assumed that the scene reflectivity is uniform and that the antenna pattern is separable in elevation and azimuth.

8.2.45. With this equation the AASR is typically found to be of the order of -20dB. At this value ambiguous signals may still be observed in images where bright ambiguities coincide with regions of low backscattering coefficient.

Range Ambiguity

8.2.46. Range ambiguities arise when echoes from preceding and succeeding pulses arrive at the antenna simultaneously with the desired return. For space-borne radars, where several inter-pulse periods elapse between transmission and reception of a pulse, range ambiguities can be significant.

8.2.47. Ambiguous signals arriving at time t_i do so from ranges given by

$$R_{ij} = \frac{c}{2}\left(t_i + \frac{j}{PRF}\right) \qquad \text{(Eq. 14)}$$

where the integer *j* is zero for the desired pulse. The integrated range ambiguity to signal ratio (RASR) is obtained by taking the ratio of integrated power of the range ambiguities to the desired pulse returns. The definition of the RASR as a function of slant range is given by (Curlander, 1991):

$$RASR(R_{i0}) = \frac{R_{i0}^3 \sin\eta_{i0}}{G^2(\theta_{i0})} \sum_{\substack{j=-N_n \\ j\neq 0}}^{j=N_f} \frac{G^2(\theta_{ij})}{R_{ij}^3 \sin\eta_{ij}} \quad \text{(Eq. 15)}$$

where η_{ij} is the incidence angle for the j^{th} ambiguity, and θ_{ij} is the beam angle for the same ambiguity.

8.2.48. Generally the RASR is lower than the AASR, although the two may have commensurate values.

Polarization

8.2.49. The recommendation for soil moisture is at minimum dual-polarization (HH and VV) and preferably full-polarization or failing that compact-polarimetry (transmit circular, receive linear orthogonal). For space-borne SAR a single-polarization on-transmit offers twice the swath width compared to full polarization. This is linked to SAR system design issues as previously discussed: full-polarimetric operation requires two Tx pulses of orthogonal polarizations and therefore doubles the required PRF, which, as per the preceding discussion, implies a reduction in swath width, for example the ALOS PALSAR, swath width reduced from 70km for the dual-pol (HH, HV) mode to 30km for the full polarization mode.

8.2.50. Note that dual-polarization (HH and VV, dual-like polarization) also implies a doubling of PRF and therefore offers no advantage over full-pol operation beyond system processing bandwidth considerations, and actually risks reduced calibration accuracy.

8.2.51. The reduced swath-width in full-polarization mode has a detrimental impact on revisit times. A compact-polarimetric mode where the transmit polarization is circular, and the only constraint on the two receiving polarizations is independence, has advantages for SAR system design. The choice of the polarizations of the two receive channels is not significant as any polarization on-receive can be synthesized from two orthogonal polarization measurements.

8.2.52. At a low frequency (L-band or lower, S-band doesn't suffer so much from ionospheric effects) where the ionosphere has a significant effect, the circular transmit polarization is the only sensible option, as it provides an effective constant polarization as seen by the scattering surface: an essential condition for a meaningful multi-temporal analysis.

8.2.53. The pseudo-covariance matrix for Tx-circular Rx-orthogonal compact polarimetry is very similar to the full polarimetric covariance matrix, and carries much the same information for soil moisture retrieval. Reconstruction of the cross-polarized backscattering coefficient from compact polarimetry has been shown to have very low sensitivity to Faraday rotation,

suggesting that land cover scattering class separation essential to the correct application of retrieval algorithms would be possible for compact-polarimetric operation (Dubois, 2008). However there has been some evidence to suggest that HV reconstructed from compact polarimetry data is not entirely reliable.

8.2.54. A procedure has been developed to correct for the ionospheric effects in compact polarimetry mode and the technique appears robust (Dubois, 2008). The calibration of CTLR (Circular Tx, Linear Rx) compact polarimetry SAR data has been addressed quite recently (Chen, 2011) indicating that this can be achieved through a combination of passive and active polarimetric calibration targets and Total Electron Content (TEC) measurements from the Global Navigation Satellite System. It has also been proposed that the Faraday rotation angle can be estimated from raw SAR data obtained in full-polarimetric mode from a few pulses, and that the CP–mode Faraday rotation correction is possible if the angle is known.

8.2.55. Thus CTLR compact-polarimetric mode, having been recommended for soil moisture retrieval, offers a significant advantage for SAR system design as it preserves swath width and reduces the revisit interval and appears to present little risk for calibration.

8.2.56. However a full analysis of the impact of the use of compact polarimetric mode SAR as opposed to full polarimetric mode for soil moisture retrieval should be undertaken for those algorithms accessible to the compact polarimetric mode data. For example, the effects of terrain slope on compact polarimetry data are not fully understood, and the implications for antenna design must be investigated. It is noted that the design of compact polarimetric mode is compatible with full polarimetric mode so that compact polarimetric mode can be integrated readily with full polarimetric architectures. Thus, having compact polarimetric mode as an option on an otherwise full polarimetric mode system would give the opportunity of enhanced system performance without additional risk.

Faraday Rotation

8.2.57. Faraday rotation is mentioned in the previous discussion and a brief description is given here.

8.2.58. As microwave radiation propagates through the ionosphere, the linearly polarized field components are rotated by an angle Ω (Faraday rotation), depending on the geomagnetic field and the ionospheric electron content. The Faraday rotation angle may be expressed approximately as

$$\Omega = 13557 f^{-2} N_f < B_o \cos\alpha \sec\chi > \quad \text{(Eq. 16)}$$

where Ω is the rotation angle in degrees, f is the radio frequency in GHz, N_f is the ionospheric total electron content (TEC) in TEC units, where 1 TECU = 10^{16} electrons m^{-2}, B_o is the Earth's magnetic field in Tesla, α is the angle between the magnetic field and the wave propagation direction, and χ is the angle between the wave propagation direction and the vertical to the Earth's surface.

8.2.59. The angular brackets denote an average of the enclosed quantities along the path of the wave. The TEC is significantly affected by the solar radiation. The global TEC measurements performed by a network of GPS receivers have shown significant temporal and latitudinal variations. In the equatorial and mid-latitude areas, the TEC varies from a few TECU at night to as high as 60 TECU at noon, while the TEC has less temporal variation with a nominal value of about 20 TECU in the polar regions. By assuming a typical worst-case geometry (χ = 45°, α = 0°) and a high-latitude value of B_o = 5.44 ×10^{-5} at 300 km altitude near the peak of the electron density, an upper bound estimate for Ω in degrees at 1.4GHz for a satellite operating above the ionosphere is

$$\Omega = 0.53 N_f \quad \text{(Eq. 17)}$$

8.2.60. Therefore, the Faraday rotation at a frequency of 1.4GHz can be as low as a few degrees at night and as high as 20 to 30° at noon local time.

8.2.61. Farady rotations of a few degrees are thought acceptable in most applications but will obviously have an effect on soil moisture retrievals which depend at a minimum on the two co-polar scattering amplitudes which are mixed by the rotation according to:

$$\begin{bmatrix} M_{hh} & M_{vh} \\ M_{hv} & M_{vv} \end{bmatrix} = \begin{bmatrix} \cos\Omega & \sin\Omega \\ -\sin\Omega & \cos\Omega \end{bmatrix} \begin{bmatrix} S_{hh} & S_{vh} \\ S_{hv} & S_{vv} \end{bmatrix} \begin{bmatrix} \cos\Omega & \sin\Omega \\ -\sin\Omega & \cos\Omega \end{bmatrix} \quad \text{(Eq. 18)}$$

8.2.62. Freeman (Freeman, 2004a,b) developed a method for estimation and correction of Faraday rotation effects using fully-polarimetric SAR data. More recently Meyer and Nicoll (Meyer, 2008) demonstrated prediction, detection and correction of Farady rotation in ALOS PALSAR fully-polarimetric data.

8.2.63. My-Linh Truong-Loi et al (2009) have presented an estimation procedure for Faraday rotation with compact polarimetry mode SAR which relies on the scattering properties of bare surfaces. The selection of the bare surfaces was based on a new parameter, the conformity coefficient computed from compact polarimetry measurements shown to be Faraday rotation invariant. Once estimated, the Faraday rotation can be corrected in compact polarimetry mode SAR data by applying a simple rotation matrix to the two-component compact polarimetry mode scattering vector.

8.2.64. My-Linh Truong-Loi et al (2009) estimate the HH and VV backscattering coefficients from the compact polarimetry mode measurements over bare soil surfaces and estimated soil moisture using the Dubois *et al*. (1995) algorithm. The results obtained using compact polarimetry were shown to be in good agreement with those obtained from the standard Dubois et al. algorithm using fully polarimetric data. This suggests that, for soil moisture, compact polarimetry mode SAR can be used instead of HH and VV dual-polarized measurements, obtained from full-polarimetric SAR.

8.2.65. Thus it is anticipated that by operating in either full-polarimetric or TCRL compact

polarimetric mode it will be possible to both estimate and correct for the effects of Faraday rotation, and ultimately estimate soil moisture.

8.3. Summary

8.3.1. A full SAR system design was beyond the scope of the current task. We have reported relevant SAR system design parameters for proposed systems and discussed the likely location of the SAR system in the parameter space for a SAR that will be capable of providing soil moisture estimates.

9. ACCURACY AND FURTHER CONSIDERATIONS

This section discusses accuracy estimates for the recommended soil moisture retrieval algorithms. The risks, special cases (i.e., vegetation and terrain effects) and ancillary data requirements for soil moisture retrieval are also considered. Future R&D requirements to improve or calibrate/validate algorithms and an operational system are also discussed.

9.1. Accuracy Assessment

9.1.1. Since it is not possible to assess the SAR system accuracy without a detailed SAR system design, it is not possible to make an unambiguous determination of the proposed soil moisture retrieval algorithm(s) presented here. Even were the SAR system design to be available there are many factors that will affect the overall accuracy of the algorithm, such as the fidelity of the data-cubes to be employed in the inversion process, that are impossible to assess, and the obscurity of which prevent a meaningful assessment of algorithm performance or accuracy. Modelling of the overall soil moisture algorithm accuracy is beyond the scope of the current task.

9.1.2. The error budget for the soil moisture retrieval from a SAR system will include the items listed in Table 9.1. An estimate of the error associated with each item will strongly depend on system design and it is outside the scope of the present task.

9.1.3. It is possible however to report those accuracies either observed or predicted for existing or proposed methods and to suggest that these should be used to bound the desired retrieval accuracy of the proposed algorithm.

Table 9.1 Main component of the soil moisture Error Budget for a SAR mission for soil moisture retrieval.

SAR noise (Radiometric accuracy + Noise Equivalent Sigma Zero)
Calibration Error
physics modeling error
Ancillary data error (vegetation, soil texture, soil temperature)
Conversion error from dielectric constant to soil moisture
Effect of scaling and scene heterogeneity

9.1.4. Clearly algorithm performance will vary according to terrain, local incidence, vegetation cover, ionospheric conditions over the period of observation etc. Whatever the conditions, Walker and Houser (Walker, 2004) reported that near-surface soil moisture observations must have an accuracy better than 0.05 vol/vol to positively impact soil moisture forecasts and that satisfying the spatial resolution and accuracy requirements was much more important than repeat time. The previous section suggested that if the SAR system meets the desired resolution requirements then uncertainties of less than 0.3dB should be possible in the estimation of backscattering coefficients (ignoring DEM area and incidence angle errors). Furthermore uncertainty in co-polar backscattering coefficients due to calibration errors should be of the same order of magnitude, and the SAR system NESZ should be small enough so as not to present an issue for accuracy. Dubois et al (Dubois, 1995) reported that using their technique, an error of 0.5dB in relative calibration between HH and VV channels, commensurate with that estimated here, corresponds to a 3.5% error in soil moisture retrieval at 45° incidence. Reported calibration and stability errors for the HH/VV ratio for ALOS PALSAR for example are only a fraction of a dB, which suggests that, without any additional sources of errors, uncertainties of the order of 0.05 vol/vol in soil moisture retrieval are feasible.

9.1.5. The algorithm proposed in this document follows closely that proposed for the SMAP radar-only retrieval. The major difference is in SAR resolution. The SMAP mission has targeted 0.06 vol/vol as the accuracy goal of the radar-only 3km product, for vegetation water contents up to 5kg/m^2 (though it is acknowledged that this may not be feasible at the higher vegetation amounts, considering the challenge of radar soil moisture retrieval in the presence of roughness and vegetation). Assuming a level of noise commensurable with that suggested in this document (0.5dB or 13% of the mean), synthetic studies indicate a soil moisture

accuracy of the time series algorithm (with constant roughness) better than 0.06 vol/vol mostly for VWC up to 2kg/m^2 and m_v up to 0.4 vol/vol over simulated grass and corn surfaces Generally the soil moisture retrieval error increases with VWC. The Monte-Carlo 0.5dB noise simulation results were made with 6 time-series records corresponding to a period of 18 days considering planned SMAP's 3-day repeat cycle. These estimates did not include the accuracy of the hyper-cube modelling, nor errors due to the conversion from dielectric constant to soil moisture. The VWC error was set to 20%.

9.1.6. Assessment done with truck-mounted scatterometer data and in-situ measurements, which does include hyper-cube modelling and dielectric conversion errors, indicate a soil moisture accuracy of 0.044 vol/vol and 0.054 vol/vol respectively for bare surface and pasture. The VWC varied from site to site between 0.16 and 2.5kg/m^2. The roughness, correlation length, and VWC remained temporally constant throughout the test periods. The SMAP team suggested that the error over the grass is likely due to uncertainty of the forward modelling of the vegetation scattering.

9.1.7. The retrieval accuracy will improve when using longer time-series, provided these are short enough to not include significant changes in surface conditions (e.g., harvest, tillage, vegetation growth).

9.1.8. The analysis on system requirements presented in Section 8 suggests the soil moisture retrieval accuracies predicted for SMAP should be possible at spatial resolutions of 3km for a SAR matching the SMAP specifications, and at considerably finer spatial resolutions for SAR systems with wider bandwidths (at least 21MHz) provided NESZ and calibration accuracy are tuned so that the overall measurement error is within 0.5dB at the desired spatial resolution of soil moisture retrieval.

9.1.9. Regarding the feasibility of a frequent revisit time of 2-3 days, a suitable SAR system has already been proposed in PALSAR II which it is anticipated will provide 42MHz bandwidth for fully-polarimetric operation over a 50km wide swath with a repeat interval of 14 days. A constellation of at least four such SAR systems might be required to address the desired repeat-cycle. The preceding analysis suggested that the proposed SMART SAR TanDEM-L system will have a 350km swath in fully-polarimetric strip-map operation with a bandwidth of 85MHz, orbit altitude of 760km, repeat cycle of 8 days, and incidence angles between 26.3 and 46.6°. A constellation of three TanDEM-L type satellites would appear to satisfy the repeat-cycle requirements at the same time providing the fine spatial resolution required to achieve SMAP retrieval accuracy at 1km resolution.

9.1.10. Uncertainty due to physical modelling error will depend on the model chosen. As an example, model assessment undertaken by the SMAP team using numerical (NMM3D) and semi-empirical (Dubois) models and measurement data for bare surfaces indicate an expectable Root Mean Square difference between field-observed and model-simulated backscattering coefficients of 1.4dB (NMM3D) and 1.9dB (Dubois). Field studies have generally found semi-empirical models (Oh, Dubois) to have a variable accuracy within 0.5-3dB at L-band depending on surface conditions. Since the sensitivity of backscattering coefficient to soil moisture observed in field studies is in the range 0.1-0.6dB/(%vol/vol) (Narayan et al., 2004), the impact of the model uncertainty on soil moisture retrieval could be significant especially on wet conditions (>30%vol/vol), due to a certain saturation of the backscattered signal to soil moisture. This stresses the importance of the development and validation of accurate hyper-cubes as a development task.

9.1.11. Errors due to ancillary data will strongly depend on the source of the data selected for a processor and therefore it is not possible to comment on the accuracy of each ancillary data set here. Nevertheless, it can be anticipated that, assuming that as a minimum a dual-pol channel system is available so that surface roughness can be retrieved, the main source of ancillary data error will be that on the Vegetation Water Content. Analysis by the SMAP team indicates that, even with a VWC error of 20% the 0.06 vol/vol error should be achievable.

9.1.12. Using the best current dielectric model, the conversion from dielectric constant to soil moisture is accurate to about 0.02 vol/vol (Mironov *et al.* 2009). This would minimally affect the total error budget when added to the total error by root-square-sum. Errors in ancillary information on soil texture and soil temperature will also affect the conversion to soil moisture. However, these will be of second order relatively to the sources of error discussed in earlier sections, provided that reasonable estimate for such quantities can be derived from ancillary sources of data.

9.1.13. Very little research has gone into assessing the error associated to the scene heterogeneity for retrieval of soil moisture from SAR. Low resolution SAR observations like that of SMAP exacerbates this problem which introduces uncertainty due to speckle beyond that modelled using theoretical clutter distributions for homogeneous areas. By moving to finer resolution such obstacles may be largely overcome if the resolution of the final product is close to the spatial scale of the land cover.

9.1.14. NASA has recently proposed an airborne P-band system (AirMOSS) for root zone soil moisture retrieval (Chapin, 2012). Having an airborne system circumvents the bandwidth and Faraday rotation issues to which a space-borne P-band SAR is subject. NASA has estimated that their system should permit estimation of soil moisture below mixed forest (using the data-cube approach) with an error of 0.05 vol/vol provided that calibration errors are less than 0.5dB.

9.1.15. It should however be stressed again that a full-system design and analysis must be undertaken before any concrete conclusions can be drawn as to the ultimate performance of the combined SAR and soil-moisture retrieval system.

9.2. Risks and Special Cases for Soil Moisture Retrieval

9.2.1. There are a number of factors which can have a detrimental effect upon soil moisture estimation or which requires special attention. If these issues are not addressed then the range of application of the proposed soil moisture retrieval algorithm may be limited to bare soils or soils without substantial vegetation cover.

Dew

9.2.2. A strong recommendation has been made by Simmonds *et al*. (2004) that SAR observations for soil moisture retrieval should be made between the hours of 6AM and 9AM. Moreover, all current satellites for measuring soil moisture have used a 6AM overpass time. Their stated reason was that during this time surface soil moisture better reflects the water content of the underlying soil, and soil moisture gradients are at a minimum. However, this overpass time is likely to result in data acquisition under the presence of dew on the ground

in many instances, which forms generally between the hours of 6AM and 8AM.

9.2.3. In an earlier paper Riedel et al. (2001) reported that the effects of dew on L-band backscatter and quantities derived from polarimetric decompositions were largely unaffected by dew, but in a later paper De Jeu *et al*. (2005) report that the L-band Microwave Polarization Difference Index (MPDI) shows marked diurnal variations they associate with dew. If the MPDI shows variations then it is expected that the co-polar backscattering coefficients may also exhibit such variations, which in turn will affect soil moisture estimates. Conversely, it has been suggested that water on leaves is only affects microwave data when there is a complete film of water; wate droplets do not affect the microwave response (Kerr, Personal Communication). Since this issue is not fully resolved and there appears to be no strategy for dealing with early morning dew on soils and vegetation, this factor is identified as a risk to be mitigated through further study.

9.2.4. Data acquisition during or shortly after rainfall is likely to have a similar effect on the microwave data and its subsequent interpretation as dew, as both result in water on the vegetation.

Deserts

9.2.5. While most often dry, deserts are subject to a periodic rainfall. Moreover, dew forms in the desert but evaporates rapidly. The sudden variation of water content in a desert and the rapid evaporation of water could imply more frequent revisit times than those proposed, and adequate modelling of evaporation to ensure proper soil moisture estimates. Furthermore, dry sandy soils permit deep penetration of microwaves, with scattering arising from substantial depths, which could easily confuse soil moisture retrieval algorithms designed to interpret backscatter signals arising from homogeneous soil surfaces. Thus, soil moisture retrieval over desert environments warrants further study.

Vegetation

9.2.6. Overlying vegetation both scatters microwave energy back towards the radar, and attenuates the energy reaching the soil surface. The attenuation may vary according to polarization. In addition, microwave energy is scattered forward from the vegetation to the soil surface, and then returns to the radar. These effects interfere significantly with the direct-surface backscatter, which underlies soil-moisture retrieval algorithms. Dubois *et al.* (1995) found the effects to be significant for vegetation with NDVI > 0.4.

9.2.7. The soil-surface/vegetation scattering mechanism carries information on soil roughness and moisture content. Polarimetry can be used to separate the scattering mechanisms and therefore has the potential to extract soil moisture information in the presence of vegetation. Hajnsek *et al*. (2009) have demonstrated that polarimetric decomposition techniques can be used in this fashion, and have demonstrated soil-moisture retrieval accuracies of 0.01 vol/vol for soils below vegetation and crops. This is in comparison with the same techniques for bare surfaces which yielded accuracies of 0.08 vol/vol. The techniques work best with mature crops and vegetation and the studies were conducted at L-band.

9.2.8. Whilst their work suggests that polarimetric techniques are valuable in extending the range of terrain type over which soil moisture can be retrieved using SAR, there exists no specific or universal algorithm. Thus, vegetation with a NDVI > 0.4 represents a risk for soil moisture retrieval that should be mitigated through further research, perhaps using airborne system studies that mirror the required imaging geometries of proposed space-borne systems.

Forests

9.2.9. Microwave attenuation in forests starts to fall-off dramatically only below L-band, although there is some fall in forest attenuation between C-band and L-band. Whilst some direct-ground and ground-volume returns may be present at L-band, they are generally masked by direct-volume returns to the extent that, as has been suggested, soil moisture retrieval over forests at L-band is not practicable. However, it is fair to say in general that forests are to P-band SAR what crops are to L-band SAR. Thus the polarimetric SAR and PolInSAR techniques that can be employed at L-band to separate scattering mechanisms over crops could be employed to P-band data over forests.

9.2.10. Whilst a comparable analysis to the L-band crop case has yet to be undertaken at P-band, My-Linh Truong-Loï *et al*. (2012) have recently developed a simplified distorted-Born model for forest backscatter and applied it to P-band airborne SAR data over forests. They found soil moisture retrieval accuracy of 0.05 vol/vol below forests, and at the same time were able to recover soil roughness and forest biomass values. Thus, there is clear potential for P-band to yield soil moisture estimates under forests and thereby increase further the area accessible to soil moisture retrieval from radar. P-band satellite SAR data are necessarily low bandwidth and subject to Faraday rotation. Thus, although the potential exists there remains much work to be done to reach the level of an operational soil-moisture retrieval algorithm for forested areas.

Snow

9.2.11. Although covered in snow, underlying soil may be wet, or indeed frozen. The SMAP mission baseline requirements call for SMAP to provide measurements of surface freeze/thaw state for areas north of 45° north latitude. The retrieval of landscape freeze/thaw state relies on analysis of time series radar backscatter for identification of temporal changes in backscatter associated with differences in the aggregate landscape dielectric constant that occur as the landscape transitions between predominantly frozen and non-frozen conditions. This technique assumes that the large changes in dielectric constant occurring between frozen and non-frozen conditions dominate the corresponding backscatter temporal dynamics. This is generally valid during periods of seasonal freeze/thaw transitions for most areas of the cryosphere.

9.2.12. For bare soils covered in dry snow microwave penetration is good and backscatter is representative of the surface backscatter. When the snow melts, from the inside out, free water exists in a complex arrangement above the soil surface and backscatter can be strongly influenced by the wet snow layer. Areas classified as thawed by SMAP and/or the algorithm proposed in this work, can be subject to wet-snow scattering. Thus a wet snow class is required for the data-cube based inversion procedure and substantial effort will be required to generate this information.

9.2.13. In the case of SMAP, flags for frozen soil and/or snow will be used to mask areas where soil moisture retrieval will not be attempted. For Australia, snow coverage is limited to a relatively small area in the alpine area between Canberra and Melbourne, and parts of Tasmania. Frozen soil is not expected to be an issue for Australia.

Steep Terrain

9.2.14. Multichannel data have been proposed for soil moisture retrieval, and at a minimum this is the dual co-polar channel (HH and VV) data. If terrain is tilted in azimuth then the local H-polarization direction is rotated about the radar line of sight and the HH and VV received signals are mixtures of HH and VV local scattering amplitudes. To see this, imagine the extreme case whereby the terrain is tilted 90° without altering the antenna orientation. Locally H becomes V and vice-versa, so that an algorithm using HH and VV backscattering coefficients will have its inputs reversed and soil moisture retrievals will be incorrect (probably failing the VV > HH filter stage).

9.2.15. In order to correctly recover the local HH and VV backscattering coefficients from which the soil moisture must be estimated, two things are needed: i) an estimate of the terrain slope and ii) the full scattering matrix which enables the line of sight basis rotation to be reversed. This implies full-polarimetric operation; the terrain slope may be estimated from full-polarimetric SAR data, but an accurate DEM and accurate geo-referencing are an alternative.

9.2.16. This is not a severe issue for essentially flat terrain, but for steep terrain it becomes a significant problem. If the chosen solution does not employ a fully-polarimetric SAR, for example if compact polarimetry is chosen, then additional research will be required to develop an algorithm that yields accurate soil moisture estimates for steep terrain.

9.2.17. One particular risk associated with terrain slope is the presence of steep regular facets, typical in tilled agricultural fields. These can determine a strong backscattering signal due to a coherent backscattering component, which surface scattering models are not trained to take into account. This can saturate the signal and completely mask the soil moisture effect on the backscattering coefficient. This effect is strongly dependent on incidence and azimuth angle, and it peaks when the radar line of sight is specular to the facets. Therefore, the comparison of observations at different incidence angle will be useful to reveal and avoid such cases.

Water Bodies

9.2.18. Water bodies, including farm dams, flood irrigation and ponded water following heavy precipitation can all have a significant impact on radar backscatter response. Consequently, these, in addition to rivers, lakes etc. need to be identified, and either masked from the retrieval or a correction procedure developed.

Radio Frequency Contamination

9.2.19. Contamination of the measured backscattering by illegal out-of-band transmissions from other devices, or by legal transmissions from other devices operating in the same or similar waveband can significantly degrade the quality of the data, rendering it useless. While this

is not expected to be a major problem for data over Australia, its on-board identification and mitigation should be given careful consideration at the sensor design stage.

9.3. Ancillary Data Requirements

9.3.1. Based on the algorithm recommendation presented in previous sections, this section provides a list of the ancillary data sets (other than SAR observations) which will be required in order to derive a soil moisture product from SAR observation using the recommended algorithms. Indication of the most likely sources of such data is also provided.

9.3.2. Ancillary data required for such a mission fall into two categories – static ancillary data which do not change during the mission and dynamic ancillary data which require periodic updates ranging from seasonally to daily. Static data include parameters such as permanent masks (land / water / forest / urban / mountain), elevation and derived slope, permanent open water fraction, and soils information (primarily sand and clay fraction). The dynamic ancillary data include land cover, precipitation, effective soil temperature, vegetation water content and dynamic water.

9.3.3. Factors to consider when selecting adequate sources of ancillary data are inherent accuracy and impact on the soil moisture retrieval accuracy, latency, spatial resolution, temporal resolution, and coverage.

Static Ancillary Data

9.3.4. Knowledge of local topography is needed to interpret and correct SAR observations for local incidence angle and reverse the line-of-sight basis rotation. The terrain slope may be estimated from fully-polarimetric SAR data, but an accurate surface Digital Elevation Model (DEM) is an alternative. Due to the strong impact of incidence angle on the backscattering coefficients, a DEM should be available at resolution not lower than that of the final soil moisture product. Geoscience Australia and CSIRO Land & Water have recently released an improved version of the Shuttle Radar Topography Mission (SRTM) DEM mission covering all of Australia at 30 and 90 metres. The near future will also see the availability of high-resolution (~12m) global DEM from the TerraSAR-X/TanDEM-X mission. High-resolution DEM from existing LiDAR coverage is a possibility for local areas.

9.3.5. Information on high-level land use is useful to drive the selection of retrieval cases (i.e., agricultural areas, forest, bare soils, inland water bodies, ocean etc.) and the flagging/masking of special cases (permanent snow, permanent water bodies, etc). Land use information from global (e.g., MODIS IGBP Land Cover 500m, ECOCLIMAP) and national (National Dynamic Land Cover Dataset 2000-2008 250m) products, could be useful for such tasks.

9.3.6. It must be highlighted that, due to their static nature, the land cover data sets mentioned are unable to reflect changes in scattering mechanism associated to plant phonological dynamics which can determine changes in the applicable physical model (or hyper-cube). While they provide some distinction between different crop types, they might not be sufficient to discern differences in scattering mechanism required to achieve a good soil moisture accuracy. Thus, land information is also required as a dynamic data set.

9.3.7. Soil textural information (in particular sand and clay fraction and soil bulk density) is required for the conversion of the dielectric constant or soil permittivity output of the retrieval algorithms into a volumetric soil moisture value. Accurate soil textural information is costly and difficult to obtain over large areas. Moreover, the impact of the uncertainty in soil texture on the soil moisture retrieval is of second order relatively to other major sources of error (i.e., SAR measurement error, scattering model error). As a reference, the same value of dielectric constant will result in soil moisture values varying of as much as 0.03 vol/vol and 0.06 vol/vol for an estimation error in sand fraction of respectively 20% and 45%. Therefore available global, national or regional databases are considered suitable sources of textural information (e.g., Harmonized World Soil Database, Australian Bureau of Rural Science) where direct observations are not available.

Dynamic Ancillary Data

9.3.8. Information on Vegetation Water Content (VWC), the main vegetation parameter affecting microwave scattering and attenuation, may be derived from global products. Vegetation indices such as Normalized Difference Vegetation Index (NDVI) and Normalized Difference Water index (NDWI) have been used for such a task in the past (mostly from MODIS and AVHRR global product). Such products have spatial (250m-1km) and temporal (10 days - 1month) resolutions suitable to characterize vegetation dynamics.

9.3.9. An alternative for VWC estimation adopted by the SMAP mission is to derive VWC estimate from a Radar Vegetation Index (RVI) obtained from a combination of SAR backscattering coefficients (HH, VV, HV). RVI or any other parameter based on the radar backscatter should correlate with the vegetation water more strongly than the optical/infrared NDVI or NDWI, because fundamentally optical radiation cannot penetrate vegetation canopies while the L-band microwave signal can. Furthermore the RVI is concurrent with the radar observation. However, further research is needed to demonstrate the robustness of the relationship between RVI and VWC.

9.3.10. Surface temperature information is required since it affects the conversion of the dielectric constant or soil permittivity output of the retrieval algorithms into a volumetric soil moisture value. However, contrary to passive microwave soil moisture retrieval where temperature is crucial in determining the microwave emission, the impact of soil temperature on the soil reflectivity (hence on the SAR soil moisture retrieval) is of second order relative to other factors. The SMAP mission will use temperature data from global weather forecasting models, and that would be appropriate for the required use in a radar mission.

9.3.11. As indicated above, information on the dynamic nature of land cover is also important for soil moisture retrieval. Earlier sections have outlined that polarimetric analysis should complement the use of static land cover to discern separate vegetation scattering classes, rather than simply vegetation classes, to overcome this limitation. Thus, the capability to derive this information directly from the radar data itself in a semi-automated fashion is highly desirable.

9.4. The Way Forward: R&D Requirements

9.4.1. Current advances in RF technology mean that design of SAR systems is beginning to focus on Smart Multi Aperture Radar Techniques (SMART). SMART SAR systems employ multiple

elevation and/or azimuth channels combined with Digital Beam-Forming (DBF) capabilities that permit the synthesis of multiple receiver apertures, which in turn permit greater flexibility in choice of system parameters such as pulse repetition frequency (PRF) and antenna size.

9.4.2. Thus for a given geometric resolution, SMART SAR systems may have wider swaths, higher SNR and lower ASR, than traditional SAR systems. These are all key quantities for SAR systems that enable improvement of performance. For example, increased swath widths can be used to reduce the revisit times and enable more frequent observations.

9.4.3. SMART SAR technology may not however overcome the maximum echo window length limitation of monostatic pulsed SAR systems, which arises through their inability to simultaneously transmit and record echoes. For a given Pulse Repetition Interval (PRI) the transmit duty cycle thus limits the duration of ground echo reception, and imposes either a restriction on the maximum swath width (single swath operation mode) or causes gaps in the coverage (multi-swath mode). Reducing the duty cycle mitigates this effect. However, for a fixed peak power this is at the expense of the reduced average transmit power, and SNR. Advances in efficiency through Gallium Nitride (GaN) technology allow handling significantly higher amounts of peak power. Thus GaN is an attractive solution for increasing the echo window length without sacrificing average transmit power and hence SNR.

Algorithm Development

9.4.4. Clearly, the proposed algorithms are currently limited in area of application and additional algorithm development is implied. The following are suggestions for some of the research and development activities which should precede the implementation of a SAR-based soil moisture monitoring system. In the following discussion, areas to be considered are Australian, but more generally the areas will include anywhere soil moisture retrievals are required for global hydrological and climatological modelling.

9.4.5. Testing of available hyper-cubes computed for the SMAP and SAOCOM missions should be undertaken where they are considered potentially suitable to scattering classes in areas of interest.

9.4.6. Additional development and validation of hyper-cubes for terrain scattering conditions not computed for SMAP but considered necessary for areas of interest should be undertaken.

9.4.7. Optimization between dimensionality of the hyper-cubes (i.e. additional parameters in the forward model) and relative improvement in soil moisture retrieval against increased computational cost should be addressed.

9.4.8. Evaluation of the time-series algorithm with assumption of constant surface roughness over different in situ data and for different land cover classes should be performed.

9.4.9. Use of polarimetric decomposition to distinguish between different land cover scattering types and in particular crop types with different plant structure for pre-classification and selection of hyper-cubes should be undertaken. In particular this investigation should focus on the use of compact polarimety in addition to full polarimetry.

9.4.10. Use of polarimetric SAR (PolSAR) and polarimetric-interferometric SAR (PolInSAR) to derive agricultural crop structural parameters to drive forward modelling in hyper-cubes should be investigated, particularly for compact polarimetry over full polarimetry considerations.

9.4.11. A full analysis of the impact of the use of compact polarimetry mode SAR as opposed to full polarimetry mode for soil moisture retrieval is needed. In particular, the ability to recover terrain slope to correct for line of sight polarization rotation and the feasibility of correcting vegetation effects using a compact polarimetric SAR system, and the implications for antenna design should be undertaken for L-band and S-band.

9.4.12. The use of compact polarimetric and full polarimetrec PolSAR to detect and flag changes in surface conditions and the evolution of crop phenological state (e.g., tillage, harvest, vegetation growth) should be developed.

9.4.13. A study is recommended to consider the impact of changes in surface conditions, both slow (e.g. vegetation growth) and fast (e.g., tillage, harvest, vegetation growth) to the soil moisture accuracy under the assumption of constant surface roughness and vegetation. This is needed to determine the optimal length of the observation window.

9.4.14. The question of soil moisture retrieval below forests should be addressed through a program of high-fidelity modelling of full polarimetric and compact polarimetric PolSAR and PolInSAR forest returns at P-band, coupled to analysis of existing and newly acquired P-band SAR data sets. The latter, through one of the several P-band airborne systems currently operating, such as DLR's F-SAR, ONERA's SETHI and JPL/FEDI's GeoSAR, or indeed NASA's AirMOSS when available. Comparisons of simplified DBA model-based retrievals against PolSAR and PolInSAR decomposition methods should be undertaken. Data cube generation for P-band SAR over forests will be required, and particular scattering classes of interest will be tropical forests and Eucalypt savannahs.

9.4.15. If a decision is to be made to move forward with a SAR system for soil moisture retrieval, then SAR system designs should be commissioned that will address the optimal SAR system design for the chosen resolution of final soil moisture product both for the L-band and P-band SAR systems, and perhaps an S-band system if this is to be considered. The design should include the use of GaN technology and SCORE operation using digital beam forming to optimise coverage, and thereby reduce the number of satellites required to meet the frequent repeat-cycle conditions.

9.4.16. Scale is still an issue using satellite SAR. Depending on the resolution of the required soil moisture product, the scale of observation can compound the effects of multi-scale processes, e.g., topography, surface roughness, soil moisture variations and mixed scattering mechanisms. Further studies are needed on the application of spatial filtering and averaging techniques to address the scale issue.

9.4.17. If a design with early morning (6:00AM - 8:00AM) overpass times is selected, investigations on the feasibility of correction for, or at least flagging of, dew presence would improve the quality of the soil moisture product. Similarly, the impact of rain droplets on vegetation surfaces needs to be better understood.

10. CALIBRATION AND VALIDATION

10.1. Overview

10.2.1. The satellite calibration and validation requirements are an important yet often undervalued component of most satellite missions. This activity should be considered in several stages:

- Pre-launch algorithm validation
- Post-launch satellite calibration
- Post-launch algorithm validation
- Validation of derived products

10.2.2. While considerable work has been undertaken already on developing soil moisture retrieval algorithms using radar, a lot of this work has been undertaken for landscape conditions and management practices that are considerably different to those of Australia. Moreover, existing data sets are not appropriate for testing of algorithms such as the time-series candidate algorithm proposed here, as they have been undertaken for only short durations exhibiting a limited range of soil moisture conditions.

10.2.3. The back-bone of any long-term satellite algorithm validation study is the requirement of a soil moisture monitoring network. Unlike the United States and Europe, there is no operational soil moisture network in Australia. However, there are two research networks; CosmOz and OzNet.

10.2.4. While the CosmOz network has broad Australian coverage (Figure 10.1), these are individual stations in predominantly coastal grassland environments. The cosmos sensors used by this network measure cosmic rays, which are then related to the soil moisture a calibration equation (Franz *et al.*, 2013). The nature of this measurement approach results in an average soil moisture for an area of approximately 300m radius. While this measurement scale eliminates many of the point-to-pixel issues related to soil moisture measurement, the spatial resolution may be too large for radar-based soil moisture missions, especially if targeting 50m rather than 1km scales. Moreover, the measurement corresponds to a soil layer thickness of approximately the top 30cm, while the soil moisture from L-band radar corresponds much more closely to a top 5cm layer. Consequently, these data are better suited for root-zone soil moisture retrieval validation using the surface soil moisture observations.

10.2.5. The OzNet soil moisture monitoring network has coverage only for the Murrumbidgee Catchment of Australia (Figure 10.2). However, it has a total of 64 soil moisture stations distributed in both “dense” and “sparse” network arrangements (Smith *et al.*, 2012). It was established with satellite validation specifically in mind, and has been used to support both of the current dedicated soil moisture missions that are based on passive microwave technology; SMOS (Peischl *et al.*, 2012) and SMAP (Panciera *et al.*, 2013). Importantly, each of the monitoring stations make soil moisture measurements of the top 5cm, and studies have been undertaken at many of the sites to understand the relationship with soil moisture in the surrounding area. These sites are distributed across a diversity of landscape conditions, including many of the dominant crops and management practices used in Australia.

10.2.6. Although it is recommended that any dedicated satellite soil moisture mission for Australia should have national coverage, the Murray Darling Basin is clearly a very important region of Australia, and its diversity represents most of the dominant landscape conditions and management practices of Australia. Moreover, the Murrumbidgee Catchment itself is representative of climate, landscape, and management practices across much of the Murray Darling Basin. Together with the existing backbone of OzNet soil moisture infrastructure, this makes it an ideal candidate for any future satellite validation studies that would support a radar-based soil moisture mission for Australia. The three CosmOz sites located in the Murrumbidgee Catchment would also be valuable for validation studies of derived products such as root-zone soil moisture.

Figure 10.1 Locations of comisc ray soil moisture sensors installed as part of the CosmOz network operated by CSIRO (http://cosmoz.csiro.au/cosmoz/).

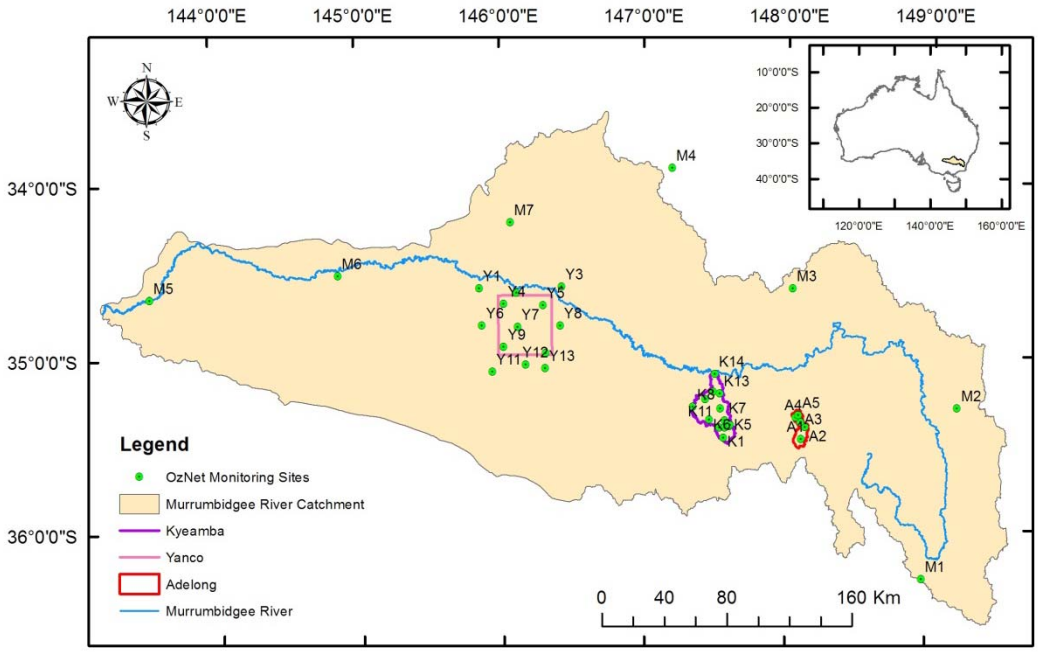

Figure 10.2 Locations of soil moisture monitoring stations installed as part of the OzNet operated jointly by Monash University and the University of Melbourne (http://www.oznet.org.au/; Smith *et al.*, 2012).

10.3. Pre-launch Algorithm Validation

10.3.1. Based on experience and extensive review of the literature, a range of algorithms have been selected for further consideration. These algorithms require further development and validation prior to launch of any dedicated Australian radar soil moisture mission, for a range of reasons:

- They have been developed under landscape conditions and land management practices that are not necessarily representative of those in Australia.
- The soil moisture, vegetation and roughness conditions have often been for limited ranges as compared to those that will be encountered in large scale application.
- The Australian experiments conducted to date have been for relatively short periods of time, which is particularly limiting for testing of time-series and temporal-change approaches.
- Most soil moisture experiments, including those recently undertaken in Australia, have been for relatively flat terrain.

10.3.2. Consequently, available data sets need to be extended to include moderate topographic relief such as is characteristic of much of the western slopes of eastern Australia, and be conducted for a range of vegetation types and soil moisture conditions representative of Australia, extending over a modest time period.

10.3.3. The pre-launch validation studies have two main requirements; i) ground-based data including soil moisture content, surface rough characteristics, and extensive vegetation characterisation for a range of land cover types, and ii) polarimetric radar backscatter data

at L-band over a long period of time and with revisit frequency suitable for soil moisture monitoring (2-3 days).

10.3.4. North American experiments for radar algorithm development have extended for as long as 8-weeks, with data collection on a 2-3day repeat (eg. SMAPVEX12). It is proposed that to cover the short comings of existing data sets for Australia, an airborne field experiment be conducted for at minimum a 3-month duration. The period September to December is most likely to capture the dynamics from wet to dry and bare soil to mature crops, being the spring growing season.

10.3.5. Soil moisture varies significantly from day-to-day, while vegetation and soil characteristics change on much longer timescales unless altered by human intervention. Consequently, it is recommended that sites be chosen around existing soil moisture monitoring stations, and that these be expanded to "core" sites, by having a minimum of three soil moisture sensors across each radar footprint under study. Vegetation and soil characteristics would be monitored on a fortnightly basis, or earlier if necessary. Addition of a webcam will assist with monitoring of human intervention, especially in cropped fields, allowing timely ground sampling of vegetation and surface roughness. The in-situ ground monitoring would be supplemented by intensive sampling on several occasions throughout the campaign, so as to fully understand the point-to-pixel scaling of these core sites.

10.3.6. It is recommended that there be at least two replicates of the core sites selected to represent each landscape type, with not more than 20 core sites in total. These core sites would also form the back-bone of post-launch validation studies as described below. It is proposed that given the network of existing sites, their characteristics and site logistics, these core sites be located in the Coleambally, Maroondah, and Kyeamba areas.

10.3.7. At the present time there are no satellites that can provide the data needed for pre-launch algorithm development and validation. The only satellite with an L-Band sensor and Australian coverage in the immediate future will be ALOS-2, and this has a 14 days repeat cycle. Soil moisture algorithm development requires exact orbit repeat with a 2-3days interval over a time frame of several months. Consequently, airborne L-band sensors will be required to provide a suitable radar data set.

10.3.8. While there are several airborne L-Band radar systems available world-wide, including UAV-SAR and PALS in the United States, these are in high demand for supporting the science and satellite missions of their respective countries. The likelihood of having them deployed to Australia for a minimum 3-month duration experiment would be highly unlikely, and the costs would be significant. Moreover, Australia has recently acquired its own airborne L-Band radar capability; the Polarimetric L-band Imaging Synthetic aperture radar (PLIS).

10.3.9. The PLIS (Figure 10.3) has full polarimetric and single-pass InSAR capabilities. It has been used in several Australian soil moisture experiments of one to three weeks duration, in support of the SMAP mission; the Soil Moisture Active Passive Experiments – SMAPEx (Panciera *et al.*, 2013).

Figure 10.3 The Polarimetric L-band Imaging Synthetic Aperture Radar (PLIS) on an Australian aircraft (left) and a sample image from the Yanco study area (right) that is shown in Figure 10.2.

10.3.10. It has been shown that PLIS can meet the calibration requirements of soil moisture retrieval algorithms, with an absolute calibration of 0.9dB for co-polarised channels. Moreover, PLIS can be made available for a 3-month duration experiment, and there is Australian expertise to conduct the campaigns, operate the sensor, and process the data.

10.3.11. Amongst other things, the data collected from this intensive pre-launch campaign will be used to test the SMAP and SAOCOM data cubes for Australian conditions.

10.3.12. Apart from soil moisture, radar based algorithms for a number of other ancillary data need to be matured and validated. Being able to derive these ancillary data from the same radar platform will substantially simplify the operational soil moisture retrieval from satellite radar algorithms. These ancillary data requirements include i) water detection, ii) vegetation classification, and iii) vegetation water content estimation. Development of these ancillary data products can be achieved from the same airborne field experiment, with minimal considerations to specific requirements. The principal consideration not already covered would be ground truthing of standing water; specifically flood irrigation and/or flood waters under vegetation.

10.3.13. In line with other soil moisture missions, a range of "optional" algorithms should be carried until well after launch, before converging on a single algorithm, or preferred algorithm according to specific conditions. The performance or each algorithm will ultimately be evaluated and decided against the post-launch validation criteria and comparisons described below. Feasibility in terms of computing load, available ancillary data, applicability of a single algorithm to a wide range of conditions, and so on, will need to be considered when making a final choice.

10.4. Post-launch Satellite Calibration

10.4.1. Although the SAR instrument can undergo internal calibration (characterising the behaviours of each individual component in the RF chain, with particular attention to the antenna pattern both *ex-situ* and *in-situ*) full calibration is always a combination of internal and external calibration: the latter involving external targets imaged by the operational system. A coherent and extended approach to radiometric and polarimetric calibration and stability appraisal is required, and will most likely involve a suitable government agency, particularly

as the SAR data will be used for scientific purposes by a global community of earth and climate scientists.

10.4.2. Australia is a very suitable site for calibration targets, having wide flat areas of low clutter over which to deploy suitable targets. However it is advisable to have calibration sites close to the equatorial regions where TEC is the lowest, and the expansive regions of the Amazon rainforest provide (mostly) stable reference targets. In addition, other countries already operate SARs in the bands considered and have established calibration sites and procedures that could be of use. A complete plan for calibration and stability studies, including target design, manufacture and deployment is beyond the scope of the current document, but should be included as part of the SAR system design.

10.4.3. The calibration technique chosen will depend upon system choice, with a risk associated with compact polarimetry mode.

10.4.4. Without full polarimetry operation, there is a risk of greater uncertainty in soil moisture retrieval because the system may not yield calibrated data. Even if a fully polarimetric calibration solution is recovered, it will only work properly when applied to fully polarimetric data.

10.5. Post-launch Algorithm Validation

10.5.1. The post-launch validation will need to establish that the soil moisture product(s) meet the agreed criterion of the mission (see discussion in Section 2). There may be staged criterion requirements, according to beta version, provisional version, and validated version.

10.5.2. Ongoing maturity of the "validated" version is also to be expected over time. Consequently, there is a requirement for long-term benchmarks that can be used to verify both product improvements resulting from algorithm upgrades, as well as product stability due to possible sensor degradation.

10.5.3. The complete validation strategy for the post-launch phase should include:

- Field experiments
- Core sites
- Sparse networks, and
- Other products.

10.5.4. Field experiments in the post-launch phase would be primarily ground-based. These would involve intensive point-based soil moisture monitoring across satellite pixels that represent the range of landscapes and management practices that dominate in Australia. These focus fields would be co-located with the soil moisture network stations, giving further understanding of the point-to-pixel relationships of those sites. These experiments would also put a significant emphasis on the ancillary data requirements of soil moisture retrieval from radar, including soil texture, soil roughness root mean square height and correlation length, vegetation water content, and vegetation structural parameters. Other techniques, such as high-resolution airborne passive microwave retrievals, could be used to supplement this validation, allowing validation across a greater number of pixels than would otherwise be possible using ground measurements alone (Walker et al., 2012). The field experiments

will yield the most reliable data for validation of satellite retrievals, but will be limited in time and space, as these are resource intensive. The field experiments should be conducted as early following launch as possible, and should capture as large a range of moisture and vegetation conditions as possible. Consequently, these would typically be conducted during the September to December growing season.

10.5.5. Core sites provide the opportunity for multiple in-situ soil moisture stations across single satellite footprints that represent the diversity of Australian conditions. Having multiple soil moisture stations in each footprint will further help to alleviate point-to-pixel uncertainties. It is recommended that there be several replicates of each landscape condition represented, limited to not more than about 20 different fields. These sites should be built off the backbone of existing sites in both crop and grassland areas, representing flat and moderate topography. The core sites will provide a long-term reference for validation of the satellite derived surface soil moisture content with a high degree of confidence, but will lack the associated ancillary data of field experiments, and will represent only a small number of pixels across the full spatial domain. These core sites should be operated for the duration of the mission.

10.5.6. Sparse networks allow for more satellite pixels to be monitored, yielding a greater diversity of landscape conditions in the validation than from core sites alone, but with significant uncertainty in the point-to-pixel scaling of the measurements. All sites with a top 5cm soil moisture value, traceable calibration standards, and latency of less than a month should be included in this comparison. However, the current understanding is that this would be limited primarily to the stations that are already included in OzNet, unless the Bureau of Meteorology (or similar) were to add soil moisture monitoring capabilities to their automatic weather stations, as recommended by the WMO. These sparse network sites should also be operated for the duration of the mission.

10.5.7. Other products should also be used as much as possible, to further extend the spatial validation through time, and thus provide greater confidence in the derived soil moisture products. Such products include soil moisture estimates from other satellites and hydrologic models. However, all other satellites with coverage of Australia have a coarser spatial resolution and/or are based on sub-optimal retrieval algorithms. Consequently, comparisons with SMOS and/or SMAP, for example, would require aggregation to scales ranging from 3km to 40km. Likewise, models are typically run on spatial resolutions greater than 1km, and due to limitations in soil properties and meteorologic forcing data, have limited predictive skill at estimating soil moisture patterns at less than about 10km.

10.6. Validation of Derived Products

10.6.1. It is anticipated that higher-order products will be derived from any L-band radar mission for Australia. While these may include vegetation and landuse mapping, flood inundation, fire front monitoring and so forth, the most relevant here is root-zone soil moisture retrieval.

10.6.2. Satellite remote sensing of soil moisture only provides direct information on the top approximately 5cm deep layer of soil. However, numerous studies (eg. Walker 1999; Walker *et al.*, 2004) have demonstrated the ability to derive soil moisture information over the root-zone through the process of "assimilating" the surface observations into a soil moisture prediction model.

10.6.3. Both the SMOS and SMAP missions plan to have what is called a Level 4 product; an estimate of the root-zone soil moisture content from assimilating the satellite surface soil moisture observations into a land surface model.

10.6.4. Soil moisture prediction models suffer from i) poor inputs of atmospheric forcing data such as precipitation, ii) inaccurate estimates of soil hydraulic parameters, and iii) miss-representation of the physical processes that redistribute the water within the soil column. However, if the correlation between the errors in the models estimate of soil moisture at the surface and at deeper depths is known, then the corrections at the surface, through comparison with satellite observations of surface soil moisture, can be propagated throughout the soil column (Walker et al., 2001).

10.6.5. The problem is that models are often a poor representation of reality, meaning that there can be large biases between model predictions at different soil depths, and between model predictions and observations (De Lannoy *et al.*, 2006). Consequently, efforts are underway to both improve the physical realism of these models, and to better understand how to account for bias in data assimilation.

10.6.6. Both the CosmOz and OzNet stations provide soil moisture information at deeper depths (30cm for CosmOz and 90cm for OzNet), which should be used for validation of any derived root-zone soil moisture product. Data from OzNet sites are already being used for pre-launch SMAP validation studies utilising surface soil moisture data from SMOS.

11. CONCLUDING SUMMARY

11.1.1. This report has considered past, present and proposed methods of soil moisture retrieval using SAR data and has presented recommendations for satellite SAR systems that could be used for soil moisture recovery over bare and vegetated surfaces and under forests.

11.1.2. The properties of SAR systems that could satisfy the soil moisture retrieval processes have been considered and, in the absence of specific system design constraints, considered the probable occupation volumes of these SAR systems in the vast SAR design space.

11.1.3. Without specific guidance on choices of antenna design, RF technologies and preferred resolution of the final soil moisture product, it is not possible to generate a SAR system design, which in any case cannot be derived without sophisticated modelling. If the process begun here is to move forward, then the next stage will involve some specific decisions being made as to what areas are of primary interest, and what final products are required, so that full system designs can be commissioned.

11.1.4. Being the stated position of the authors that they have not been tasked to comment on any existing SAR system designs, it is not assumed that any suitable designs already exist, particularly at S-band or P-band.

11.1.5. The requirement for 2-3 day repeat observation does tend to imply a constellation of satellites rather than a single satellite. However this conclusion must be justified through detailed modelling before it should be accepted, and in particular the number of required satellites in the constellation should be established.

11.1.6. The use of multiple (not necessarily identical) satellites should not complicate the radiometric and polarimetric calibration procedures since these are well established. Nor is there necessarily a requirement to calibrate one satellite against another, since each may be calibrated absolutely through the use of active and passive targets, although the existence of multiple observations of stable targets will afford the opportunity of establishing the stability of each sensor. However, the use of a time-series soil moisture retrieval algorithm will require a tight tolerance on relative calibration performance between constellation sensors.

11.1.7. In addition to the need to commission a complete SAR system design based on the chosen soil moisture product parameters, there is much work to be done to establish the algorithm for retrieval of soil moisture below heavily vegetated and forested surfaces. Recommendations for future work that would serve to establish algorithms for these problematic terrain types have been given.

11.1.8. Finally the need for strategies for calibration, validation and monitoring, both of the SAR sensor radiometry and polarimetry as well as of the retrieval algorithms, has been highlighted. These will require substantial effort, careful planning and extended execution. The outline for such a program has been provided.

REFERENCES

Allain, S., Ferro-Famil, L. and Pottier, E. (2003) Surface parameter retrieval from polarimetric and multi-frequency SAR data. *Proc. IEEE International Geoscience and Remote Sensing Symposium (IGARSS)*, Toulouse, France, 2: 1417-1419.

Altese, E., Bolognani, O., Mancini, M. and Troch, P.A. (1996) Retrieving soil moisture over bare soil from ERS-1 Synthetic Aperture Radar data: Sensitivity analysis based on a theoretical surface scattering model and field data. *Water Resources Research*, 32(3): 653-661.

Array Systems Computing Inc. (2011) Algorithm Theoretical Basis Document (ATBD) for the SMOS Level 2 Soil Moisture Processor Development Continuation Project. Prepared by CSBA, UoR, TV and INRA for ESA. Array No.: ASC_SMPPD_037, July 28.

Attema, E.P.W. and Ulaby, F.T. (1978) Vegetation Modeled as a Water Cloud. *Radio Science*, 13(2): 357-364.

Baghdadi, N., Gherboudj, I., Zribi, M., Sahebi, M., King, C. and Bonn, F. (2004) Semi-empirical calibration of the IEM backscattering model using radar images and moisture and roughness field measurements. *International Journal of Remote Sensing,* 25(18): 3593-3623.

Baghdadi, N., Holah, N. and Zribi, M. (2006) Soil moisture estimation using multi-incidence and multi-polarization ASAR data. *International Journal of Remote Sensing*, 27: 1907-1920.

Baghdadi, N., Cerdan, O., Zribi, M., Auzet, V., Darboux, F., Hajj, M.E. and Kheir, R.B. (2008) Operational performance of current synthetic aperture radar sensors in mapping soil surface characteristics in agricultural environments: Application to hydrological and erosion modelling. *Hydrol.Process*, 22: 9-20.

Balenzano, A., Mattia, F., Satalino, G. and Davidson, M.W.J. (2011) Dense temporal series of C- and L-band SAR data for soil moisture retrieval over agricultural crops. *IEEE journal of Selected Topics in Applied Earth Observations and Remote Sensing,* 4(2): 439-450.

Balenzano, A., Mattia, F., Satalino, G., Pauwels, V. and Snoeij, P. (2012) SMOSAR algorithm for soil moisture retrieval using Sentinel-1 data. *Proc. IEEE International Geoscience and Remote Sensing Symposium (IGARSS)*, Munich, Germany, pp. 1200-1203.

Barbier, C. (1996) SAR Image Data Processing at CSL. Report No. TN-CSL-SAR-95001, CSL, Leige, Belgium, 52pp.

Barrett, B.W., Dwyer, E. and Whelan, P. (2009) Soil moisture retrieval from active space-borne microwave observations: an evaluation of current techniques. *Remote Sensing*, 1: 210-242.

Beaudoin, A., Le Toan, T. and Gwyn, Q.H.J. (1990) SAR observations and modelling of the C-band backscatter variability due to multiscale geometry and soil moisture. *IEEE Transactions on Geoscience and Remote Sensing*, 28(5): 886-895.

Bernard, R., Soares, J.V. and Vidal-Madjar, D. (1986) Differential bare field drainage properties from airborne microwave observations. *Water Resources Research*, 22(6): 869-875.

Bindlish, R. and Barros, A.P. (2001) Parameterization of vegetation backscatter in radar-based, soil moisture estimation. *Remote Sensing of Environment,* 76: 130-137.

Bindlish, R. and Barros, A.P. (2002). Subpixel variability of remotely sensed soil moisture: an inter-comparison study of SAR and ESTAR. *IEEE Transactions on Geoscience and Remote Sensing*, 40(2): 326-337.

Bindlish, R., Jackson, T.J., Wood, E., Gao, H., Starks, P., Bosch, D. and Lakshmi, V. (2003) Soil moisture estimates from TRMM Microwave Imager observations over the Southern United States. *Remote Sensing of Environment*, 85: 507-515.

Boisvert, J.B., Gwyn, Q.H.J., Chanzy, A., Major, D.J., Brisco, B. and Brown, R.J. (1997) Effect of surface soil moisture gradients on modelling radar backscaterring from bare fields. *International Journal of Remote Sensing,* 18(1): 153-170.

Bolten, J.D., Lakshmi, V. and Njoku, E.G. (2003) Soil moisture retrieval using the passive/active L- and S-band radar/radiometer. *IEEE Transactions on Geoscience and Remote Sensing,* 41: 2792-2801.

Borgeaud, M. and Wegmüller, U. (1996) On the use of ERS SAR interferometry for the retrieval of geo- and bio-physical information. *Proc. Fringe Workshop on ERS SAR Interferometry*, ESA SP-406, Zurich, Switzerland, pp. 83-94.

Brocca, L., Hasenauer, S., Lacava, T., Melone, F., Moramarco, T., Wagner, W., Dorigo, W., Matgen, P., Martínez-Fernández, J., Llorens, P., Latron, J., Martin, C. and Bittelli, M. (2011) Soil moisture estimation through ASCAT and AMSR-E sensors: an intercomparison and validation study across Europe. *Remote Sensing of Environment*, 115: 3390-3408.

Brogioni, M., Pettinato, S., Macelloni, G., Paloscia, S., Pampaloni, P., Pierdicca, N. and Ticconi, F. (2010) Sensitivity of bistatic scattering to soil moisture and surface roughness of bare soils. *International Journal of Remote Sensing*, 31(15): 4227-4255.

Brown, R.J., Manore, M.J. and Poirer, S. (1992) Correlations between X-, C- and L-band imagery within an agricultural environment. *International Journal of Remote Sensing*, 13(9): 1645-1661.

Bruckler, L., Witono, H. and Stengel, P. (1988) Near surface soil moisture estimation from microwave measurements. *Remote Sensing of Environment*, 26(2): 101-121.

Chapin, E., Chau, A., Chen, J., Heavey, B., Hensley, S., Lou, Y., Machuzak, R. and Moghaddam, M. (2012) AirMOSS: An Airborne P-band SAR to measure root-zone soil moisture, *Proc. IEEE Radar Conference (RADAR)*, pp. 693–698.

Chanzy, A., Bruckler, L. and Perrier, A. (1995) Soil evaporation monitoring: A possible synergism of microwave and infrared remote sensing. *Journal of Hydrology*, 165: 235-259.

Chanzy, A., Kerr, Y., Wigneron, J.-P. and Calvet, J.-C. (1997) Soil moisture estimation under sparse vegetation using microwave radiometry at C-band. *Proc. IEEE International Geoscience and Remote Sensing Symposium (IGARSS)*, Singapore, pp. 1090-1092.

Chen, K.S., Yen, S.K. and Huang, W.P. (1995) A simple model for retrieving bare soil moisture from radar-scattering coefficients. *Remote Sensing of Environment*, 54: 121-126.

Chen, J., and Quegan, S. (2011) Calibration of spaceborne CTLR compact polarimetric low-frequency SAR using mixed radar calibrators. *IEEE Transactions on Geoscience and Remote Sensing*, 49(7): 2712-2723.

Cloude, S.R. (2007) The dual polarisation entropy/alpha decomposition: A PALSAR case study. *Proc. International Workshop on Science and Applications of SAR Polarimetry and Polarimetric Interferometry (PolInSAR)*, Frascati, Italy.

Cloude, S.R. and Pottier, E. (1996) A review of target decomposition theorems in radar polarimetry. IEEE Transactions on Geoscience and Remote Sensing*, 34*: 498-518.

Cloude, S.R. and Pottier, E. (1997) An entropy based classification scheme for land applications of polarimetric SAR. *IEEE Transactions on Geoscience and Remote Sensing*, 35: 68-78.

Cloude, S.R., Papathanassiou, K. and Hajnsek, I. (2000) An eigenvector method for the extraction of surface parameters in polarimetric SAR. *Proc. CEOS SAR Workshop, European Space Agency*, Toulouse, France, pp. 693-698.

Cloude, S.R. and Corr, D.G. (2002) A new parameter for soil moisture estimation. *Proc. IEEE International Geoscience and Remote Sensing Symposium (IGARSS)*, Toronto, Canada, 1: 641-643.

Cloude S.R. and Williams M.L. (2005a) The negative alpha filter: A new processing technique for polarimetric SAR interferometry. *IEEE Geoscience and Remote Sensing Letters*, 2: 187-191.

Cloude S.R. and Williams M.L. (2005b) Estimating sub-canopy soil moisture using PolInSAR. *Proc. PolInSAR, ESA/ESRIN*.

Curlander, J. C. and McDonough, R.N. (1991) Synthetic aperture radar systems and signal processing. John Wiley & Sons, New York, NY, USA.

Cutrona , L.J. (1970) Synthetic aperture radar. *Radar Handbook*, Ch. 23 (Skolnik, M.I.,ed.) McGraw-Hill, New York.

Das, N.N., Entekhabi, D. and Njoku, E.G. (2011) An algorithm for merging SMAP radiometer and radar data for high-resolution soil moisture retrieval. *IEEE Transactions on Geoscience and Remote Sensing*, 49(5): 1504-1512.

Davidson, M.W.J., Thuy Le Toan, Mattia, F., Satalino, G., Manninen, T., Borgeaud, M. (2000) On the characterization of agricultural soil roughness for radar remote sensing studies. *IEEE Transactions on Geoscience and Remote Sensing*, 38(2): 630-640.

Davidson, M.W.J., Thuy Le Toan, Mattia, F., Manninen, T., Borderies, P., Chenerie, I. and Borgeaud, M. (1998) A validation of multi-scale roughness description for the modelling of radar backscattering from bare soil surfaces. *Retrieval of Bio- and Geo-Physical Parameters from SAR Data for Land Applications Workshop*, ESA/ESTEC.

De Jeu, R.A.M., Holmes, T.R. H. and Owe, M. (2005) Determination of the effect of dew on passive microwave observations from space. *Proc. SPIE International Society for Optical Engineering*, vol. 5976.

De Lannoy, G.J.M., Houser, P.R., Pauwels, V.R.N. and Verhoest, N.E.C. (2006). State and bias estimation for soil moisture profiles by an ensemble Kalman filter: effect of assimilation depth and frequency. *Water Resources Research*, 43(6), W06401, doi:10.1029/2006WR005100

Demircan, A., Rombach, M. and Mauser, W. (1993) Extraction of soil moisture from multitemporal ERS-1 SLC data of the Freiburg test-site. *Proc. IEEE International Geoscience and Remote Sensing Symposium (IGARSS)*, Tokyo, Japan, pp. 1794-1796.

De Rosnay, P., Calvet, J.-C., Kerr, Y., Wigneron, J.-P., Lemaître, F., Escorihuela, M.J., Sabater, J.M., Saleh, K., Barrié, J. and Bouhours, G. (2006) SMOSREX: A long term field campaign experiment for soil moisture and land surface processes remote sensing. *Remote Sensing of Environment*, 102: 377-389.

Dobson, M.C., Ulaby, F.T., Hallikainen, M.T. and El-Rayes, M.A. (1985) Microwave dielectric behaviour of wet soil – Part II: Dielectric Mixing Models. *IEEE Transactions on Geoscience and Remote Sensing*, GE-23(1): 35-46.

Dobson, M.C. and Ulaby, F.T. (1986) Active microwave soil moisture research. *IEEE Transactions on Geoscience and Remote Sensing*, GE-24(1): 23-36.

Dobson, M.C., Pierce, L., Sarabandi, K., Ulaby, F.T. and Sharik, T. (1992) Preliminary analysis of ERS-1 SAR for forest ecosystem studies. *IEEE Transactions on Geoscience and Remote Sensing*, 30(2): 203-211.

Dorigo, W.A., Wagner, W., Hohensinn, R., Hahn, S., Paulik, C., Xaver, A., Gruber, A., Drusch, M., Mecklenburg, S., van Oevelen, P., Robock, A. and Jackson, T. (2011) The International Soil Moisture Network: a data hosting facility for global in situ soil moisture measurements. *Hydrol. Earth Syst. Sci.*, 15: 1675-1698.

Doubkova, M., Van Dijk, A.I.J.M., Sabel. D., Wagner, W. and Bloschl, G. (2012) Evaluation of the predicted error of the soil moisture retrieval from C-band SAR by comparison against modelled soil moisture estimates over Australia. *Remote Sensing of Environment*, 120: 188-196.

Draper, C.S., Walker, J.P., Steinle, P.E., de Jeu, R.A.M. and Holmes, T.R.H. (2009) An evaluation of AMSR-E derived soil moisture over Australia. *Remote Sensing of Environment,* 113(4): 703-710.

Du, Y., Ulaby, F.T. and Dobson, M.C. (2000) Sensitivity to soil moisture by active and passive microwave sensors. *IEEE Transactions on Geoscience and Remote Sensing*, 38: 105-114.

Dubois, P.C and van Zyl, J. (1994) An empirical soil moisture estimation algorithm using imaging radar. *Proc. IEEE International Geoscience and Remote Sensing Symposium (IGARSS),* Pasadena, USA, pp. 1573-1575.

Dubois, P.C., van Zyl, J. and Engman, T. (1995a) Measuring soil moisture with active microwave: effect of vegetation. *Proc. IEEE International Geoscience and Remote Sensing Symposium (IGARSS)*, Firenze, Italy, pp. 495-497.

Dubois, P.C., van Zyl, J. and Engman, T. (1995b) Measuring soil moisture with imaging radars. *IEEE Transactions on Geoscience and Remote Sensing*, 33(4): 915-926.

Dubois-Fernández, P.C., Souyris, J.-C., Angelliaume, S. and Garestier, F. (2008) The compact polarimetry alternative for space-borne SAR at low frequency. *IEEE Transactions on Geoscience and Remote Sensing*, 46(10): 3208-3222.

Eagleman, J.R. and Lin, W.C. (1976) Remote sensing of soil moisture by a 21 cm passive radiometer. *J. Geophys. Res.*, 81: 3660-3666.

Engman, E.T. (1990) Progress in microwave remote sensing of soil moisture. *Canadian Journal of Remote Sensing*, 16(3): 6-14.

Engman, E.T. and Chauhan, N. (1995) Status of microwave soil moisture measurements with remote sensing. *Remote Sensing of Environment*, 51: 189-198.

Franz, T.E, M. Zreda, R. Rosolem and T.P.A. Ferre (2013) A universal calibration function for determination of soil moisture with cosmic-ray neutrons. *Hydrology and Earth System Sciences*, 17:453-460, doi:10.5194/hess-17-453-2013.

Freeman, A. and Durden, S.L. (1998) A three-component scattering model for polarimetric SAR data. *IEEE Transactions on Geoscience and Remote Sensing*, 36: 963-973.

Freeman, A., Johnson, W., Huneycutt, B., Jordan, R., Hensley, S., Siqueira, P. and Curlander, J. (2000) The "myth" of the minimum SAR antenna area constraint. *IEEE Transactions on Geoscience and Remote Sensing*, 38(1): 320-324.

Freeman, A. (2004a) Calibration of linearly polarized polarimetric SAR data subject to Faraday rotation. *IEEE Transactions on Geoscience and Remote Sensing*, 42(8): 1617-1624.

Freeman, A. and Saatchi, S. (2004b) On the detection of Faraday rotation in linearly polarized L-band SAR backscatter signatures. *IEEE Transactions on Geoscience and Remote Sensing,* 42(8): 1607–1616.

Frisch, U. (1986) Wave propagation in random media. *Probabilistic Methods in Applied Mathematics*, Barucha-Reid, A.T. (Ed), Academic Press.

Frolich, H. (1949). Theory of Dielectrics, Oxford Clarendon Press.

Frulla, L., Medina, J., Milovich, J., Ortega, G.R. and Thibeault, M. (2011) SAOCOM mission overview. *Proc. CEOS SAR Calibration and Validation Workshop*, Fairbanks, Alaska, USA.

Fung, A.K., Li, Z. and Chen, K.S. (1992) Backscattering from a randomly rough dielectric surface. *IEEE Transactions on Geoscience and Remote Sensing*, 30(2): 356-369.

Fung, A.K. (1994) Microwave scattering and emission models and their applications. Norwood, MA, Artech House.

Gaiser, P.W., St. Germain, K.M., Twarog, E.M., Poe, G.A., Purdy, W., Richardson, D., Grossman, W., Linwood Jones, W., Spencer, D., Golba, G., Cleveland, J., Choy, L., Bevilacqua, R.M. and Chang, P.S. (2004) The WindSat spaceborne polarimetric microwave radiometer: Sensor description and early orbit performance. *IEEE Transactions Geoscience and Remote Sensing*, 42(11): 2347-2361.

Galantowicz, J.F. and Entekhabi, D. (1996) Soil moisture and temperature determined by recursive assimilation of multifrequency observations using simplified models of soil heat and moisture flow and emission. *Proc. International Geoscience and Remote Sensing Symposium (IGARSS)*, Lincoln, Nebraska, USA.

Giacomelli, A., Bacchiega, U., Troch, P.A. and Mancini, M. (1995) Evaluation of surface soil moisture distribution by means of SAR remote sensing techniques and conceptual hydrological modelling. Journal of Hydrology, 166: 445-459.

Goutorbe, J.P., Lebel, T., Tinga, A., Bessemoulin, P., Brouwer, J., Dolman, A.J., Engman, E.T., Gash, J.H.C., Hoepffner, M. and Kabat, P. (1994) HAPEX-Sahel: a large-scale study of land-atmosphere interactions in the semi-arid tropics. *Annals of Geophysics*, 12: 53-64.

Gray, D., Yang, R., Yardley, H., Walker, J., Bates, B., Panciera, R., Hacker, J., McGrath, A. and Stacy, N. (2011) PLIS: An airborne polarimetric L-band interferometric synthetic aperture radar. *Proc. IEEE International Asia-Pacific Conference on SAR*, Seoul, Korea, pp. 845-848.

Hajnsek, I. (2001) Inversion of surface parameters from polarimetric SAR data. PhD Thesis, Friedrich Schiller University of Jena (FSU): Jena, Germany.

Hajnsek, I., Papathanassiou, K.P., Moreira, A. and Cloude, S.R. (2002) Surface parameter estimation using interferometric and polarimetric SAR. *Proc. IEEE International Geoscience and Remote Sensing Symposium (IGARSS)*, Toronto, Canada, 1: 420-422.

Hajnsek, I., Alvarez-Pérez, J.L., Papathanassiou, K.P., Moreira, A. and Cloude, S.R. (2003a) Surface parameter estimation using interferometric coherences at different polarisations. *Workshop on Applications of SAR Polarimetry and Polarimetric Interferometry (PolInSAR)*, ESA/ESRIN, Frascati, Italy.

Hajnsek, I., Pottier, E., and Cloude, S.R. (2003b) Inversion of surface parameters from polarimetric SAR. *IEEE Transactions on Geoscience and Remote Sensing*, 41(4): 727-744.

Hajnsek, I., Jagdhuber, T., Schön, H. and Papathanassiou, K.P. (2009) Potential of estimating soil moisture under vegetation cover by means of PolSAR. *IEEE Transactions Geoscience and Remote Sensing*, 47(2): 442-454.

Hoeben, R., Troch, P.A., Su, Z., Macini, M. and Chen, K. (1997) Sensitivity of radar backscattering to soil surface parameters: a comparison between theoretical analysis and experimental evidence. *Proc. International Geoscience and Remote Sensing Symposium (IGARSS)*, Singapore, 1368-1370.

Hornacek, M., Wagner, W., Sabel, D., Hong-Linh Truong, Snoeij, P., Hahmann, T., Diedrich, E. and Doubkova, M. (2012a) Potential for high resolution systematic global surface soil moisture retrieval via change detection using Sentinel-1. *IEEE Journal of Selected Topics in Applied Earth Observations and Remote Sensing*, 5(4): 1303-1311.

Hornacek, M., Wagner, W. and Sabel, D. (2012b) GNSS positioning in support of surface soil moisture retrieval and flood delineation in near real time. *United Nations/Latvia Workshop on the Applications of Global Navigation Satellite Systems*, Riga, Latvia.

Hornik, K. (1989) Multilayer feed forward network are universal approximators. *Neural Networks*, 2(5): 359-366.

Ichoku, C., Karnieli, A., Arkin, Y., Chorowicz, J., Fleury, T. and Rudant, J.P. (1998) Exploring the utility potential of SAR interferometric coherence images. *International Journal of Remote Sensing,* 19: 1147-1160.

Jackson, T.J. (1993) Measuring surface soil moisture using passive microwave remote sensing. *Hydrological Processes*, 7: 139-152.

Jackson, T.J., Chang, A. and Schmugge, T.J. (1981) Active microwave measurements for estimating soil moisture. *Photogrammetric Engineering and Remote Sensing*, 47: 801-805.

Jackson, T.J. and Schmugge, T.J. (1989) Passive microwave remote sensing system for soil moisture: Some supporting research. *IEEE Transactions Geoscience and Remote Sensing*, 27(2): 225-235.

Jackson,T.J. and Schmugge, T.J. (1991) Vegetation effects on the microwave emission of soils. *Remote Sensing of the Environment*, 36: 203-212.

Jackson, T.J., Le Vine, D.M., Swift, C.T., Schmugge, T.J. and Schiebe, F.R. (1995) Large area mapping of soil moisture using the ESTAR passive microwave radiometer in Washita'92. *Remote Sensing of Environment*, 53: 27-37.

Jackson, T.J., Schmugge, T.J. and Engman, E.T. (1996) Remote sensing applications to hydrology: soil moisture. *Hydrological Sciences Journal*, 41(4): 517-530.

Jackson, T.J., Bindlish, R., Gasiewski, A.J., Stankov, B., Klein, M., Njoku, E.G., Bosch, D., Coleman, T.L., Laymon, C.A. and Starks, P. (2005) Polarimetric scanning radiometer C- and X-band microwave observations during SMEX03. *IEEE Transactions on Geoscience and Remote Sensing*, 43: 2418-2430.

Jackson, T.J., Cosh, M., Bindlish, R., Dinardo, S., Laymon, C., O'Neill, P., Piepmeier, J., Rincon, R. and Yueh, S. (2008) Soil Moisture Active Passive Validation Experiment 2008. *GRSS Lecture* (http://www.grss-ieee.org/talk/soil-moisture-active-passive-validation-experiment-2008-smapvex08/)

Kalman, R.E. (1960) A new approach to linear filtering and predicting problems. *J. Basic Engineering*, 82: 35-45.

Kerr, Y.H., Waldteufel, P., Wigneron, J-P., Martinuzzi, J-M., Font, J. and Berger, M. (2001) Soil moisture retrieval from space: the Soil Moisture and Ocean Salinity (SMOS) mission. *IEEE Transactions on Geoscience and Remote Sensing*, 39(8): 1729-1735.

Kerr, Y.H., Waldteufel, P., Richaume, P., Davenport, P., Ferrazzoli, P. and Wigneron, J.-P. (2006) SMOS Level 2 processor soil moisture algorithm theoretical basis document (ATBD). SM-ESL (CBSA), CESBIO, Toulouse, SOTN-ESL-SM-GS-0001, V5.a, 15/3/2006.

Kerr, Y.H., Waldteufel, P., Wigneron, J.-P., Delwart, S., Cabot, F., Boutin, J., Escorihuela, M.J., Font, J., Reul, N., Gruhier, C., Juglea, S.E., Drinkwater, M.R., Hahne, A., Martín-Neira, M. and Mecklenburg, S. (2010). The SMOS Mission: new tool for monitoring key elements of the global water cycle. *Proceedings of the IEEE*, 98(5): 666-687.

Kim, S-B., Huang, S., Tsang, L., Johnson, J. and Njoku, E. (2011) Soil moisture retrieval over low-vegetation surfaces using time-series radar observations and a lookup table representation of forward scattering. *Proc. IEEE International Geoscience and Remote Sensing Symposium (IGARSS)*, Vancouver, Canada, pp. 146-149.

Kim, Y. and van Zyl, J.J. (2009) A time-series approach to estimate soil moisture using polarimetric radar. *IEEE Transactions on Geoscience and Remote Sensing*, 47: 2519-2527.

Koike, T., Nakamura, Y., Kaihotsu, I., Davva, G., Matsuura, N. and Tamagawa, K. (2004) Development of an advanced microwave scanning radiometer (AMSR-E) algorithm of soil moisture and vegetation water content. *Annual Journal of Hydraulic Engineering,* JSCE, 48: 217-222.

Kong, X. and Dorling, S.R. (2008) Near-surface soil moisture retrieval from ASAR wide swath imagery using a principal component analysis. *International Journal of Remote Sensing*, 29(10): 2925-2942.

Koster, R.D., Dirmeyer, P.A., Guo, Z., Bonan, G., Chan, E., et al. (2004) Regions of Strong Coupling Between Soil Moisture and Precipitation. *Science*, 305(5687):1138-1140.

Lee, J-S., Schuler, D.L. and Ainsworth, T.L. (2000). Polarimetric SAR data compensation for terrain azimuth slope variation. *IEEE Transactions on Geoscience and Remote Sensing,* 38(5): 2153-2163.

Lee, K-H. and Anagnostou, E.N. (2004). A combined passive/active microwave remote sensing approach for surface variable retrieval using Tropical Rainfall Measuring Mission observations. *Remote Sensing of Environment,* 92: 112-125.

Lee, J.S., Boerner, W.M., Schuler, D.L., Ainsworth, T.L., Hajnsek, I., Papathanassiou, K.P. and Lüneburg, E. (2004) A review of polarimetric SAR algorithms and their applications. *Journal of Photogrammetry and Remote Sensing,* 9: 31-80.

Le Vine, D.M., Jackson, T.J., Swift, C.T., Isham, J., Haken, M., Hsu, A. (1998) Passive microwave remote sensing with the synthetic aperture radiometer, ESTAR, during the Southern Great Plains experiment. *Proc. IEEE International Geoscience and Remote Sensing Symposium (IGARSS)*, Seattle, USA, pp. 2606-2608.

Lillesand, T.M. and Kiefer, R.W. (1994) Remote Sensing and Image Interpretation, 3rd ed., John Wiley and Sons, New York, 750pp.

Lin, D-S. and Wood, E.F. (1993) Behaviour of AirSAR signals during MAC-Europe'91. *Proc. IEEE International Geoscience and Remote Sensing Symposium (IGARSS)*, Tokyo, Japan, pp. 1800-1802.

Linden, A. and Kinderman, J. (1989) Inversion of multi-layer nets. *Proc. International Joint Conference on Neural Networks*, II: 425-43.

Liu, Y.Y., Dorigo, W.A., Parinussa, R.M., de Jeu, R.A.M., Wagner, W., McCabe, M.F., Evans, J.P. and van Dijk, A.I.J.M. (2012) Trend-preserving blending of passive and active microwave soil moisture retrievals. *Remote Sensing of Environment,* 123: 280-297.

Lozza, H.F. (2009). Simulations of remotely-sensed surface soil moisture assimilations for future Earth Observations missions. *WMO Symposium on Data Assimilation*, Melbourne, Australia.

Lu, Z. and Meyer, D.J. (2002) Study of high SAR backscattering caused by an increase of soil moisture over a sparsely vegetated area: implications for characteristics of backscattering. *International Journal of Remote Sensing*, 23: 1063-1074.

Luo, X., Askne, J., Smith, G. and Dammert, P. (2001). Coherence characteristics of radar signals from rough soil. *Progress in Electromagnetic Research (PIER)*, 31: 69-88.

Ma, L., Li, Z.F. and Liao, G.S. (2011) System error analysis and calibration methods for multi-channel SAR. *Progress in Electromagnetics Research (PIER)*, 112: 309-327.

MacDonald, Dettwiler and Associates Ltd. (2011) Sentinel-1 Product Definition. MDA Document No. SEN-RS-52-7440, Mar 21, MDA, Richmond, Canada.

Maggioni, V., Panciera, R., Walker, J.P., Rinaldi, M., Paruscio, V., Kalma, J.D. and Kim, E.J. (2006) A multi-sensor approach for high resolution airborne soil moisture mapping. *Proc. Hydrology and Water Resources Symposium*, Launceston, Tasmania, Australia.

Malhotra, S., Kasilingam, D. and Schuler, D. (2003) The dependence of polarimetric coherence on surface roughness for very rough surfaces. *Proc. IEEE International Geoscience and Remote Sensing Symposium (IGARSS)*, Toulouse, France, pp. 1654-1656.

Manninen, T. (1997) Multiscale surface roughness and backscattering. *Proc. Progress in Electromagnetic Research Symposium (PIER)*, 16: 175-203.

Mattia, F., Le Toan, T., Souyris, J.C., De Carolis, C., Floury, N., Posa, F. and Pasquariello, N.G. (1997) The effect of surface roughness on multifrequency polarimetric SAR data. *IEEE Transactions on Geoscience and Remote Sensing*, 35: 954-966.

Merlin, P., Walker, J.P., Chehbouni, A. and Kerr, Y. (2008) Towards deterministic downscaling of SMOS soil moisture using MODIS derived soil evaporative efficiency. *Remote Sensing of Environment*, 112(10): 3935-3946.

Merlin, O., Walker, J.P., Panciera, R., Escorihuela, M.J. and Jackson, T.J. (2009) Assessing the SMOS soil moisture retrieval parameters with high resolution NAFE'06 data. *IEEE Geoscience and Remote Sensing Letters*, 6(4): 635-639.

Merlin, O., Bitar, A.A., Walker, J.P. and Kerr, Y. (2010) An improved algorithm for disaggregating microwave-derived soil moisture based on red, near-infrared and thermal-infrared data. *Remote Sensing of Environment,* 114: 2405-2316.

Merlin, O., Rüdiger, C., Al Bitar, A., Richaume, P., Walker, J.P. and Kerr, Y. (2012). Disaggregation of SMOS Soil Moisture in Southeastern Australia. *IEEE Transactions on Geoscience and Remote Sensing*, 50(5), doi:10.1109/TGRS.2011.2175000.

Meyer, F.J. and Nicoll, J.B. (2008) Prediction, detection and correction of Faraday rotation in full-polarimetric L-Band SAR data. *IEEE Transactions on Geoscience and Remote Sensing*, 46(10): 3076-3086.

Mironov, V.L., Kosolapova, L.G. and Fomin, S.V. (2009) Physically and mineralogically based spectroscopic dielectric model for moist soils. . IEEE Transactions on Geoscience and Remote Sensing, 47: 2059-2070.

Mladenova, I., Lakshmi, V., Jackson, T.J., Walker, J.P., Merlin, O. and de Jeu, R.A.M. (2011) Validation of AMSR-E soil moisture using L-band airborne radiometer data from National Airborne Field Experiment 2006. *Remote Sensing of Environment,* 115(8): 2096-2103.

Monerris, A., Walker, J.P., Panciera, R., Jackson, T.J., Gray, D., Yardley, H. and Ryu, D. (2011) The third Soil Moisture Active Passive Experiment. *Proc. International Congress on Modelling and Simulation (MODSIM)*, Perth, Australia, pp. 1980-1986.

Moran, M.S., Vidal, A. Troufleau, D., Inoue, Y., Qi, J., Clarke, T.R., Pinter, P.J., Mitchell, Jr.T. and Neale. C.M.U. (1997) Combining multi-frequency microwave and optical data for farm management. *Remote Sensing of Environment*, 61: 96-109.

Moran, M.S., Hymer, D.C. Qi, J. and Sano, E.E. (2000) Soil moisture evaluation using multitemporal synthetic aperture radar SAR in semiarid rangeland. *Agricultural and Forest Meteorology*, 105: 69-80.

Moran, M.S., McElroy, S., Watts, J.M. and Peters Lidard, C.D. (2006) Radar remote sensing for estimation of surface soil moisture at the watershed scale. *Proc.ARS/INIFAP Binational Symposium on Modeling and Remote Sensing in Agriculture*, Aguascalientes, Mexico, pp. 91-106.

Moreira, A., Krieger, G., Younis, M., Hajnsek, I., Papathanassiou, K., Eineder, M. and De Zan, F. (2011) TanDEM-L: A mission proposal for monitoring dynamics Earth processes. *Proc. IEEE International Geoscience and Remote Sensing Symposium (IGARSS)*, Vancouver, Canada, pp. 1385-1388.

Morse, P. M. and Feshbach, H. (1953) Methods of Theoretical Physics vols I and II, McGraw-Hill.

My-Linh Truong-Loï, Freeman, A., Dubois-Fernández, P. C. and Pottier, E. (2009) Estimation of soil moisture and Faraday rotation from bare soil surfaces using compact polarimetry. *IEEE Transactions on Geoscience and Remote Sensing*, 47(11): 3608–3615.

My-Linh Truong-Loï, Saatchi, S. and Jaruwatanadilok, S. (2012) A parameterized inversion model for soil moisture and biomass from polarimetric backscattering coefficients. *Proc. IEEE International Geoscience and Remote Sensing Symposium (IGARSS)*, Munich, Germany, pp. 5145-5148.

Narayan, U., Lakshmi, V. and Njoku, E.G. (2004) Retrieval of soil moisture from passive and active L/S band sensor (PALS) observations during the Soil Moisture Experiment in 2002 (SMEX02). Remote Sensing of Environment, 92: 483-496.

Narayan, U., Lakshmi, V. and Jackson, T.J. (2006) High-resolution change estimation of soil moisture using L-band radiometer and radar observations made during the SMEX-2 experiments. *IEEE Transactions on Geoscience and Remote Sensing*, 44: 1545-1554.

Nesti, G., Tarchi, D., Bedidi, A., Despan, D., Rudant, J.P., Bachelier, E. and Borderies, P. (1998) Phase shift and decorrelation of radar signal related to soil moisture changes. *Retrieval of Bio- and Geo-Physical Parameters from SAR Data for Landsat Applications Workshop*, ESA/ESTEC, Noordwijk, The Netherlands, pp. 423-430.

Neumann, M., Ferro-Famil, L. and Reigber, A. (2010) Estimation of forest structure, ground, and canopy layer characteristics from multibaseline polarimetric interferometric SAR data. *IEEE Transactions Geoscience and Remote Sensing*, 48(3): 1086-1104.

Njoku, E.G. and Entekhabi, D. (1996) Passive microwave remote sensing of soil moisture. *Journal of Hydrology*, 184: 101-129.

Njoku, E., Jackon, T., Lakshmi, V., Chan, T. and Nghiem, S. (2003) Soil moisture retrieval from AMSR-E. *IEEE Transactions on Geoscience and Remote Sensing*, 41: 215-229.

Ogilvy, J.A. (1991) Theory of wave scattering from random rough surfaces, IOP Publishing, Bristol, UK.

Oh, Y., Sarabandi, K. and Ulaby, F.T (1992) An empirical model and an inversion technique for radar scattering from bare soil surfaces. *IEEE Transactions on Geoscience and Remote Sensing*, 30(2): 370-381.

Oh, Y., Sarabandi, K. and Ulaby, F.T. (1994) An inversion algorithm for retrieving soil moisture and surface roughness from polarimetric radar observations. *Proc. IEEE International Geoscience and Remote Sensing Symposium (IGARSS)*, Pasadena, USA, pp. 1582-1584.

Owe, M., de Jeu, R. and Walker, J. (2001) A methodology for surface soil moisture and vegetation optical depth retrieval using the microwave polarization difference index. *IEEE Transactions on Geoscience and Remote Sensing*, 39: 1643-1654.

Paloscia, S., Pettinato, S., Santi, E., Pierdicca, N., Pulvirenti, L., Notarnicola, C., Pace, G. and Reppucci, A. (2012) An algorithm for soil moisture mapping in view of coming Sentinel-1 satellite. *Proc. IEEE International Geoscience and Remote Sensing Symposium (IGARSS)*, Munich, Germany, pp. 7023-7026.

Panciera, R., Walker, J.P., Kalma, J.D., Kim, E.J., Saleh, K. and Wigneron, J-P. (2009a) Evaluation of the SMOS L-MEB passive microwave soil moisture retrieval algorithm. *Remote Sensing of Environment*, 113: 435-444.

Panciera, R., Walker, J.P. and Merlin, O. (2009b) Improved understanding of soil surface roughness parameterization for L-band passive microwave soil moisture retrieval. *IEEE Geoscience and Remote Sensing Letters*, 6(4): 625-629.

Panciera, R., Walker, J.P., Kalma, J. and Kim, E. (2011) A proposed extension to the soil moisture and ocean salinity Level 2 algorithm for mixed forest and moderate vegetation pixels. *Remote Sensing of Environment,* 115: 3343-3354.

Panciera, R., Walker, J. P., Jackson, T. J., Gray, D., Tanase, M. A., Ryu, D., Monerris, A., Yardley, H., Rüdiger, C., Wu, X., Gao, Y., Hacker, J. (2013) The Soil Moisture Active Passive Experiments (SMAPEx): Towards soil moisture retrieval from the SMAP mission. *IEEE Transactions on Geoscience and Remote Sensing*, doi: 10.1109/TGRS.2013.2241774.

Pathe, C., Wagner, W., Sabel, D., Doubkova, M. and Basara, J.B. 2009. Using ENVISAT ASAR Global Mode data for surface soil moisture retrieval over Oklahoma, USA. *IEEE Transactions on Geoscience and Remote Sensing*, 47, 2: 468-480.

Pauwels, V.R.N., Timmermans, W., Loew, A. 2008. Comparison of the estimated water and energy budgets of a large winter wheat field during AgriSAR 2006 by multiple sensors and models. *Journal of Hydrology,* 349: 425-440.

Peischl, S., Ye, N., Walker, J.P., Ryu, D. and Kerr, Y.H. 2011. Soil moisture retrieval from multi-incidence angle observations at L-band. 19th International Congress on Modelling and Simulation, Perth, Australia, 12-16 December.

Peplinski, N.R., Ulaby, F.T. and Dobson, M.C. (1995) Dielectric properties of soils in the 0.3-1.3GHz range. *IEEE Transactions on Geoscience and Remote Sensing,* 33(3): 803-807.

Pierdicca, N., Pluvirenti, L. and Bignami, C. (2010) Soil moisture estimation over vegetated terrains using multitemporal remote sensing data. *Remote Sensing of Environment,* 114: 440-448.

Pierdicca, N. and Pulvirenti, L. (2012) Future use of the data from the ESA Sentinel-1 mission for operational soil moisture mapping: a multitemporal algorithm. *Proc. SPIE International Society for Optical Engineering*, Edinburgh, UK, vol. 8536.

Powles, J.G., Williams, M.L. and Evans, W.A.B. (1987) Does a microscopically inhomogeneous polar liquid have a dielectric constant? *Journal of Physics C: Solid State Physics*, 21: 1639.

Powles, J.G., Williams, M.L. and Evans, W.A.B. (1988) The dynamic dielectric constant of an inhomogeneous polar liquid: Direct approach from simulation. *Molecular Physics*, 66: 1107.

Quesney, A., Hegarat-Mascle, S.Le., Taconet, O., Vidal-Madjar, D., Wigneron, J.-P., Loumagne, C. and Normand, M. (2000) Estimation of watershed soil moisture index from ERS/SAR data. *Remote Sensing of Environment,* 72: 290-303.

Ragab, R. (1995) Towards a continuous operational system to estimate the root-zone soil moisture from intermittent remotely sensed surface moisture. *Journal of Hydrology*, 173: 1-25.

Rao, K.J., Raju, S. and Wang, J.R. (1993) Estimation of soil moisture and surface roughness parameters from backscattering coefficient. *IEEE Transactions on Geoscience and Remote Sensing,* 31(5): 1094-1099.

Rice, S.O. (1963) Reflection of EM waves by slightly rough surfaces. The Theory of Electromagnetic waves, M. Kline (Ed.), Interscience, New York.

Richards, L.A. (1931) Capillary conduction of liquids through porous mediums. *Physics*, 1 (5): 318-333.

Riedel, T., Pathe, C., Thiel, C., Herold, M. and Schmullius, C. (2001) Systematic investigation on the effect of dew and interception on multi-frequency and multi-polarimetric radar backscatter signals, *Proc. International Symposium on Retrieval of Bio- and Geophysical Parameters from SAR Data for Land Applications*, Sheffield, UK, pp. 99-104.

Robock A., K.Y. Vinnikov, G. Srinivasan, J.K. Entin, S.E. Hollinger, N.A. Speranskaya, S. Liu and A. Namkhai (2000) The global soil moisture data bank. *Bulletin of the American Meteorological Society*, 81(6): 1281-1300.

Rombach, M. and Mauser, W. (1997) Multi-annual analysis of ERS surface soil moisture measurements of different land uses. *Proc. ERS Symposium: Space at the Service of our Environment*, Florence, Italy, ESA-SP-414: 27-34.

Rosen, P.A., Eisen, H., Shen, Y., Hensley, S., Shaffer, S., Veilleux, L., Dubayah, R., Ranson, K.J., Dress, A., Blair, J.B., Luthcke, S., Hager, B.H. and Joughin, I. (2011) The proposed DESDynI mission - From science to implementation. *Proc. Radar Conference (RADAR)*, pp.1129-1131.

Saleh, K., Kerr, Y.H., Richaume, P., Escorihuela, M.J., Panciera, R., Delwart, S., Boulet, G., Maisongrande, P., Walker, J.P., Wursteisen, P. and Wigneron, J.-P. (2009) Soil moisture retrievals at L-band using a two-step inversion approach (COSMOS/NAFE'05 Experiment). *Remote Sensing of Environment*, 113: 1304-1312.

Sano, E.E., Huete, A.R., Troufleau, D., Moran, M.S. and Vidal, A. (1998) Relation between ERS-1 Synthetic Aperture Radar data and measurements of surface roughness and moisture content of rocky soils in a semiarid rangeland. *Water Resources Research,* 34(6): 1491-1498.

Schmugge, T.J. (1983) Remote sensing of soil moisture: Recent advances. *IEEE Transactions on Geoscience and Remote Sensing*, GE-21(3): 336-344.

Schmugge, T.J. (1985) Remote sensing of soil moisture. Anderson, M.G. and Burt, T.P. (Eds), *Hydrological Forecasting*, John Wiley and Sons, New York, Ch. 5, pp. 101-124.

Schmulluis, C. and Furrer, R. (1992) Frequency dependence of radar backscattering under different moisture conditions of vegetation-covered soils. *International Journal of Remote Sensing*, 13(12): 2233-2245.

Schuler, D.L., Jong-Sen, L., Kasilingam, D. and Nesti, G. (2002) Surface roughness and slope measurements using polarimetric SAR data. *IEEE Transactions on Geoscience and Remote Sensing*, 40: 687-698.

Sellers, P.J., Hall, F.G., Asrar, G., Strebel, D.E. and Murphy, R.E. (1992) An overview of the first international satellite land surface climatology project, (ISLSCP) field experiment (FIFE). *J. Geophys. Res. Atmosph.*, 97: 18345-18371.

Shi, J., Wang, J., Hsu, A., O'Neill, P. and Engman, E.T. (1997) Estimation of bare surface soil moisture and surface roughness parameter using L-band SAR image data. *IEEE Transactions on Geoscience and Remote Sensing*, 35(5): 1254-1266.

Shoshany, M., Svoray, T., Curran, P.J., Foody, G.M. and Perevolotsky, A. (2000) The relationship between ERS-2 SAR backscatter and soil moisture: generalization from a humid to semi-arid transect. *International Journal of Remote Sensing*, 21(11): 2343.

Simmonds, L.P. *et al*. (2004) Soil moisture retrieval by a future space-borne Earth observation mission, ESA/ESTEC contract #14662/00/NL/DC.

Smith, A.B., Walker, J.P., Western, A.W., Young, R.I., Ellett, K., Pipunic, R.C., Grayson, R.B., Siriwardena, L., Chiew, F.H.S. and Richter, H. (2012) The Murrumbidgee soil moisture monitoring network data set, *Water Resources Research*, doi:10.1029/2012WR011976.

Srivastava, S.K. and Jayaraman, V. (2001) Relating interferometric signature of repeat pass ERS-1 SAR signals to dynamic land cover changes. *Acta Astronaut*, 48: 37-44.
Srivastava, H.S., Patel, P., Manchanda, M.L., Adiga, S. (2003) Use of multi-incidence angle RADARSAT-1 SAR data to incorporate the effect of surface roughness in soil moisture estimation. *IEEE Transactions on Geoscience and Remote Sensing,* 41: 1638-1640.

Su, Z., Troch, P.A., de Troch, F.P., Nochtergale, L. and Cosyn, B. (1995) Preliminary results of soil moisture retrieval from ESAR (EMCA 94) and ERS-1/SAR, Part II: Soil moisture retrieval. *Proc. workshop on hydrological and microwave scattering modelling for spatial and temporal soil moisture mapping from ERS-1 and JERS-1 SAR data and macroscale hydrologic modelling (EV5V-CT94-0446)*.

Tansey, K.J. and Millington, A.C. (2001) Investigating the potential for soil moisture and surface roughness monitoring in drylands using ERS SAR data. *International Journal of Remote Sensing*, 22: 2129-2149.

Thorsos, E.I. and Jackson, D.R. (1991) Studies of scattering theory using numerical methods. *Waves in Random Media*, 1(3): 165-190.

Topp, G.C. (1992) The measurement and monitoring of soil water content by TDR. *Proc. of National Hydrology Research Centre Workshop*, Saskatoon, Saskatechewan, Canada, pp. 155-161.

Tsang, L., Kong, J.A. and Shin, R.T. (1985) Theory of microwave remote sensing. Wiley Series in Remote Sensing.

Ulaby, F.T. and Batlivala, P.P. (1976) Optimum radar parameters for mapping soil moisture. *IEEE Transactions on Geoscience Electronics*, 14: 81-93.

Ulaby, F.T., Batlivala, P.P. and Dobson, M.C. (1978) Microwave backscatter dependence on surface roughness, soil moisture, and soil texture: Part I-bare soil. *IEEE Transactions on Geoscience Electronics*, 16: 286-295.

Ulaby, F.T., Moore, R.K. and Fung, A.K. (1982) Microwave Remote Sensing: Active and Passive, Vol. I - Microwave Remote Sensing Fundamentals and Radiometry, Addison-Wesley, Reading, Massachusetts, 456 pp.

Ulaby, F.T., Moore, R.K. and Fung, A.K. (1986a) Microwave Remote Sensing: Active and Passive, Vol. II - Radar Remote Sensing and Surface Scattering and Emission Theory, Addison-Wesley, Reading, Massachusetts, 1982, 609 pp.

Ulaby, F.T., Moore, R.K., Fung, A.K. (1986b) Microwave Remote Sensing: Active and Passive, Vol. III - Volume Scattering and Emission Theory, Advanced Systems and Applications, Artech House, Dedham, Massachusetts, 1986, 1100 pp.

Ulaby, F.T., Dubois, P.C. and van Zyl, J. (1996) Radar mapping of surface soil moisture. *Journal of Hydrology*, 184: 57-84.

van de Griend, A.A. and Engman, E.T. (1985) Partial area hydrology and remote sensing. *Journal Hydrology*, 81: 211-251.

vanZyl, J.J. (1993) The effects of topography on the radar scattering from vegetated areas. *IEEE Transactions on Geoscience and Remote Sensing*, 31(1): 153-160.

van Zyl, J.J., Njoku, E.G. and Jackson, T.J. (2003) Quantitative analysis of SMEX'02 AIRSAR data for soil moisture inversion. *Proc. IEEE International Geoscience and Remote Sensing Symposium (IGARSS)*, Toulouse, France, pp. 404-406.

Verhoest, N.E.C., Troch, P.A., Paniconi, C. and De Troch, F.P. (1998) Mapping basin scale variable source areas from multitemporal remotely sensed observations of soil moisture behaviour. *Water Resources Research*, 34(12): 3235-3244.

Vivoni, E.R., Gebremichael, M., Watts, C.J., Bindlish, R. and Jackson, T.J. (2008) Comparison of ground-based and remotely-sensed surface soil moisture estimates over complex terrain during SMEX04. *Remote Sensing of Environment*, 112: 314-325.

Wagner, W. (1998) Soil moisture retrieval from ERS scatterometer data. Vienna, Austria, Vienna University of Technology.

Wagner, W., G. Lemoine, M. Borgeaud and H. Rott. (1999a) A study of vegetation cover effects on ERS scatterometer data. *IEEE Transactions on Geoscience and Remote Sensing,* 37(2II): 938-948.

Wagner, W., Lemoine, G. and Rott, H. (1999b) A method for estimating soil moisture from ERS scatterometer and soil data. *Remote Sensing of Environment*, 70(2): 191-207.

Wagner, W., Noll, J., Borgeaud, M. and Rott, H. (1999c) Monitoring soil moisture over the Canadian Prairies with the ERS scatterometer. *IEEE Transactions on Geoscience and Remote Sensing*, 37: 206-216.

Wagner, W. and Scipal, K. (2000) Large-scale soil moisture mapping in western Africa using the ERS scatterometer. *IEEE Transactions of Geoscience and Remote Sensing*, 38(4): 1777-1782.

Wagner, W., K. Scipal, C. Pathe, D. Gerten, W. Lucht and B. Rudolf (2003) Evaluation of the agreement between the first global remotely sensed soil moisture data with model and precipitation data. *Journal of Geophysical Research D: Atmospheres*, 108(D19): Art. No. 4611.

Wagner, W., Sabel, D., Doubkova, M., Bartsch, A. and Pathe C. (2009) The potential of Sentinel-1 for monitoring soil moisture with a high spatial resolution at global scale. *Proc. The Earth Observation and Water Cycle Science Conference*, ESA/ESRIN, Frascati, Italy.

Walker, J.P. (1999) Estimating soil moisture profile dynamics from near-surface soil moisture measurements and standard meteorological data. PhD Thesis, Department of Civil, Surveying and Environmental Engineering, The University of Newcastle.

Walker, J.P., Houser, P.R. and Willgoose, G.R. (2004) Active Microwave Remote Sensing for Soil Moisture Measurement: A Field Evaluation Using ERS-2. *Hydrological Processes*, 18: 1975-1997. doi:10.1002/hyp.1343.

Walker, J.P., Merlin, O., Panciera, R., Kalma, J., Kim, E. and Hacker, J. (2006) National Airborne Field Experiments for soil moisture remote sensing. *Proc. Hydrology and Water Resources Symposium*, Launceston, Tasmania, Australia.

Walker J.P., Panciera, R. and Kim, E. (2008) High resolution airborne soil moisture mapping. *Proc. Australasian Remote Sensing and Photogrammetry Conference*, Darwin, Australia.

Wang, J.R., Engman, E.T., Shiue, J.C., Rusek, M. and Steinmeier, C. (1996). The SIR-B observations of microwave backscatter dependence on soil moisture, surface roughness and vegetation covers. *IEEE Transactions on Geoscience and Remote Sensing*, 24(4): 510-516.

Wang, J.R. and Schmugge, T.J. (1980) An empirical model for the complex dielectric permittivity of soils as a function of water content. *IEEE Transactions on Geoscience and Remote Sensing*, 18: 388-295.

Wang, J.R., Hsu, A., Shi, J.C., O'Neill, P.E., Engman, E.T. (1997) A comparison of soil moisture retrieval models using SIR-C measurements over the Little Washita River watershed. *Remote Sensing of Environment*, 59: 308-320.

Wang, C., Qi, J., Moran, S. and Marsett, R. (2004) Soil moisture estimation in a semiarid rangeland using ERS-2 and TM imagery. *Remote Sensing of Environment*, 90: 178-189.

Wang, W-Q. (2012) Virtual antenna array analysis for MIMO synthetic aperture radars. *International Journal of Antennas and Propagation*, Article ID 587276.

Wegmüller, U. (1997) Soil moisture monitoring with ERS SAR interferometry. *Proc. ERS Symposium: Space at the Service of our Environment*, ESA-SP-414, Florence, Italy, pp. 47-52.

Wever, T. and Henkel, J. (1995). Evaluation of the AIRSAR system for soil moisture analysis. *Remote Sensing of Environment*, 53: 118-122.

Wiemann, A. (1998) Inverting a microwave backscattering model by the use of a neural network for the estimation of soil moisture. *Proc. IEEE International Geoscience and Remote Sensing Symposium (IGARSS)*, Seattle, WA, USA, p. 1837-1839.

Wigneron, J.-P., Schmugge, T., Chanzy, A., Calvet, J.-C. and Kerr, Y. (1998) Use of passive microwave remote sensing to monitor soil moisture. *Agronomie*, 18(1): 27-43.

Wigneron, J.-P., Waldteufel, P., Chanzy, A., Calvet, J.-C., Marloie, O., Hanocq, J.-F. and Kerr, Y. (2000) Retrieval capabilities of L-band 2-D interferometric radiometry over land surfaces (SMOS mission). *Proc. Microwave Radiometry and Remote Sensing of the Earth's Surface and Atmosphere*, P. Pampaloni and S. Paloscia (Eds.) Utrecht, The Netherlands.

Wigneron, J.-P., Kerr, Y.H., Waldteufel, P., Saleh, K., Escorihuela, M.J. and Richaume, P. (2007) L-band Microwave Emission of the Biosphere (L-MEB) model: Description and calibration against experimental data sets over crop fields. *Remote Sensing of Environment*, 107: 639-655.

Williams, M.L. (2006) PolSARproSim: A coherent, polarimetric SAR simulation of forests (version 1.0), Available online at: http://earth.esa.int/polsarpro/Manuals/PolSARproSim_Design.pdf

Williams, M.L. (2008). Potential for surface parameter estimation using compact polarimetric SAR. *IEEE Geoscience and Remote Sensing Letters*, 5: 471-473.

Wu, T.D. and Chen, K.S. (2004). A reappraisal of the validity of the IEM model for backscattering from rough surfaces. *IEEE Transactions on Geoscience and Remote Sensing*, 42(4): 743-753.

Wu, X., Walker, J.P., Rüdiger, C., Panciera, R., Monerris, A. and Das, N.N. (2011) Towards medium-resolution brightness temperature retrieval from active and passive microwave. *Proc. International Congress on Modelling and Simulation (MODSIM)*, Perth, Australia, pp. 2023-2029.

Wuthrich, M. (1997) In-situ measurement and remote sensing of soil moisture using time domain reflectometry, thermal infrared and active microwaves. PhD Thesis, Naturwissenschaftlichen Fakultät der Universität Basel.

Younis, M., Patyuchenko, A., Huber, S., Krieger, G., Moreira, A. (2010) A concept for high performance reflector-based Synthetic Aperture Radar, *Proc. IEEE International Geoscience and Remote Sensing Symposium (IGARSS)*, Honolulu, Hawaii, USA.

Yueh, S.H. (2000) Estimates of Faraday rotation with passive microwave polarimetry for microwave remote sensing of Earth surfaces. *IEEE Transactions on Geoscience and Remote Sensing*, GE-38(5): 2434-2438.

Zebker, H.A. and Villasenor, J. (1992) Decorrelation in interferometric radar echoes. *IEEE Transactions on Geoscience and Remote Sensing*, 30: 950-959.

Zhan, X., Houser, P.R., Walker, J.P. and Crow, W.T. (2006) A method for retrieving high-resolution surface soil moisture from HYDROS L-band radiometer and radar observation. *IEEE Transactions on Geoscience and Remote Sensing*, 44(6): 1534-1544.

Zhang, T., Zeng, Q., Li, Y. and Xiang, Y. (2008) Study on relation between InSAR coherence and soil moisture. *Proc. International Society for Photogrammetry and Remote Sensing Congress*, Beijing, China.

Zribi, M., Le Hegarat-Mascle, S., Ottle, C., Kammoun, B. and Guerin, C. (2003) Surface soil moisture estimation from the synergistic use of the (multi-incidence and multi-resolution) active microwave ERS Winder Scatterometer and SAR data. *Remote Sensing of Environment,* 86: 30-41.

APPENDIX A. SOME SIGNIFICANT MODEL PARAMETERS

Table A.1. Model parameters. Theoretical backscatter models.

Model and author(s)	Formulation	Model parameters
Approximate version of IEM **(Altese *et al.* 1996)**	$\sigma_{pq}^{o} = \frac{k_o^2}{2}\exp(-2k_{zo}^2\sigma^2)\sum_{n=1}^{\infty}\sigma^{2n}\left\|I_{pq}^{n}\right\|^2\frac{W^n(-2k_{xo},0)}{n!}$	$I_{pq}^{n} = (2k_{zo})^n f_{pq}\exp(-\sigma^2 k_{zo}^2) + \frac{k_{zo}^n\left[F_{pq}(-k_{xo},0)+F_{pq}(k_{xo},0)\right]}{2}$ $f_{vv} = \frac{2R_v}{\cos\vartheta}$ $f_{hh} = \frac{-2R_h}{\cos\vartheta}$ $F_{vv}(-k_{xo},0)+F_{vv}(k_{xo},0) = \frac{2\sin^2\vartheta(1+R_v)^2}{\cos\vartheta}\cdot\left[\left(1-\frac{1}{\varepsilon_r}\right)+\frac{\mu_r\varepsilon_r-\sin^2\vartheta-\varepsilon_r\cos^2\vartheta}{\varepsilon_r^2\cos^2\vartheta}\right]$ $F_{hh}(-k_{xo},0)+F_{hh}(k_{xo},0) = \frac{-2\sin^2\vartheta(1+R_h)^2}{\cos\vartheta}\cdot\left[\left(1-\frac{1}{\mu_r}\right)+\frac{\mu_r\varepsilon_r-\sin^2\vartheta-\mu_r\cos^2\vartheta}{\mu_r^2\cos^2\vartheta}\right]$ $R_h = \frac{\cos\vartheta-\sqrt{\varepsilon_r-\sin^2\vartheta}}{\cos\vartheta+\sqrt{\varepsilon_r-\sin^2\vartheta}}$ $R_v = \frac{\varepsilon_r\cos\vartheta-\sqrt{\varepsilon_r-\sin^2\vartheta}}{\varepsilon_r\cos\vartheta+\sqrt{\varepsilon_r-\sin^2\vartheta}}$ $R_0 = \frac{1-\sqrt{\varepsilon_r}}{1+\sqrt{\varepsilon_r}}$ $W^n(u,v) = \frac{1}{2\pi}\int_{-\infty}^{+\infty}\rho^n(\xi,\varsigma)\exp(-iu\xi-iv\varsigma)d\xi d\varsigma$ f_{pq} Kirchhoff coefficient F_{pq} complementary field coefficient R_v and R_h vertical and horizontal Fresnel reflection coefficients

		R_0 Fresnel reflection coefficient at nadir ε_r relative dielectric constant k_0 free space wave number k_{z0} z component of free space wave number k_{x0} x component of free space wave number σ RMS surface height (cm) l correlation length (cm) μ_r relative magnetic permeability W^n roughness spectrum of surface related to nth power of 2 parameter surface correlation function $\rho(\xi,\varsigma)$ by the Fourier transformation, and is usually simplified to a single parameter isotropic case

Table A.2 Model parameters. Empirical backscatter models.

Model and author(s)	Formulation	Model parameters
Oh's model **(Oh *et al.* 1992)**	$\sigma_{vv}^{o} = \frac{g\cos^3\vartheta}{\sqrt{p}}[\Gamma_v + \Gamma_h]$ $\sigma_{hh}^{o} = g\sqrt{p}\cos^3\vartheta[\Gamma_v + \Gamma_h]$ $\sigma_{hv}^{o} = q\sigma_{vv}^{o}$	$\sqrt{p} = 1 - \left(\frac{2\vartheta}{\pi}\right)^{\frac{1}{3\Gamma_0}}\exp(-k_o\sigma)$ $g = 0.7\left[1 - \exp\left(-0.65(k_o\sigma)^{1.8}\right)\right]$ $q = 0.23\sqrt{\Gamma_0}\left[1 - \exp(-k_o\sigma)\right]$ $\Gamma_h = \left\lvert\frac{\cos\vartheta - \sqrt{\varepsilon_r - \sin^2\vartheta}}{\cos\vartheta + \sqrt{\varepsilon_r - \sin^2\vartheta}}\right\rvert^2$ $\Gamma_v = \left\lvert\frac{\varepsilon_r\cos\vartheta - \sqrt{\varepsilon_r - \sin^2\vartheta}}{\varepsilon_r\cos\vartheta + \sqrt{\varepsilon_r - \sin^2\vartheta}}\right\rvert^2$ $\Gamma_0 = \left\lvert\frac{1 - \sqrt{\varepsilon_r}}{1 + \sqrt{\varepsilon_r}}\right\rvert^2$ ϑ incidence angle (deg.) Γv Vertical Fresnel reflectivity Γh Horizontal Fresnel reflectivity $\Gamma 0$ Fresnel reflectivity at nadir εr Dielectric constant relative to free space

Table A.3 Model parameters. Semi-empirical backscatter models.

Model and author(s)	Formulation	Model parameters
Shi *et al.* (1997)	$\sigma^{o}_{pq} = \lvert\alpha_{pq}\rvert^{2}\left[\frac{S_R}{a_{pq}(\vartheta)+b_{pq}(\vartheta)S_R}\right]$	$S_R = (k_o\sigma)^2 W(-2k_{xo})$ $W(K) = \int_0^{\infty} \rho(\xi) J_0(K\xi)\xi d\xi$ $\alpha_{vv} = 4k_o\left[R_v \cos^2\vartheta + \frac{\sin^2\vartheta(1+R_v)^2}{2}\left(1-\frac{1}{\varepsilon_r}\right)\right]$ $\alpha_{hh} = -4k_o R_h \cos^2\vartheta$ $a_{vv}(\vartheta) = \exp(-3.118 + 5.302\vartheta)$ $b_{vv}(\vartheta) = \exp(-3.013 + 2.361\tan^{6.8}\vartheta)$ $R_h = \frac{\cos\vartheta - \sqrt{\varepsilon_r - \sin^2\vartheta}}{\cos\vartheta + \sqrt{\varepsilon_r - \sin^2\vartheta}}$ $R_v = \frac{\varepsilon_r\cos\vartheta - \sqrt{\varepsilon_r - \sin^2\vartheta}}{\varepsilon_r\cos\vartheta + \sqrt{\varepsilon_r - \sin^2\vartheta}}$ Where: W roughness spectrum related to one-parameter surface correlation function $\rho(\xi)$. $J_0()$ Bessel function to zeroth order k_0 free space wave number k_{x0} x component of free space wave number ϑ incidence angle (deg.) a_{pq} and b_{pq} empirically derived coefficients α_{pq} approximation of parameter I_{pq} in IEM R_v and R_h vertical and horizontal Fresnel reflection coefficients ε_r relative dielectric constant - By using 2 polarisation measurements and rearranging the above equations, the roughness parameter S_R was eliminated to obtain: $10\log_{10}\left[\frac{\lvert\alpha_{vv}\rvert^2 + \lvert\alpha_{hh}\rvert^2}{\sigma^{o}_{vv} + \sigma^{o}_{hh}}\right] = a_{vh}(\vartheta) + b_{vh}(\vartheta)10\log_{10}\left[\frac{\lvert\alpha_{vv}\rvert\lvert\alpha_{hh}\rvert}{\sqrt{\sigma^{o}_{vv}\sigma^{o}_{hh}}}\right]$

		- This equation is used to solve for the dielectric constant of the near-surface soil layer from vv and hh polarisation observations. The base equation is then used to solve for the surface roughness parameter. Where: $a_{vh}(\vartheta) = \exp\left(\begin{matrix}-12.37 + 37.206\sin\vartheta - \\ 41.187\sin^2\vartheta + 18.89\sin^3\vartheta\end{matrix}\right)$ $b_{vh}(\vartheta) = 0.649 + 0.659\cos\vartheta - 0.306\cos^2\vartheta$

APPENDIX B. ACRONYMS

AASR	Azimuth ASR	**MPDI**	Microwave Polarisation Difference Index
AIRSAR	Airborne Synthetic Aperture Radar	**NAFE**	National Airborne Field Experiment
ALOS	Advanced Land Observation Satellite	**NASA**	National Aeronautics and Space Administration
AMSR-E	Advanced Microwave Scanning Radiometer - Earth Observing System	**NDVI**	Normalized Difference Vegetation Index
ANN	Artificial Neural Network	**NDWI**	Normalized Difference Water Index
ARD	Annotated Raw Data	**NESZ**	Noise Equivalent Sigma Zero
ASAR	Advanced Synthetic Aperture Radar	**NMM3D**	Numerical Maxwell Model in 3 Dimensions
ASAR	Advanced Synthetic Aperture Radar	**OSSE**	Observing System Simulation Experiment
ASCAT	Advanced SCATterometer	**OzNet**	Australian Hydrological Monitoring Network
ASI	Agenzia Spaziale Italiana	**PALS**	Passive/Active L-band Sensor
ASR	Ambiguity to Signal Ratio	**PALSAR**	Phased Array L-band SAR
ASR	Ambiguity to Signal Ratio	**PBTG**	Physical Based Two Grid
AWRA	Australian Water Resources Assessment system	**PCA**	Principal Components Analysis
CONAE	Comisión Nacional de Actividades Espaciales	**PLIS**	Polarimetric L-band Imaging Synthetic aperture radar
COSMOS	Campaign for validating the Operation of SMOS	**PLMR**	Polarimetric L-band Multibeam Radiometer
CosmOz	Australian National Cosmic Ray Soil Moisture Monitoring Facility	**PolInSAR**	Polarimetric Interferometric SAR
CP	Compact Polarimetry	**PolSAR**	Polarimetric SAR
DBF	Digital Beam Forming	**POM**	Physical Optics Method
DEM	Digital Elevation Model	**PR**	Polarisation Ratio
DESDynI	Deformation, Ecosystem Structure, and Dynamics of Ice	**PRF**	Pulse Repetition Frequency
DiSPATCh	Disaggregation based on Physical And Theoretical scale Change	**PRI**	Pulse Repetition Interval
EASE	Equal-Area Scalable Earth grid	**RFI**	Radio Frequency Interference
EKF	Extended Kalman Filter	**RMS**	Root Mean Square

ENVISAT	ENVironmental SATellite	**RMSE**	Root Mean Square Error
ERS	European Remote Sensing	**SA**	Strategic Applications
ESA	European Space Agency	**SAOCOM**	SAtélite Argentino de Observación COn Microondas
EUMETSAT	European Organisation for the Exploitation of Meteorological Satellites	**SAR**	Synthetic Aperture Radar
FP	Full Polarimetry	**SCORE**	Scan On Receive algorithm
GCOM	Global Change Observation Mission	**SLC**	Single Look Complex
GMES	Global Monitoring for Environment and Security	**SM**	Soil Moisture
GPS	Global Positioning System	**SMAP**	Soil Moisture Active Passive
GSFC	Goddard Space Flight Center	**SMAPEx**	Soil Moisture Active Passive Experiment
IEM	Integral Equation Method	**SMART**	Smart Multi Aperture Radar Techniques
INA	Instituto Nacional del Agua	**SMC**	Soil Moisture Content
InSAR	Interferometric SAR	**SMCG**	Sparse Matrix Canonical Grid
INTA	Instituto Nacional de Tecnología Agropecuaria	**SMOS**	Soil Moisture and Ocean Salinity
IWS	Interferometric Wide Swath	**SMOSAR**	Soil MOisture retrieval from multi-temporal SAR data
JAXA	Japan Aerospace Exploration Agency	**SMP**	Soil Moisture Processor
JPL	Jet Propulsion Laboratory	**SNR**	Signal to Noise Ratio
KA	Kirchhoff Approach	**SPM**	Small Perturbation Model
LIA	Local Incidence Angle	**TDR**	Time Domain Reflectometry
L-MEB	L-band microwave emission of the biosphere model	**TEC**	Total Electron Content
LOS	Line Of Sight	**TMI**	TRMM Microwave Imager
LUT	Look-Up Table	**TRMM**	Tropical Rainfall Measuring Mission
MAP	Bayesian Maximum Posterior Probability	**VWC**	Vegetation Water Content
MODIS	Moderate Resolution Imaging Spectroradiometer	**WCM**	Water Cloud Model